5-5-2020

The Role of Bacterial Symbionts and Bioluminescence in the Pyrosome, Pyrosoma atlanticum

Alexis Berger
Nova Southeastern University

Thesis of
Alexis Berger

Submitted in Partial Fulfillment of the Requirements for the Degree of

Master of Science
M.S. Marine Biology

Nova Southeastern University
Halmos College of Natural Sciences and Oceanography

May 2020

Approved:
Thesis Committee

Major Professor: Dr. Jose Lopez

Committee Member: Dr. Patricia Blackwelder

Committee Member: Dr. Tamara Frank

HALMOS COLLEGE OF NATURAL SCIENCES AND OCEANOGRAPHY

The Role of Bacterial Symbionts and Bioluminescence in the Pyrosome, *Pyrosoma atlanticum*

By

Alexis Berger

Submitted to the Faculty of
Halmos College of Natural Sciences and Oceanography
in partial fulfillment of the requirements for
the degree of Master of Science with a specialty in:

Marine Biology

Nova Southeastern University

June 5, 2020

Table of Contents

Abstract

The pelagic tunicate, *Pyrosoma atlanticum*, is known for its brilliant bioluminescence, but the mechanism causing this bioluminescence has not been fully characterized. This study identifies the bacterial bioluminescent symbionts of *P. atlanticum* collected in the northern Gulf of Mexico using various methods such as electron microscopy, light microscopy, and molecular genetics. The bacteria are localized within a specific pyrosome light organ. Bioluminescent symbiotic bacteria of Vibrionaceae composed >50% of taxa in tunicate samples (n=13), which was shown by utilizing current molecular genetics methodologies. While searching for bacterial lux genes in 2 tunicate samples, we also serendipitously generated a draft tunicate mitochondrial genome which was used for *P. atlanticum* pyrosome identification. Furthermore, a total of 396K MiSeq 16S rRNA reads provided pyrosome microbiome profiles to determine bacterial symbiont taxonomy. After comparing with the Silva rRNA database, a 99% sequence identity matched a *Photobacterium sp. R33*-like bacterium (referred to as *Photobacterium Pa-1*) as the most abundant bacteria within *P. atlanticum* samples. Specifically-designed 16S rRNA V4 probes for fluorescence in situ hybridization (FISH) verified the *Photobacterium Pa-1* location around the periphery of each pyrosome luminous organ. Scanning and transmission electron microscopy (SEM, TEM respectively) confirmed a rod-like bacterial presence which also appears intracellular in the light organs. This intracellular bacterial localization may represent a bacteriocyte formation reminiscent of other invertebrates.

Keywords: symbiosis, bioluminescence, Pyrosome, microscopy, 16S, high throughput sequencing

Acknowledgements

First, I would like to thank my family for their endless support and encouragement throughout this journey. I would like to thank my mother, Annie, for your unending words of encouragement and unshakable faith in me – you have helped keep my head above water when it all felt like too much. I would like to thank my father, Hector, for supporting my craziness and always making sure I ate. I would like to thank my brother, Max, for continuing to push me to be better and wanting to make you proud. Thanks for always being a phone call away when I needed you. I would also like to thank Colleen McMaken, for reading and rereading my drafts and listening to all of my talks for hours on end. I could not have done this without you and your confidence in my abilities. Thank you for keeping me company in the lab while I yell at the Qubit and gels. Thank you for all of the little things you did that kept me smiling. I would not have been able to get through this, especially during the quarantine without my family.

I would like to thank my advisor, Dr. Jose Lopez, for the opportunity to study such a unique organism and shed light to a decades long unanswered question. Thank you for guiding me through the microbiology world and its intricacies. I would also like to thank my committee member Dr. Patricia Blackwelder, for opening the door and fostering my love for microscopy. You have introduced a whole new world and I could not be more excited to see where it takes me. I would also like to thank Dr. Tamara Frank for sharing your unending knowledge of bioluminescence and the deep-sea. I truly appreciate every member of my committee for their dedication and effort to getting this thesis done and ready to defend on time. I would also like to thank Mickie Edwards, Murphy McDonald, Dr. Lauren Krausfeldt, and every member of the Lopez Genetics and Microbiology Lab. You all have made my time at Nova Southeastern University unforgettable. In addition to everyone at HALMOS, I would like to thank Dr. Tracey Sutton, Dr. Rosanna Milligan, Natalie Slayden, and Nina Pruzinsky as well as DEEPEND for making this project possible. I would also like to thank NOAA and the DeepSearch crew for collecting additional samples. I would finally like to thank the Scripps Institute, specifically Alta Johnson, and the University of Miami Microscopy Center for allowing us to use their facilities.

Introduction

Pyrosoma atlanticum

Pyrosomes derive their name from the Greek words pyro ("fire") and soma ("body") because of the "fiery" bioluminescence that was viewed at night (Sutherland et al., 2018). They were classified by Lamarck and Huxley under the subphylum Tunicata (previously known as Urochordata) due to their tunic encased zooids (Huxley, 1851;Lemaire and Piette, 2015). The zooids are encased in an extracellular sheath (tunic) made in part of cellulose (Holland, 2016). Subphylum Tunicata is divided into three classes: Ascidiacea, Thaliacea, and Appendicularia. Class Ascidiacea and Appendicularia have tadpole larvae with notochords and hollow nerve chords while the tadpole larvae in Class Thaliacea do not. Another notable difference between the classes are that Class Thaliacea and Appendicularia are pelagic while Class Ascidiacea is sessile (Holland, 2016). Class Thaliacea encompasses Orders Pyrosomatida, Salpida, and Doliolida. Pyrosomes, and more specifically *Pyrosoma atlanticum*, are found within the order Pyrosomatida. The presence of an intricate cellular network of individual zooids within a chitinous tunic suggests a phylogenetic relationship between the pyrosomes and other colonial Ascidians and Thaliacians (Hirose et al., 1999;Sutherland et al., 2018). Pyrosomes have several different cell types within the tunic. These cells are capable of phagocytosis, conduction of impulses, contraction of the tunic, and locomotion (Hirose et al., 1999).

Pyrosomes are approximately 95% water and are extremely well adapted for rapid growth and efficient energy use. Transparency makes pyrosomes difficult to see at any depth, which is why they can be found throughout the pelagic realm. Aside from being transparent, and of limited nutritional value, pyrosomes have few sensory or predator-avoidance adaptations. (Alldredge and Madin, 1982). They can reproduce both sexually and asexually, via internal fertilization (hermaphroditic) and budding (Holland, 2016). Once fertilized the embryo cleaves into a group of cells (cyathozooid) and is released it after it buds into 4 zooids. The budding continues once released from the parent (Holland, 2016). Individual pyrosomes can reach lengths of up to 20 m and are composed of thousands of individual zooids. The zooids are oriented so the buccal siphons direct water inward and the atrial siphons channel the water to flow through the central cavity (Fig. 1). This flow allows the pyrosome to propel itself through the water. Each

zooid contains a pair of light organs with intracellular symbionts located near the buccal siphon (Fig. 2) (Haygood, 1993). Although the presence of light organs has been observed, the bioluminescent mechanism has not been unequivocally elucidated in *P. atlanticum.*

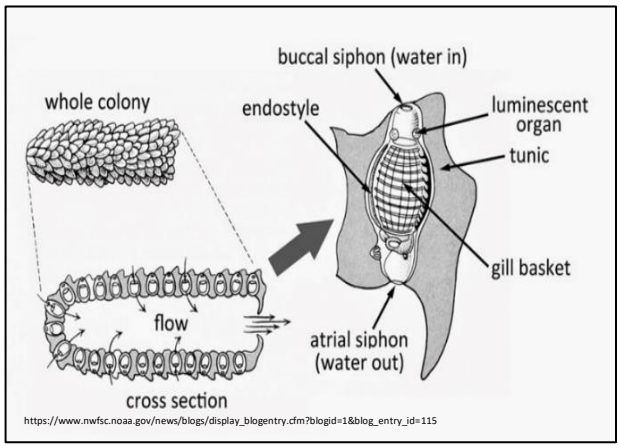

Figure 1. Individual *P. atlanticum* zooid (Ruppert and Barnes, 1994)

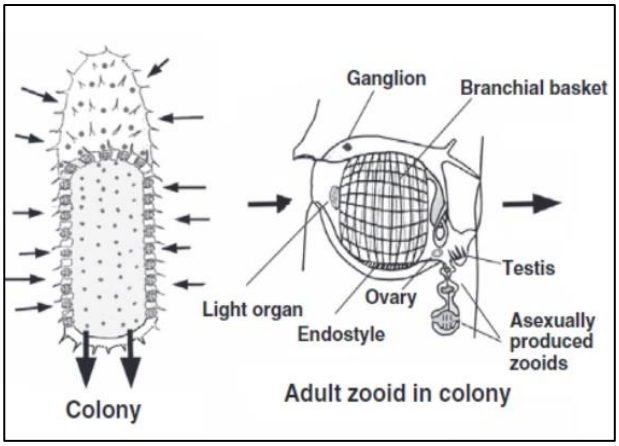

Figure 2. Detailed diagram of an individual *P. atlanticum* zooid (Holland, 2016).

Pyrosomes occupy marine habitats from shallow water (near shore) to open ocean and deep sea (Holland, 2016). Their typical habitat range is from 45°N to 45°S, which includes tropical to temperate waters. However, their range is expanded in warmer waters (Fig. 3) (Holland, 2016). This expansion is related to pyrosome sensitivity to the physical environment. Temperature, light, salinity, dissolved oxygen, and even current flow have a significant impact on the biology and behavior of these tunicates, which facilitates habitat expansion (Sutherland et al., 2018). Pyrosomes remain one of the least studied planktonic grazers, despite their widespread distribution and ecological significance. Pyrosomes are characterized as highly successful planktonic grazers, and swarms of these colonies can consume substantial amounts of phytoplankton (Alldredge and Madin, 1982;Décima et al., 2019). They have been noted for their potential to restructure the food web when aggregating in large quantities (Sutherland et al., 2018). It has been recently confirmed that pyrosomes are major modifiers of the food web. They can cycle energy from shallow water depths to deeper in the water column by eating phytoplankton and excreting carbon rich fecal matter (Holland, 2016). Some pyrosome species have been shown to graze on deeper dwelling phytoplankton at the base of the euphotic zone

(Décima et al., 2019). Pyrosome remains also play a role in carbon flux as they make up a significant proportion of marine snow and serve as a benthic food source (Holland, 2016;Sutherland et al., 2018). The remains are colonized by bacteria and viruses, and they provide shelter for other species inhabiting the water column (Holland, 2016).

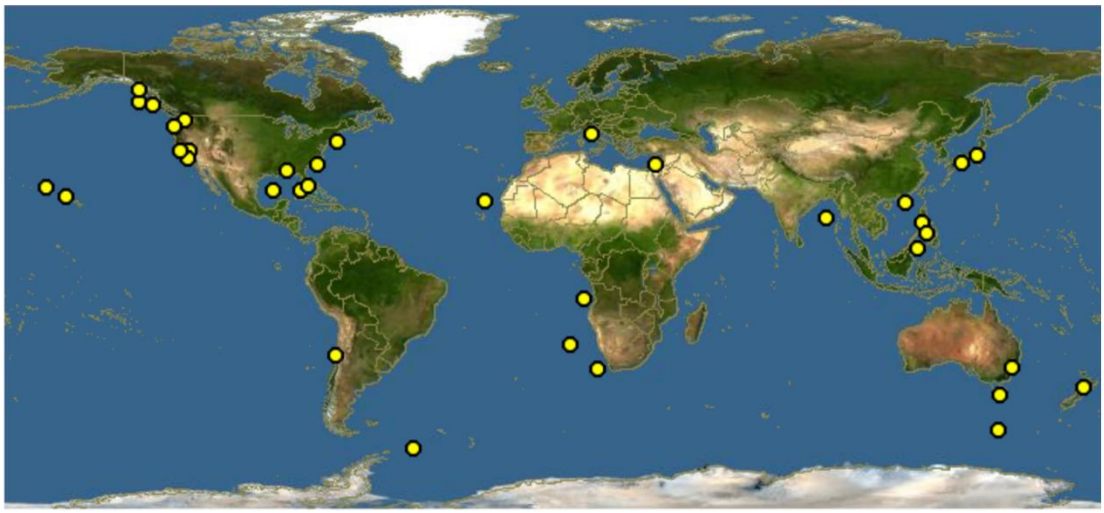

Figure 3. Sightings of *P. atlanticum* globally.
https://www.discoverlife.org/mp/20m?kind=Pyrosoma+atlanticum

Generating Light at Ocean Depths

The emission of light by organisms has evolved independently over 40 times in marine and terrestrial organisms (Haddock et al., 2010). Bioluminescence is an important adaptive trait in ocean dwelling taxa, and appears to be more prevalent than previously thought (Martini and Haddock, 2017). Over 700 animal genera are known to include luminous species, with more than 80% being marine organisms (Widder, 2010). Within this group, 90% of pelagic organisms between 200-1000m are known to have bioluminescent capabilities. In addition, fishes, squid, and shrimp are able to modify aspects of their light production, such as the intensity, kinetics, wavelength, and angular distribution. This emphasizes the evolutionary importance of the bioluminescence mechanism (Haddock and Case, 1999). There are several critical ways bioluminescence can aid an organismal survival. Bioluminescence can facilitate food location and capture, attract a mate, allow for species recognition, and functions as a defense mechanism (Widder, 2010).

Bioluminescence is produced by the oxidation of a light emitting molecule, called a luciferin, with an enzyme, luciferase (Haddock et al., 2010). Luminous and non-luminescent

organisms have luciferins. However, in order for bioluminescence to occur they have to evolve the luciferase enzyme or photoproteins, which allows for the "easy" evolution of bioluminescence (Haddock et al., 2010). There are four luciferins responsible for most light production in oceanic species: bacteria luciferin, dinoflagellate luciferin, coelenterazine, and cypridina luciferin (Widder, 2010). Invertebrates display a variety of bioluminescent mechanisms. The northern krill, *Meganyctiphanes norvegica,* has ten ventral photophores that produce the luminescence using dinoflagellate luciferin (Herring, 1985;Widder, 2010). The comb jelly, *Beroe forskalii,* uses calcium-activated proteins and coelenterazine to trigger their bioluminescent mechanism (Haddock et al., 2010). The vampire squid, *Vampyroteuthis infernalis,* produces its intrinsic bioluminescence by using a luciferin along with its individual luciferase to luminesce in two large mantle light organs and small light organs across the body (Haddock et al., 2010). Organismal light organs can be very complex structures, with features that range from canals to tubules that are highly vascularized (Nealson et al., 1981). The light organ within pyrosome zooids is located near the buccal siphon and is known to have a ball-like structure (Fig. 1). However, this is the extent of knowledge concerning the structure of the light organ.

Other studies have focused on the mechanisms of bioluminescent light propagation in several species such as the hydromedusae, *Euphysa japonica*, the squid, *Abralia veranyi*, and the myctophid fish, *Ceratoscopelus maderensis* (Mackie and Bone, 1978;Nealson et al., 1981;Johnsen et al., 2004). These studies focused on how bioluminescence could be utilized for counterillumination. The difference between pyrosomes and most other bioluminescent organisms is that they do not respond similarly (Bowlby et al., 1990). One of the mechanisms of pyrosome luminescence is producing luminescence in response to external light flashes, as well as responding to conspecifics and stimulated bioluminescence (Polimanti, 1911;Burghause, 1914;Mackie and Bone, 1978;Bowlby et al., 1990). In many bioluminescent organisms the luminescence is autogenic, i.e. does not require bacterial symbionts (Haddock et al., 2010). However, bioluminescent bacteria are common in temperate to warmer waters and are associated with colonial animals as saprophytes, commensals, and parasites (Kita-Tsukamoto et al., 2006;Haddock et al., 2010). Bioluminescent bacteria have been studied in a wide array of ctenophores, ceratioids, ophiuroids, and cephalopods (Haddock et al., 2010). For example, the Hawaiian bobtail squid, *Euprymna scolopes*, and the bioluminescent bacteria, *Vibrio fischeri* (a

recent taxonomic revision now calls the genus *Allivibrio*), have been one model for beneficial symbioses for over 25 years (McFall-Ngai, 2014). This model is used to understand host-bacterial interactions, host-symbiont specificity, and signaling between the innate immune system and symbiotic bacteria. *A. fischeri* is the only bacteria that can colonize the light organ in the bobtail squid (Rader and Nyholm, 2012). This high specificity has also been proposed in pyrosomes since their morphology includes light organs (Nealson et al., 1981).

Microbial symbionts occur in almost every organism, and have not been sufficiently studied (McFall-Ngai et al., 2013). They are widespread throughout the oceans and found in tropical and temperate coastal regions and throughout midwater and deep-sea habitats. The bacterial origin of luminescence is generally proposed on the basis of microscopic observation of bacteria in the light organ. Luminous bacteria are all Gram-negative, non-spore-forming, have cell walls difficult to penetrate, are motile, and are generally chemoorganotrophic (Dunlap, 2009). Bioluminescent symbiosis is fundamentally different that other types of symbiotic associations (Dunlap, 2009). With most bacterial mutualisms with flora and fauna, the host relies nutritionally on the bacteria, and without these symbionts, host growth suffers significantly (Dunlap, 2009). In bioluminescent symbioses, the host without bacterial symbionts has been found in laboratory settings to grow and develop at the same level as its counterparts with bioluminescent bacterial symbionts (Dunlap, 2009). Another difference in bioluminescent symbioses from other types is that most bacterial bioluminescent symbionts are extracellular whereas in obligate symbiosis the bacteria are found intracellularly (Dunlap, 2009). Even though most bacterial symbionts are extracellular, there are a few that appear intracellularly. The intracellular luminescent bacteria differ morphologically and biochemically from almost all other bacteria since they appear oval or as subspherical rods and without granules (Mackie and Bone, 1978).

Bacterial bioluminescence employs a specific mechanism that allows symbionts to produce light. The luciferase produced by the symbionts oxidizes reduced flavin mononucleotide and a long chain aldehyde, with energy released in the form of light instead of heat (Fig. 4) (Dunlap, 2009). Luciferins and luciferases are highly variable in their chemical structure (Schnitzler et al., 2012). Species differentiation and identification, especially in bacteria, is possible through studying luciferase kinetics. Different species of luminous bacteria can exhibit

similar or even the same cell density-dependent expression of luminescence, even though the auto-inducers (signaling molecules that are produced in response to changes in cell-population density) involved in the reaction are species-specific (Baldwin et al., 1989;Schauder and Bassler, 2001). The molecular mechanisms and gene arrangements of bioluminescent bacteria are unique, even though they exhibit similar patterns of bioluminescence control (Baldwin et al., 1989).

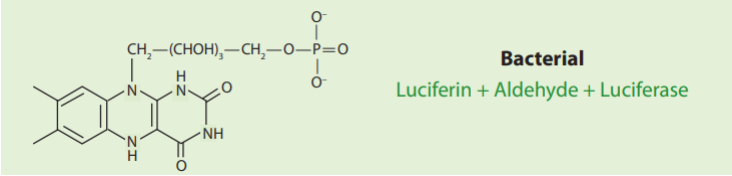

Figure 4. Molecular structure and mode of operation of bacterial luciferase (Haddock et al., 2010).

Luminous bacteria carry the *lux* genes (also referred to as *lux* operons) *luxCDABEG.* Bacterial luciferase is coded by the alpha and beta subunits, *luxA* and *luxB*, respectively. These genes have been found in three closely related *Gammaproteobacteria* families: Vibrionaceae, Enterobacteriaceae, and Shewanellaceae. Most luminous bacteria are from family Vibrionaceae, and mainly from the genera of *Aliivibrio*, *Vibrio*, and *Photobacterium*. These genera occur in the marine environment, and a few species form symbioses with fishes and squids (Dunlap and Urbanczyk, 2013). In deep-sea ceratioid anglerfishes, the esca (lure) microbial population is complex and can be composed of one of at least six species in the genera *Aliivibrio*, *Enterovibrio*, and *Photobacterium* (Hendry et al., 2018).

Morphological accounts symbiotic bacteria of luminous fishes describe bacteria as oval or sub-spherical rods, sometimes with conspicuous storage granules (Munk, 1998). Specifically, *Aliivibrio* and *Vibrio sp.* are round-bodied or small, straight, slightly curved or curved while *Photobacterium* are small, plump, and rod-shaped (Farmer and Hickman-Brenner, 2006;Farmer III et al., 2015). The known morphology of *Vibrio* and *Photobacterium* provides background for comparisons with pyrosome symbiont morphology. The bacteria-like cells in the light organ of *Pyrosoma* are intracellular, and may have undergone considerable biochemical specialization (Mackie and Bone, 1978). However, since these symbionts have not been successfully cultivated, little is known about the physiology of the microbial symbionts associated with bioluminescence. Haygood (1993) speculated that the bacterial symbionts in fishes may be highly specialized for the light organ environment, and consequently they are unable to compete in other environments.

The degree to which this specialization is similar in pyrosomes in terms of the organelles and symbionts involved is not known.

There are multiple ways to characterize bioluminescent bacteria including microscopy, molecular genetics, and decay kinetics. Through the use of decay kinetics, luminescent bacteria can be identified to the genus level. This is accomplished by analyzing the rate of turnover of the luciferase. The rate of turnover is dependent on the aldehyde present, so identification can only be made by measuring the luciferase decay (Leisman et al., 1980). *Photobacterium* has a fast decay, and extracted samples from *Pyrosoma sp.* have yielded luciferase activity with fast decay kinetics (Leisman et al., 1980). Much of the literature suggests the need for continuing work and utilizing molecular genetics to verify bioluminescent sources in pelagic organisms including pyrosomes (Mackie and Bone, 1978;Bowlby et al., 1990;Haddock et al., 2010;Widder, 2010). With improved technology and methodology, additional characterization is possible to resolve the question of whether the bioluminescence in pyrosomes is bacterial.

Tunicate Microbiome

The most extensively tunicate microbiome studied is from ascidians. Classical techniques, or culture dependent techniques, have shown that both bacteria and fungi can be isolated from these tunicates. Six bacterial phyla have been identified as well as three fungal phyla. These include Actinobacteria, Proteobacteria, Firmicutes, Cyanobacteria, Bacteriodetes, Verrucomicrobia, Ascomycota, Zygomycota, and Basidiomycota (Bauermeister et al., 2018). With next generation sequencing and methods based on metagenomics and community sequencing, Proteobacteria has been identified as the most abundant phylum in the ascidian microbiome. Classes Alpha- and Gammaproteobacteria are the most commonly detected while classes Beta- and Deltaproteobacteria are detected at lower abundances (Bauermeister et al., 2018). Studies have found that species-specific core-microbiomes are seen throughout all life stages, and different geographical locations of ascidian species from orders Aplousobranchia, Phlebobranchia, and Stolidobranchia. Four species in particular, *Ciona robusta, Ciona savignyi, Botrylloides leachi*, and *Botryllus schlosseri*, reinforce the concept that ascidians can foster defined microbiomes (Cahill et al., 2016). A study of *Didemnum fulgens,* has shown maternal vertical transmission of a stable and unique microbiome composed primarily of both Alpha- and

Gammaproteobacteria (Bauermeister et al., 2018). Little is known regarding the microbiomes of the other classes of tunicates, but none of the above encompass bioluminescent taxa.

Characterizing Microbial Bioluminescence

Microscopy

Microbial communities were first analyzed microscopically using methods related to laboratory cultured bacteria. Light microscopy is the simplest method to identify bacteria cell morphology using various staining techniques such as the Gram stain. The earliest record of use of light microscopy to identify microorganisms was by Antonie van Leeuwenhoek. He first described protozoa in 1675 and bacteria in 1683 by using only simple microscopes equipped with single uncorrected lenses that had short focal lengths (Barer, 1974). Today the compound optical microscope is commonly used in almost every microbiology laboratory and many have access to a variety of special optical microscopes, including electron microscopes (Barer, 1974). In light microscopy, the maximum upper magnification is 1000x. The resolution is limited by the wave nature of light. This limitation of magnification and resolution led to the development of the transmission electron microscope (TEM) by Ernst Ruska.

Today, standard TEM can achieve good resolution up to a magnification of up to a million times. The wavelength of electrons is about 100,000 times shorter than photons which allows for much higher magnification. However, TEM resolution is partially limited by spherical aberration. Scanning electron microscopy (SEM) resolution is about one order of magnitude lower than TEM, but still far higher than light microscopy. The SEM can image larger specimens such as those up to a few centimeters in size, while TEM images sections that are about 90 nanometers thick. Another advantage of SEM is that energy-dispersive X-ray spectroscopy (EDS) can be used while imaging a sample. EDS measures the energy of the x-rays emitted when electrons hit the sample which are elementally unique. Electron microscopy is a key technique that has allowed researchers to see atomic scale structures (Datye, 2003). These fine-scale techniques provide further evidence needed to characterize microbes.

Nearly 99% of bacteria are unculturable, so other techniques are needed beyond light and electron microscopy for microbial characterization. rRNA techniques have been employed to study and classify these elusive microorganisms (Woese, 1987;Krishnaveni et al., 2018). As

these methods have been improved and expanded upon, one of the most important is '*in situ* hybridization', which is particularly applicable to this study. In this case, rRNA of intact whole cells are targeted in their natural microhabitat (Amann et al., 1995). One of the most common '*in situ* hybridization' techniques used today for identifying microbial/microorganismal populations is fluorescence *in situ* hybridization (FISH). This method uses fluorescence microscopy, which is an optical microscope technique used to study both organic and inorganic materials. It is excellent for studying fluorescing material that either exhibits auto or secondary fluorescence. Autofluorescence occurs when a material fluoresces in its natural form. Secondary fluorescence happens when a material is treated with chemicals that are capable of fluorescing (Blackwelder, 2019). Fluorescence microscopy utilizes a fundamentally different approach than light microscopy. The sample is illuminated by light of a selected wavelength that causes fluorescence. The light emitted by fluorescence is longer than that of the wavelength of illumination. There are two filters used, one for excitation and the other for detection (Blackwelder, 2019).

These methods are universally applied to studying the microbial community. More specifically, FISH has been used globally to describe the temporal and spatial distribution of aquatic bacteria (Bouvier and Del Giorgio, 2003). Several examples include use for identification, enumeration, and localization of bacteria symbionts in gutless siboglinid tube worms and the gutless marine worm *Inanidrilus leukodermatus* (Schimak et al., 2012;Schimak et al., 2016). FISH and electron microscopy have been used to study the genus *Vibrio.* The genus *Vibrio* includes bioluminescent bacterial symbionts. FISH has been particularly helpful in this endeavor since these symbionts are "viable but not culturable" (Thompson et al., 2004). These studies have been successful in describing the spatial distribution of not only aquatic bacteria but in symbionts as well.

Whole Genome Sequencing and Analysis

Whole genome sequencing is the complete DNA sequencing of an organism's genome for accurate phylogenetic inferences that allow for selection of the most informative gene set (Lewin et al., 2018). On average, a bacterial genome is about 3 - 5 million base pairs and encodes around 5,000 proteins (Land et al., 2015). Luminous bacteria have the genome size typical of their non-symbiotic and free-living relatives (Baker et al., 2019). Within these genomes, the key genes to identify are the *lux* genes. Bacterial *lux* genes over time have become useful for taxonomic and phylogenetic analysis of luminous bacteria (Urbanczyk et al., 2011), which in this study will be useful for characterizing the symbionts. The *lux* genes *luxCDABEG* are found in all luminescent bacteria and are responsible for coding the luciferase subunits (Dunlap, 2009). If these genes, at minimum *luxA* and *luxB,* can be identified through sequencing it would provide evidence of luminescent bacteria residing in the pyrosome (Pace, 1997;Urbanczyk et al., 2011;Dunlap and Urbanczyk, 2013).

16S rRNA Bacterial Systematics

The small subunit ribosomal ribonucleic acid (SSU rRNA) can be characterized to determine the potential source of microbial bioluminescence. The 16S rRNA molecule is the smallest of the two major RNA components of the ribosome and has emerged as a reliable tool for phylogenetics and molecular ecology. For example, phylogenetics can utilize the 16S rRNA gene to build trees that can be considered a rough map of the evolution of the genetic core of cellular lineages (Pace, 1997) or use the 16S rRNA gene to identify how algal communities and nutrient pollution affect coral microbiomes (Zaneveld et al., 2016). These SSU rRNAs are present in all living organisms, and are functionally constant and highly conserved (Sfanos et al., 2005). Bacterial taxonomic identification can be accomplished through numerous methods, but the most modern is utilizing high-throughput sequencing (HTS), which is also referred to as next generation sequencing (NGS) of the 16S rRNA gene (Pace, 1997;Thompson et al., 2017). It is the most common housekeeping genetic marker in bacteria, and utilized for a variety of reasons, including the fact that it is present in almost all bacteria. It also exists as a multigene family(also referred to as a "multigene operon"), the function of the gene is conserved over time, and its sequence composition is long enough for information purposes (Janda and Abbott, 2007). Bacteria are considered different species if they share less than 97.5% 16S rRNA sequence similarity and different genera if they share less than 93% sequence similarity (Sfanos et al.,

2005). The characteristics of the 16S gene make it a viable candidate for sequencing and developing FISH (fluorescence *in situ* hybridization) probes (Thompson et al., 2004;Negandhi et al., 2010).

The Lopez Microbiology and Genetics Laboratory at Nova Southeastern University has employed molecular genetics including 16S rRNA methods to identify bacteria and bacterial communities from a wide variety of organisms and habitats (Cuvelier et al., 2014;Hughes et al., 2018). Such methods have been utilized in describing the dynamics of bacterial communities in coastal waters and variation in the microbiome of coastal waters along the South Florida's Atlantic coast and in sponges found on the reef tracts (Lopez, 2019). In these earlier studies, six localities were examined and the microbiome was profiled using high-throughput sequencing of the 16S rRNA (Campbell et al., 2015;Freed, 2018). Similar to the work of Campbell and colleagues, the Port Everglades Inlet microbiome was characterized using high throughput sequencing using the 16S rRNA gene (Campbell et al., 2015;O'Connell et al., 2018). The 16S rRNA gene is also useful in lower throughput taxonomic surveys for microbial diversity found in deep-water marine invertebrates (Sfanos et al., 2005). In addition to invertebrates, the 16S rRNA gene was used in the characterization of the bioluminescent symbionts from ceratiids (deep-sea anglerfish) (Freed, 2018). Based on all the previous research conducted in the Lopez Laboratory, the best path determined to identify the bacterial symbionts within *P. atlanticum* was to utilize the 16S rRNA gene in conjunction with different microscopy techniques. This approach facilitates addressing the following hypotheses.

Hypotheses

The main goal of this project is to identify and characterize the holobiont, which is host and bacterial symbiont taxa, responsible for bioluminescence in *Pyrosoma atlanticum.* In addition, the following hypotheses will be addressed.

I. H_1: Bioluminescence is bacterial based in the pyrosome, *P. atlanticum.*

- **a.** H_O: Bioluminescence is not bacterial based but is induced by some other mechanism.

II. H_2: If present, bioluminescent bacterial symbionts are located intracellularly in the luminous organ of *P. atlanticum*.

a. H_O: Bioluminescent bacterial symbionts are not located intracellularly in the luminous organ of the *P. atlanticum.*

III. H_3: The *Pyrosoma atlanticum* bioluminescent symbiont community will be relatively simple and homogeneous compared to the surrounding environment, with low species richness dominated by just a few bacterial taxa.

a. H_O: The bioluminescent symbiont community will be heterogeneous with more than 5 bacterial taxa indication a high microbial abundance distribution.

Materials and Methods

Sample Collection and Fixation

The samples were collected with the help of the Deep Pelagic Nekton Dynamics of the Gulf of Mexico (DEEPEND) consortium. In 2017, a number of midwater trawls were conducted on DEEPEND Cruise DP05, during which various species of fish, crustaceans, cephalopods, and other pelagic species were collected from the Gulf of Mexico. Among those was *P. atlanticum* (Fig. 5, 6). Thirty samples were stored in 1.5 mL tubes and stored in a -80°C freezer as well as 5 individuals in dimethyl sulfoxide (DMSO) in the Lopez Microbiology and Genetics Laboratory at Nova Southeastern University. In addition to these 2017 samples, 29 more samples were collected from the Gulf of Mexico on the July 2018 DEEPEND Cruise DP06. Samples were collected from depths of 0-1500 meters at multiple collection sites for both cruises. These samples were stored in either a 2% Glutaraldehyde in Sodium Cacodylate Buffered Sea-water fixative for EM or RNALater in 45 mL Falcon tubes for genetic study. In 2019, an additional 12 *P. atlanticum* samples in the Gulf of Mexico were collected during the NOAA DeepSearch Cruise aboard the R/V Point Sur (Fig. 7). These samples were stored in 2% Glutaraldehyde in Sodium Cacodylate Buffered Sea-water fixative, paraformaldehyde in 4% PBS (phosphate-buffered saline), or RNALater. A total of 15 samples from 3 cruises to utilize for the several methodologies employed in this study (Table 1).

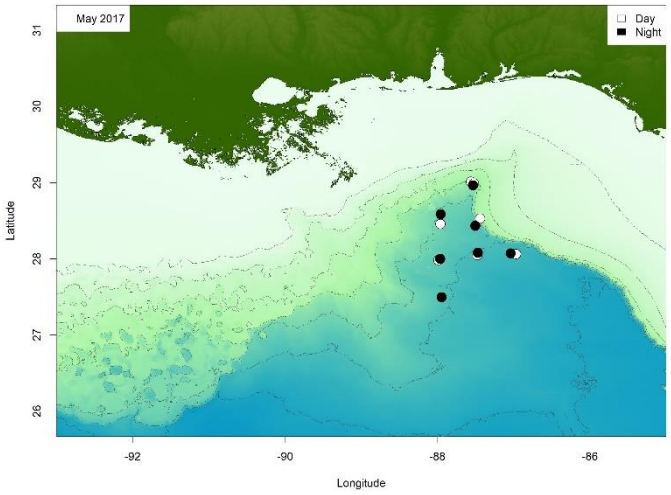

Figure 5. Map of DP05 Cruise collection sites for *Pyrosoma atlanticum.* Courtesy of Dr. Rosanna Milligan.

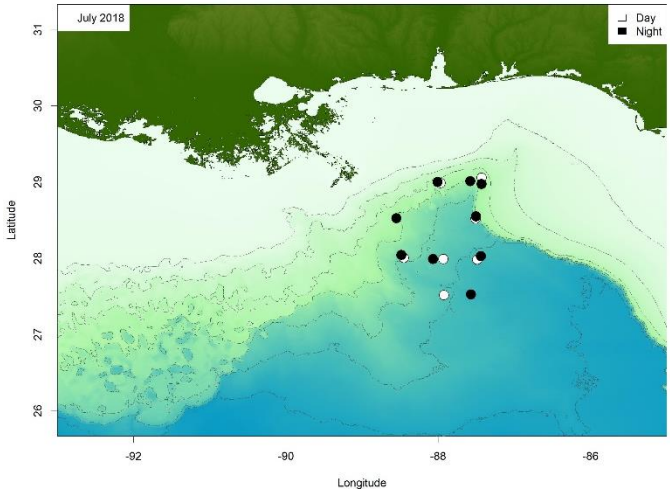

Figure 6. Map of DP06 Cruise collection sites for *Pyrosoma atlanticum.* Courtesy of Dr. Rosanna Milligan

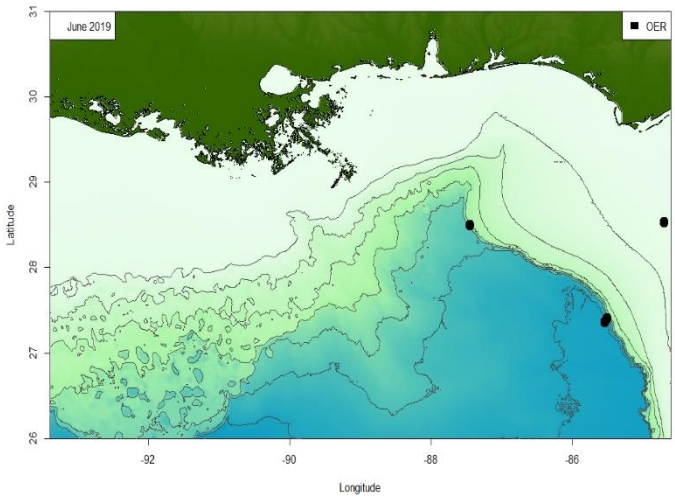

Figure 7. Collection site (red) of R/V Point Sur for NOAA DeepSearch Research Cruise in June 2019.

Table 1. Collection Data from the 15 samples used from all three research cruises with DEEPEND and NOAA - DP05, DP06, OER.

Sample ID	Sample Type	Count	Cruise Designation	Sample Date	Start Lat	Start Lon	Trawl Depth (m)	Protocol Used
RNALater6	RNALater	1	DP06-25JUL18-MOC10-B250N-108-N0	25-Jul-18	27°59'21.588"N	88°30'36.612"W	0-1503	16S Sequencing & Genome Sequencing
RNALater7	RNALater	1	DP06-26JUL18-MOC10-B250D2-109-N0	26-Jul-18	27°59'27.6"N	88°30'20.412"W	0-1504	16S Sequencing & Genome Sequencing
DMSO1	DMSO	1	DPO5-02MAY17-MOC10-B082N-085-N0	2-May-17	28°0'58.5612"N	88°2'53.98"W	0-1500	16S Sequencing & Genome Sequencing
PYRG1_6.19	Gluteraldehyde	1	15JUN19-OER2019T07	15-Jun-19	27°21'47" N	85°31'93" W	0-1200	TEM & SEM
PYRG2_6.19	Gluteraldehyde	1	15JUN19-OER2019T07	15-Jun-19	27°21'47" N	85°31'93" W	0-1200	TEM & SEM
PYRG3_6.19	Gluteraldehyde	1	15JUN19-OER2019T07	15-Jun-19	27°21'47" N	85°31'93" W	0-1200	TEM & SEM
PYRG4_6.19	Gluteraldehyde	1	15JUN19-OER2019T07	15-Jun-19	27°21'47" N	85°31'93" W	0-1200	TEM & SEM
PYRP1_6.19	Paraformaldehyde	1	15JUN19-OER2019T07	15-Jun-19	27°21'47" N	85°31'93" W	0-1200	Fluorescence in situ hybridization
PYRP2_6.19	Paraformaldehyde	1	15JUN19-OER2019T07	15-Jun-19	27°21'47" N	85°31'93" W	0-1200	Fluorescence in situ hybridization
PYRP3_6.19	Paraformaldehyde	1	16JUN19-OER2019T09	16-Jun-19	27°23'67" N	85°30'56" W	0-1200	Fluorescence in situ hybridization
PYRP4_6.19	Paraformaldehyde	1	16JUN19-OER2019T09	16-Jun-19	27°23'67" N	85°30'56" W	0-1200	Fluorescence in situ hybridization
PYRRNA1_6.19	RNALater	1	16JUN19-OER2019T09	16-Jun-19	27°23'67" N	85°30'56" W	0-1200	DNA Extraction
PYRRNA2_6.19	RNALater	1	17JUN19-OER2019T10	17-Jun-19	28°29'34" N	87°27'14" W	1000-1500	DNA Extraction
PYRRNA3_6.19	RNALater	1	17JUN19-OER2019T10	17-Jun-19	28°29'34" N	87°27'14" W	1000-1500	DNA Extraction
PYRRNA4_6.19	RNALater	1	18JUN19-OER2019T10	18-Jun-19	28°31'58" N	84°42'27" W	0-200	DNA Extraction

Microscopy

Light Microscopy (Histology)

Samples were fixed in 2% Glutaraldehyde in Sodium Cacodylate Buffered Sea-water fixative. They were placed in 70% EtOH overnight and processed through a graded series of ethanols, cleared, and infiltrated with molten *Paraplast Plus*®, and embedded in *Paraplast Xtra*®. Using a Leica RM 2125 microtome, 4 μm thick sections were cut and mounted on microscope slides. Sections were then stained with Harris's hematoxylin and eosin. Slides were examined using an Olympus BX43 light microscope at 4–60x magnification.

Fluorescence in situ hybridization (FISH)

Pyrosome (*P. atlanticum*) samples were stored in paraformaldehyde and dehydrated through an ethanol series, cleared in xylenes, and infiltrated with paraffin. Serial sections were cut at 4 μm and 8 μm and mounted. They were then deparaffinized with xylene and ethanol series (100-70%). After mounting the sections, specialized probes were added to localize the bacteria within the light organs of the pyrosome. These probes were designed by using MAFFT, or the Multiple Alignment using Fast Fourier Transform program (Katoh and Standley, 2013). MAFFT utilized the 16S rRNA sequence of *Photobacterium sp. r33* (referred to as *Photobacterium Pa-1)* from the Illumina MiSeq run, combined with previously determined 16S sequences from various bacterial species (DQ889917, DQ889916, DQ889915, DQ889914, DQ889913) from NCBI database to find the most specific V4 region of *Photobacterium Pa-1* for the probe to identify bioluminescent symbiont location within the pyrosome zooid (Table 2).

MAFFT aligns the 16S rRNA sequences from the selected samples. The *Photobacterium* sequence, TTCAGGTGTAGCGGTGAAATGC, was chosen because it was the most variable region in the alignment. This signifies that there is no overlap in this sequence with the various bacterial sequences chosen for this alignment. The high specificity is required in order to highlight just the *Photobacterium* in the samples. The probes were then tested on NCBI PROBE Database (www.ncbi. nlm.nih.gov/probe) and Microbial Ribosomal Databases Probe Match (http://rdp.cme.msu.edu/probe match/search.jsp) (Negandhi et al., 2010).

The dye used for the *Photobacterium* probe was Cy3, which is a standard orange-fluorescent label for nucleic acids and was attached at the 5' end (Table 3). The control probe EUB338 is a universal bacteria probe and was dyed with 6-FAM (fluorescein). FAM

(fluorescein) is the most commonly used fluorescent dye attachment for oligonucleotides and this particular dye was attached at the 3' end and will appear green. The probes attach to one end or the other to allow for overlap. This is possible because the two probes' nucleotide sequences are at different location on the ribosome (either the 5' or 3' end). When imaging the samples, only orange and green fluorescence should appear, and red fluorescence should be excluded due to double binding. This means both probes should bind to the targeted *Photobacterium sp.* which will present the orange fluorescence with the rest of the bacteria appearing green.

Table 2. Bacteria used to develop target FISH probe for *Photobacterium sp. r33* accession numbers from NCBI.

Species Used	**Accession Number**
MiSeq *Photobacterium sp. r33*	N/A
Uncultured *Cytophaga sp*. clone EC64	DQ889917
Uncultured *Vibrio sp*. clone EC66	DQ889916
Uncultured beta proteobacterium clone EC67	DQ889915
Uncultured beta proteobacterium clone EC69	DQ889914
Uncultured alpha proteobacterium clone EC75	DQ889913

Table 3. FISH probe sequences and dye used to identify the *Photobacterium* in samples.

Probe	**Sequence with TAG**	**Base Pairs**	**5' or 3' Attachment**	**Absorbance Max**	**Emission Max**
Photobacterium sp.	/5Cy3/TTCAGGTGTAGCGGTGAAATGC	22	5' End	550 nm	564 nm
EUB3338	GCTGCCTCCCGTAGGAGT/36-FAM/	18	3' End	495 nm	520 nm

After the designing and testing probes, hybridization buffer (35% formamide) was made. The hybridization buffer contains 360 µl 5M NaCl, 40 µl 1M Tris-HCl, 700 µl formamide, 900 µl H_2O, and 2 µl 10% SDS. Once made, 45 µl of hybridization buffer was mixed with 5 µl of the desired probe (5 ng/µl), for a total of 50 µl per slide. Pyrosome tissues were then incubated inside a humidity chamber with a paper towel that was moistened with the hybridization buffer for 2 hours at 46°C. After hybridization, slides were put in a buffer wash for 20 minutes at 48°C (buffer consists of 700 µl 5M NaCl, 1 ml 1M Tris-HCl, 500 µl 0.5 EDTA, 50 ml H_2O, and 50 µl 10% SDS). Slides were quickly rinsed with dH_2O and air dried.

As in Negandhi et al (2010), two control runs were carried out in order to test for non-specific binding of the probes. FISH was performed on three blocks with two sections each. The control runs utilized probe EUB338. In addition to the control, slide with no probes as well as slides with both EUB338 and *Photobacterium* probes were run. This allowed for an autofluorescence assessment and aided in eliminating background noise. Slides were examined using an Olympus IX70 Fluorescence Microscope with green (500-570nm) and red (610 ~750nm) filter cubes.

Scanning and Transmission Electron Microscopy (SEM & TEM)

SEM samples were stored in a 2% glutaraldehyde in sodium cacodylate buffered seawater fixative. Pyrosomes were dissected in the fixative and divided into three sections per sample. They were rinsed three times in sodium cacodylate buffered sea water, postfixed in 1% osmium tetroxide, rinsed in the sea water buffer, dehydrated through a graded series of ethanol (20, 50, 70, 95, and 100%), and dried in hexamethyldisilazane (HMDS). Dried samples were outgassed overnight, coated with palladium in a sputter coater, and examined in a Philips XL-30 Field Emission SEM at the University of Miami Center for Microscopy (UMCAM) located in the Chemistry Department at the University of Miami Coral Gables Campus.

TEM samples were prepared similarly to SEM except that samples at the last dehydration step (100% ETOH) were embedded in Spurr resin and polymerized for 3 days at 60°C. Blocks were trimmed, sectioned, floated onto grids, stained with either Uranyl Acetate and/or Lead Citrate and examined in a JEOL 1400X TEM located at the University of Miami Miller School of Medicine TEM Core Lab. Semi-thin sections of TEM prepared samples were examined in an IX-70 fluorescent microscope to examine gross structures.

Sequencing Methods

DNA Extraction and Polymerase Chain Reaction (PCR)

Microbial DNA was extracted from tissues stored in RNALater and DMSO using the standard protocol for the MO BIO PowerLyzer PowerSoil kit. The Polymerase Chain Reaction (PCR) is the repeated copying of a selected region of a DNA molecule (Brown, 2007). Since

almost all of 16S sequence data are products of PCR amplification of the 16S rRNA gene that uses between 15 and 25 nucleotide primers (Tringe and Hugenholtz, 2008), this study focused on amplifying the 16S gene of the unknown bacteria in the luminescent organ of the pyrosome. Once DNA extractions were completed, PCR was run using Invitrogen Platinum Hot Start PCR Master Mix (2x) and the universal primers 515F and 806R.The 515F and 806R primers were used to amplify the 200bp sequence of the V3 and V4 region of the 16S gene (Caporaso et al., 2011;Easson and Lopez, 2019). Another 1% agarose gel was run to ensure successful PCR products were produced. The PCR products were cleaned via AMPure XP beads. This process was used to purify the 16S V3 and V4 amplicon away from free primers and primer dimer species. (Chakravorty et al., 2007). The final DNA concentration was checked using a Qubit2.0 (Life Technologies). Attempts were made to isolate the light organ for a purer sample using laser capture microdissection, however, they did not work (Appendix 1 for more information).

Illumina High- Throughput Metagenomic Sequencing

The 16S rRNA gene fragment is the target for this section of high throughput sequencing (Easson and Lopez, 2018;O'Connell et al., 2018). Samples were prepared for sequencing following the 16S Illumina Amplicon Protocol per the Earth Microbiome Project (Kuczynski et al., 2011;Thompson et al., 2017). The final PCR products were checked for their DNA concentrations using a Qubit 2.0, which is a fluorometer created to precisely measure nucleic acids or proteins. Once concentrations were obtained, each sample was diluted to a normalization of 4pM. All DNA samples were library pooled and rechecked on the Qubit to make sure the concentration is between 4-6 ng/μL. A final quality check was done using an Agilent Bio analyzer Tapestation 2000, which checks the quality of the DNA and for any possible contamination. The tape station analysis checks the quality of DNA and for potential contamination. The final product was loaded into an Illumina MiSeq system for 16S metagenomics DNA at 500 cycles. The sequencing followed a modified Illumina workflow protocol.

Sequencing and Symbiont Analysis: QIIME2& CosmosID

The Quantitative Insights into Microbial Ecology v.2 (QIIME2) pipeline was used to demultiplex, quality filter, assign taxonomy, reconstruct phylogeny, and produce diversity analysis and visualizations from the FASTQ DNA sequence files (Caporaso et al., 2010). The quality filtering and trimming of the data was conducted in DADA2, which was used to create a feature table that was utilized in R Studio. The QIIME2-generated sequences were assigned taxonomy through a learned SILVA classifier (silva-132-99- 515-806-nb-classifier.qza). This feature table was used for SIMPER statistical analysis in R Studios. A SIMPER analysis was used to determine which taxa are driving the differences in the water and pyrosome samples (Rees et al., 2004). Additional comparisons were made in CosmosID, a bioinformatic pipeline used for microbial analysis that employs a phylogenetic and k-mer based approach to metagenomics. FASTQ files were uploaded to the CosmosID.com analysis platform, which provided various statistical tests such as, Chai alpha diversity estimates, PCoA, and beta diversity relative abundance counts visualized in a heatmap comparison. Further data analysis used 16S rRNA alignments with MAFFT (Katoh and Standley, 2013) in order to generate a phylogeny to compare the extracted 16S sequence from the MiSeq run with known luminescent bacterial species. Pyrosome microbiome sequences have been deposited to the NCBI Sequence Read Archive (#PRJNA636187).

Genome Sequencing and Analysis

For genome sequencing, the Illumina Nextera XT DNA Sample Prep Kit was used for library preparation. A final quality check was done using an Agilent Bio Analyzer Tapestation 2000 as well. The Illumina MiSeq was used for sequencing, running samples at 300 cycles (for 150 bp library) due to the small library sizes of 254 and 292 bp. For genome assembly and annotation, Galaxy and Blast2Go were utilized (Götz et al., 2008;Afgan et al., 2018).

Results

Structure and Morphology of the Light Organ: Light and Fluorescence Microscopy

The focus for light and fluorescent microscopy was to identify the *P. atlanticum* luminous organ, and image morphology as well as any potential microbes observed. The FISH methodology was additionally utilized to employ genomic techniques to visually identify the bacteria present and discriminate their location within the pyrosome light organ and tissue. Due to their relatively fixed location in the tissue, it was straightforward to determine where the organs were in thin section, and structural features were evident even in unstained sections. The light organ and bacteria were well resolved under light microscopy, with the buccal siphon and the light organs, located on each side, clearly identified (Fig. 8). The left and right light organs were usually fully intact (Fig. 8, 9) with the 30-50 µm luminous organ well resolved (Fig. 10). The light organs were oval shaped structures, with each exhibiting a nodule at the end. Within the light organ, there was a clear space in the center, with the bacteria clustered around the interior. At higher magnification, it is evident that what appear to be bacteria are clustered in the light organ with as many as 72 individual bacteria or more likely bacteriocytes evident in a single light organ (Fig. 10).

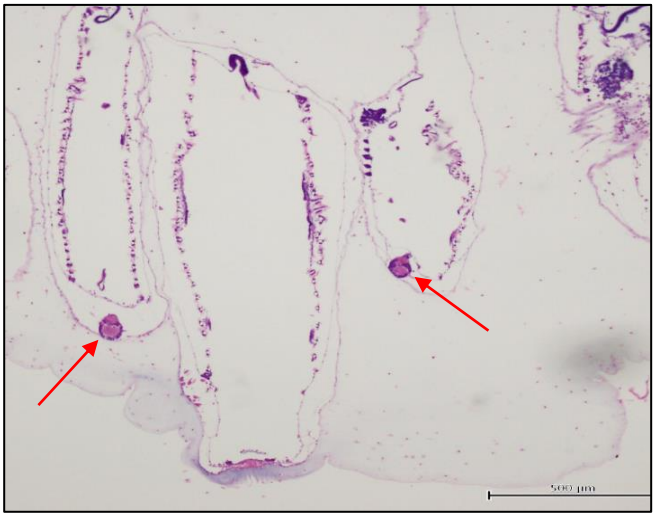

Figure 8. Orientation of both light organs (red arrows) on either side of buccal siphon.

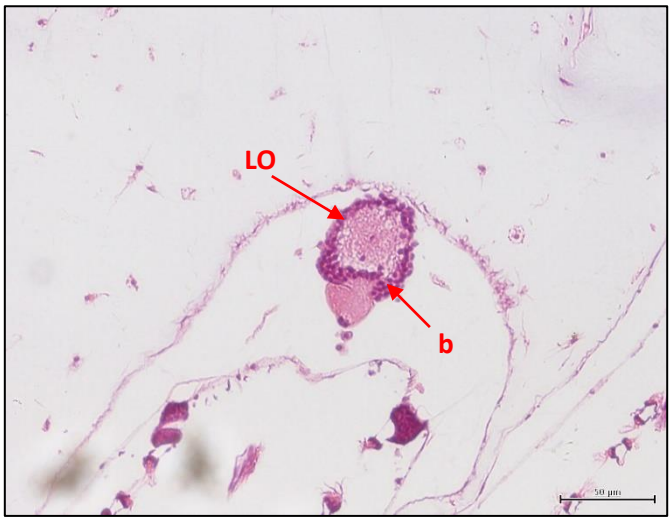

Figure 9. Higher magnification of individual light organ (LO) with bacteria (or more likely bacteriocytes) (b).

Figure 10. Individual light organ (LO) with bacteria or bacteriocytes (b) found intracellularly with a clear space in the middle.

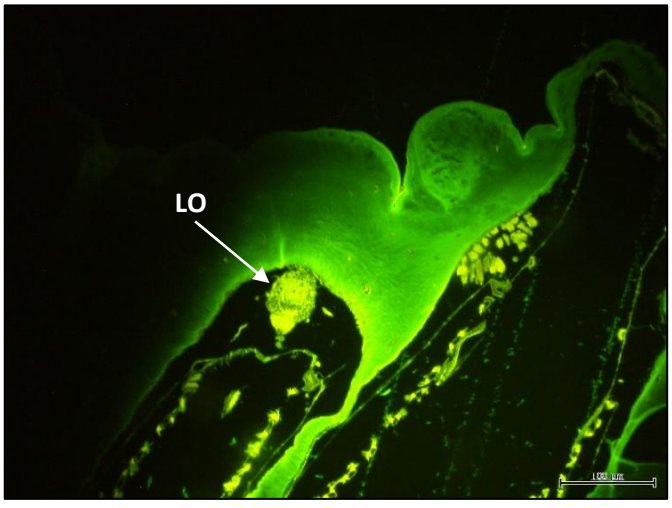

Figure 11. Light organ (LO) on the left side of the buccal siphon.

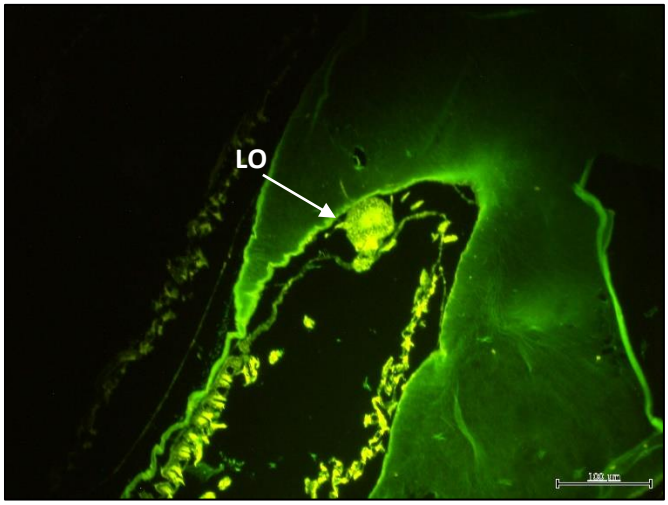

Figure 12. Light organ (LO) on the right side of the buccal siphon.

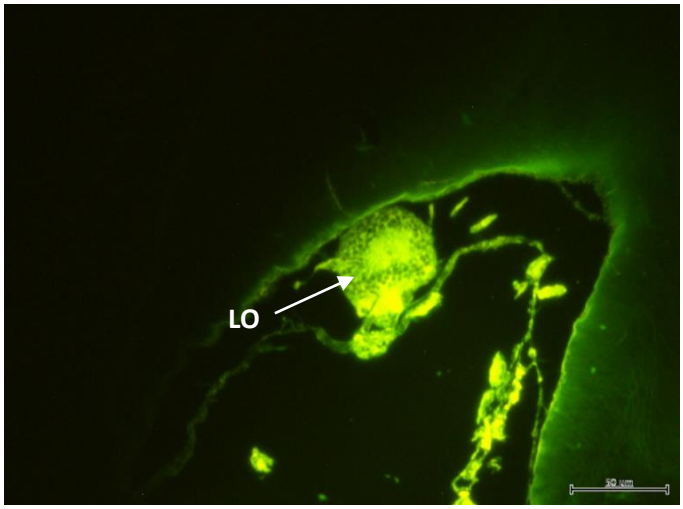

Figure 13. Higher magnification of the right light organ (LO) with bacteria seen on the outer portion of the organ, with clear space in the middle in the left luminous organ.

Fluorescence *in situ* Hybridization (FISH)

Under fluorescence microscopy, the pyrosome exhibited a considerable amount of autofluorescence (Figs. 11,12,13). However, the bacteria were clearly discernable (Fig. 13). If histology sections are compared with those prepared for FISH analyses, similar orientation, and morphology of the two light organs is evident (Fig. 14a and b). Shown in both methodologies are the putative "bacteriocytes" containing bacteria concentrated at the outer edges of the organ with a clear space in the center. This also suggests that the light organ is hollow, at least without discrete cells.

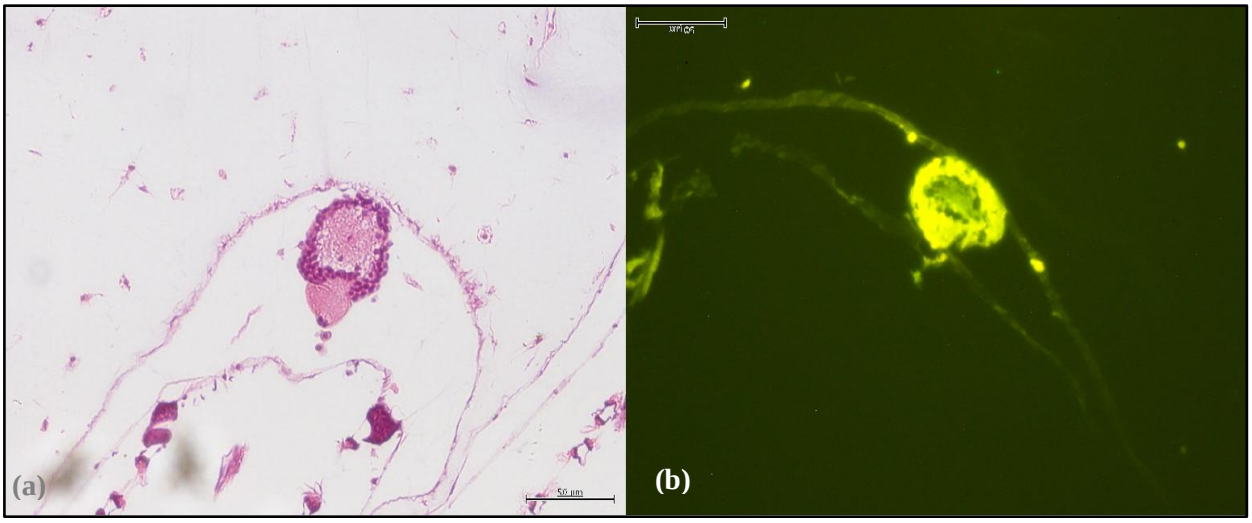

Figure 14. Light micrograph of Hematoxylin and Eosin stained light organ (a). FISH section of both EUB338 and *Photobacterium* probe attached to the light organ (b). Scale bar = 50 µm.

In light microscopy, the oval organ can be seen anchored to part of the tunic with the concentrated bacteria or "bacteriocytes" distributed in the interior surface (Fig 15a). When FISH was employed, the light organ section exhibited additional interior structures. The only bacteria fluorescing is *Photobacterium Pa-1*. around the outer edges. The probe produced a more yellow/yellow orange signal than expected (Fig. 15b).

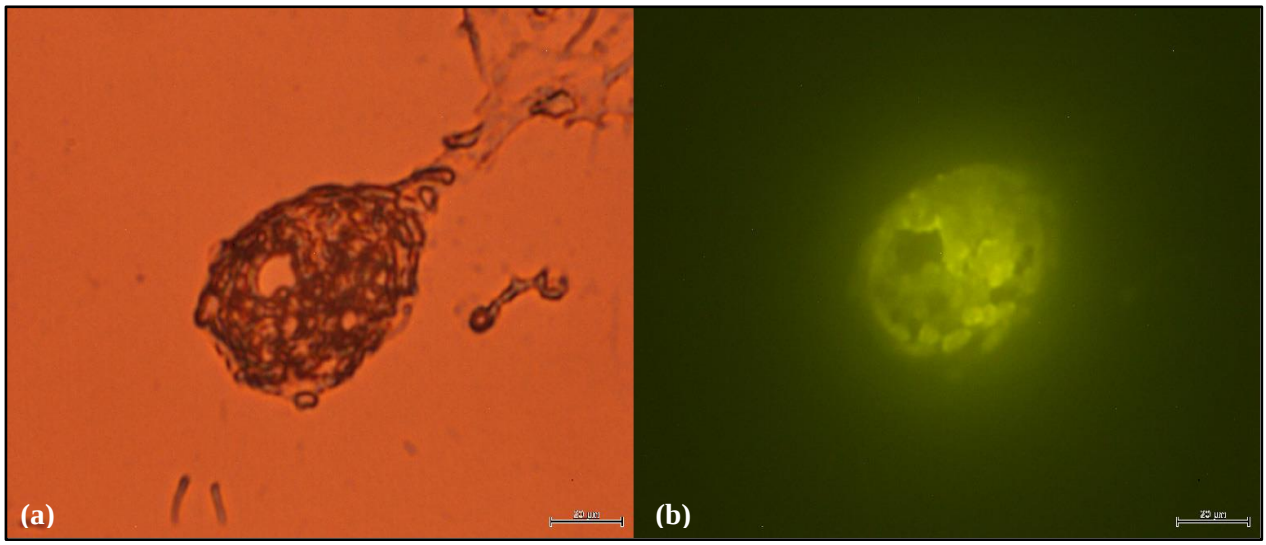

Figure 15. Light microscope image of the light organ (a) compared to Cy3 labeled *Photobacterium* probe (b). Scale bar = 20 µm.

Controls included pyrosome sections that was incubated with no fluorescent probes. The control sections reflected native background autofluorescence and did not display the degree of fluorescence seen in sections hybridized with probes (Fig. 16a). This comparison shows that the probes appear to be annealing specifically to their respective DNA targets and producing a signal

after stringent washing. The pair of light organs illuminated without a probe, but not as brilliantly as when the EUB338 and *Photobacterium* probes were used (Fig. 16a and b). The signal produced with both probes was very intense and, as anticipated, bacteria other than those in the light organ, can be seen emitting a signal. Due to the light intensity, the shutter on the microscope was partially closed for the sections hybridized with probes while the sections with no probes were imaged with the shutter remain fully open.

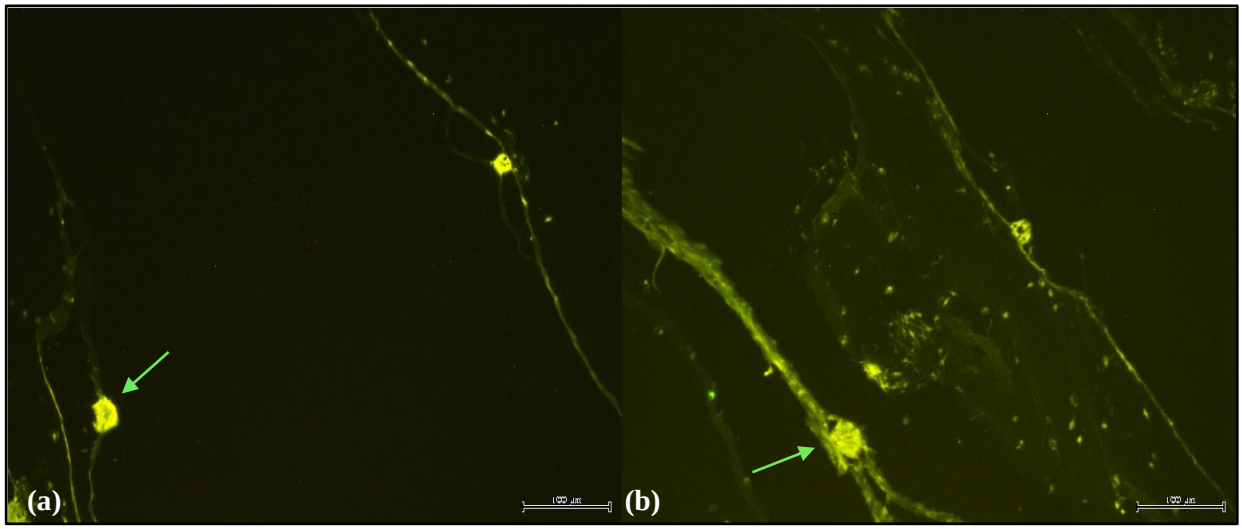

Figure 16. The light organs (green arrows) with no probe and the shutter wide open (a) vs. 4 µl of both EUB338 and *Photobacterium* probe with the shutter partially closed (b). Scale bar = 100 µm.

The sections hybridized with just the general EUB338 probe exhibited intense signals as well (Fig. 17). The light organ fluoresced using both green and red filters (green = 500-570nm, red = 610~ 750nm). The bacteria are more discernable using the green filter and were concentrated at the outer edges of the organ and throughout the tunic. When the red filter was used, the signal was intense as well, and the bacteria can still be seen concentrated towards the edges, but not as clearly (Fig. 17). However, the EUB338 probe does not discriminate between the *Photobacterium* and other bacteria found within the pyrosome or even within the area surrounding the light organ.

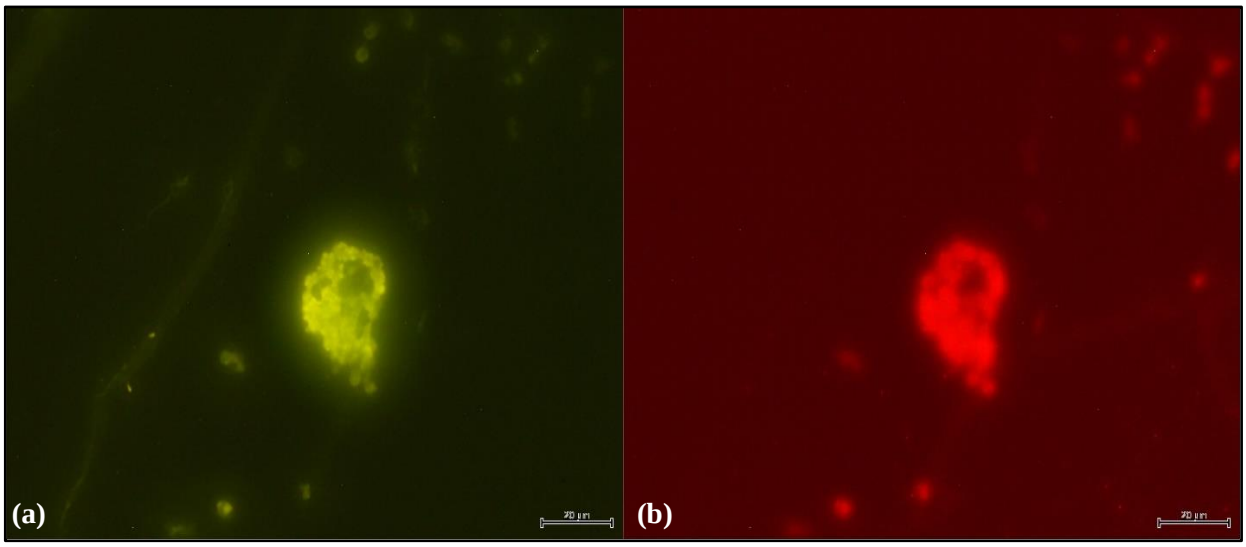

Figure 17. Green (a) vs. red (b) filters of a section with the EUB338 probe attached to the light organ (LO). Scale bar = 20 μm.

The EUB338 probe is designated as the universal bacteria probe and is designed to bind to almost all bacteria within the sample. As expected, the fluorescent signal is apparent not only in the light organ, but also in surrounding tissue as well (Fig 18a). Most bacteria emit a slightly green signal. The morphology of bacteria is different in the tissue throughout the section, ranging from coccoid in the light organ, to bacterium with flagella-like structures in the tunic. When the *Photobacterium* probe was employed, only the light organ emitted a signal (Fig. 18b). Other areas of the tunic do not emit a signal, confirming that the photobacteria were concentrated in, and were not present outside, the light organ.

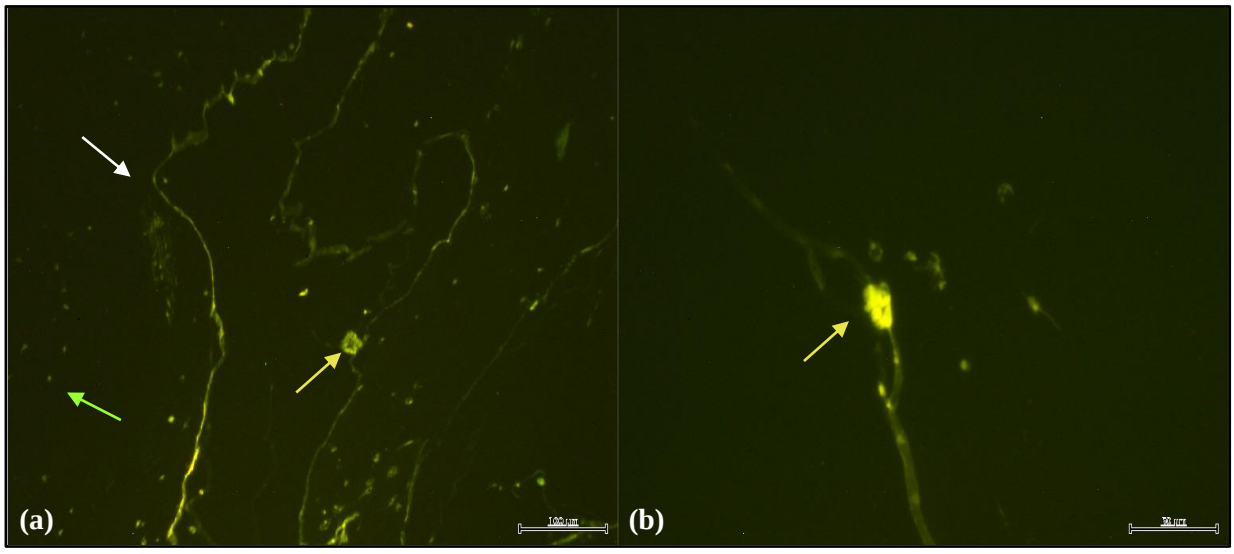

Figure 18. EUB338 probe (a) vs. *Photobacterium* probe (b). The EUB338 probe binds to many bacteria (green arrow) within the tunic (white arrow) and the light organ (yellow arrow). In contrast, the *Photobacterium* probe only illuminated the light organ. Scale bar = 100 μm and 50 μm, respectively.

When the EUB338 and *Photobacterium* probes were combined, variability in the intensity of signal emission was evident. *Photobacterium Pa-1.* was brightest when both probes were combined. For example, under the green filter, the bacteria are seen as in previous observations, concentrated around the outer edges of the light organ with a clear space in the center (Fig. 19). When the red filter is used, the same outer edges are packed with *Photobacterium Pa-1.* fluorescing orange (Fig. 19b). This orange fluorescence confirms the presence of *Photobacterium Pa-1* in the light organ.

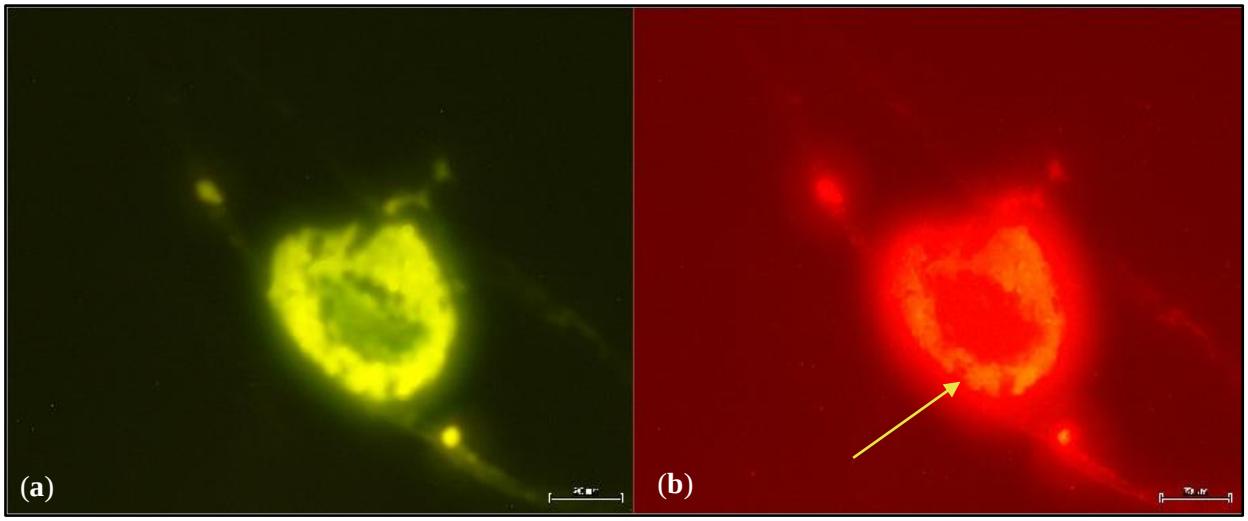

Figure 19. EUB338 and *Photobacterium* probes in green (a) vs. red (b). The orange fluorescence in *Photobacterium Pa-1.* is found exclusively concentrated around the edges of the light organ (yellow arrow). Scale bar = 20 μm.

Fine Structure and Bacterial Cluster Location in *P. atlanticum* (SEM)

SEM was utilized to discern high resolution three dimensional fine structural details of *P. atlanticum* and the bacteria associated with the light organ. Confirmation of observations made in the light microscopy and FISH analysis described in the previous section was a goal of this analyses. Fine structural details of the gill basket and tunic (Fig. 20) were important to examine in order to orient zooids and possible light organs. Areas were observed that were adjacent to zooids which contained intracellular clusters of cells approximately 1-2 microns in diameter and were morphologically similar to bacteria (Fig. 21, 22, 23). The openings of each zooid contain numerous bacterial clusters (Fig. 21), and higher magnification shows the clusters packed together (Fig. 22). Previous studies have questioned whether the luminescent bacteria are

intracellular or extracellular. SEM images suggest bacterial clusters are located intracellularly, since a cell membrane was evident covering the clusters (Fig. 24, 25).

During SEM analysis, crystals were observed in the pyrosome tissue which were similar to descriptions in the literature of paracrystalline bodies. These have been described as associated with luminescence in invertebrates (Thuesen et al., 2010). The crystals found around the bacterial clusters exhibit intricate formations (Fig. 24, 26, 27), in which each crystal is approximately 50-60 μm in length (Fig. 24, 27). These crystals are similar in size to the hemihydrates found in the bioluminescent deep-sea medusae (Tiemann et al., 2002). Energy Dispersive X-Ray Spectroscopy (EDS) of the structures indicates they contained the elements calcium and sulfur, suggesting they are composed of the mineral gypsum (Fig. 28). Calcium and sulfur have been seen associated with other crystalline structures in bioluminescent organisms (Liu et al., 2000). In some cases, the light organ was located intact within parts of the tunic, with crystalline structures near the bacterial clusters (Fig. 29). Bacterial clusters in some specimens shown in the literature exhibit a more scattered pattern (Nyholm and McFall-Ngai, 1998), which is different from our observations of clusters of bacteria in the light organ of *P. atlanticum* which exhibited a more organized distribution (Fig. 25).

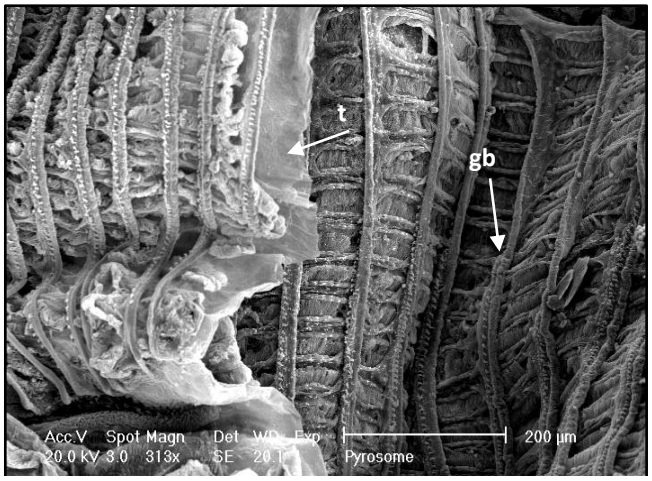

Figure 20. *Pyrosoma atlanticum* tunic structure with gill basket (gb) and tunic (t) present.

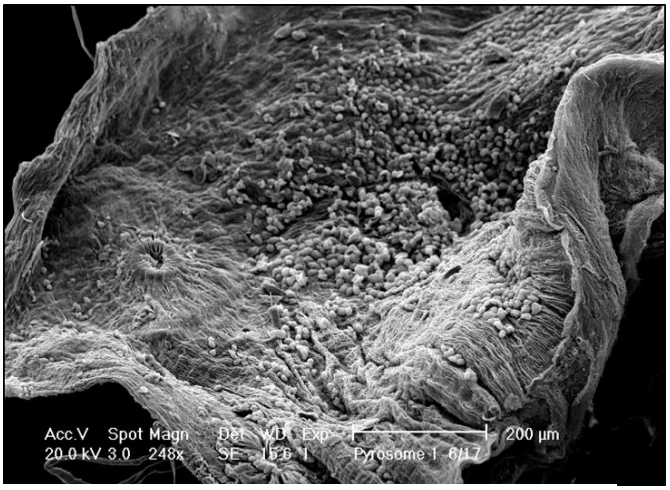

Figure 21. Bacterial clusters detached from the tetrazooids.

Figure 22. Higher magnification of bacterial clusters in the zooid.

Figure 23. Single opening of zooid with bacterial clusters populating the area.

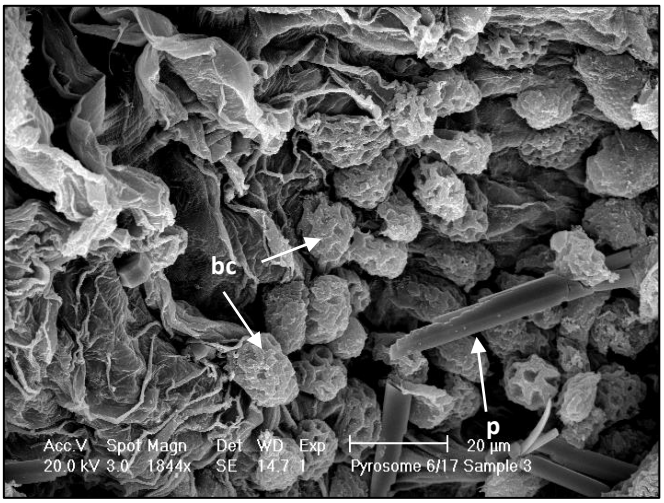

Figure 24. Bacterial clusters (bc) and paracrystalline (p) structures are present.

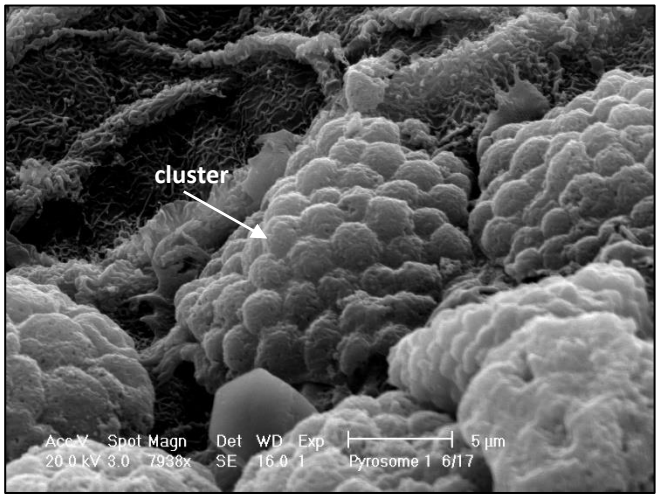

Figure 25. High magnification of an intact bacterial cluster in a bacteriocyte cell. Clusters range from 5-10 µm with individual intact bacteria ranging from 1-2 µm.

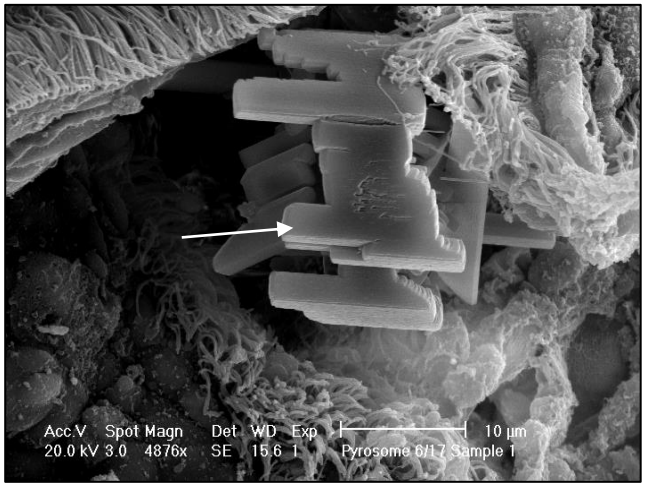

Figure 26. Calcium and sulfur paracrystalline structure identified as Gypsum.

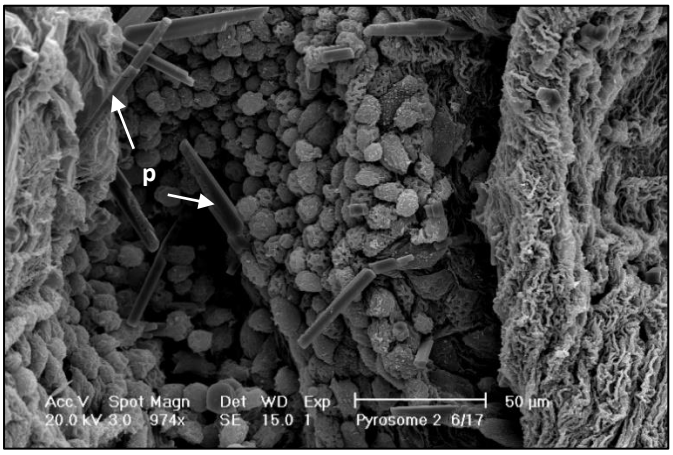

Figure 27. *In situ* higher density of paracrystalline (p) structures associate with intracellular bacteria. Each crystal is approximately 50-60 µm in length.

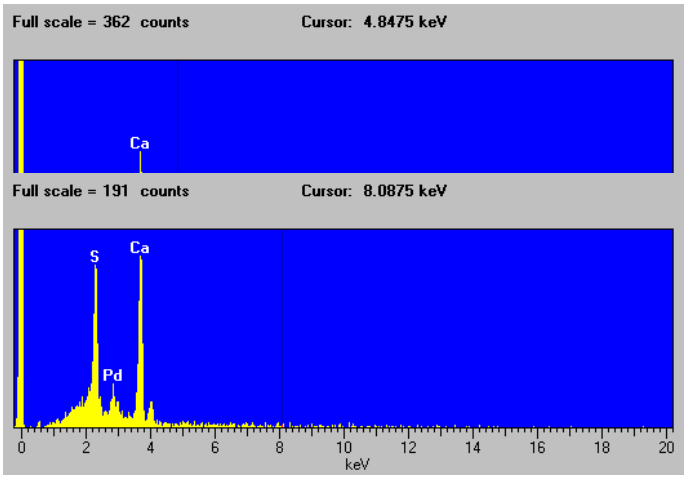

Figure 28. EDS of paracrystalline structures observed indicating they are composed of CaS. Pd is from the coating.

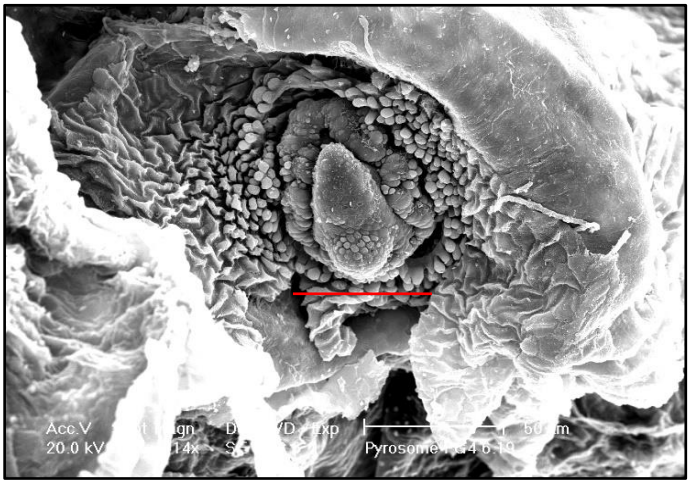

Figure 29. Intact light organ (~30 µm diameter) semi encased in the tunic. Red scale bar is set at 50 µm.

Ultrastructure of the Microbial Population in *P. atlanticum* (TEM)

When the light organ was captured in TEM sections, the overall structure and intracellular clusters of bacteria were apparent and analogous to light and SEM microscopy observations. In some cases, the pair of light organs can be viewed in the same plane, with many organelles distinguishable (Fig. 31). Intact light organs were isolated, and ultrastructurally they exhibit two distinct regions (Fig. 31-34). Within the light organ, the bacteria typically are clustered towards one end with organelles such as the nucleus surrounded by mitochondria (Fig. 31-34).

TEM examination of the pyrosome epithelial tissue in thin section revealed the presence of approximately 1-2 micron cells morphologically typical of bacteria (Fig. 31-40). These bacterial cells had a coccoid morphology and were opaque in the TEM sections. They were characterized by a "fuzzy" appearance with cells walls of unequal thickness, which produced distinct ring-like structures within the microbes (Fig. 31, 32). They exhibited thick cells walls and had a double membrane around each cell, typical of Gram-negative bacteria (Fig. 31,32) (Beveridge, 2006).

The microbial cells are intracellular and associated with mitochondria (Fig. 35). Their intracellular location is confirmed by observation of a cell membrane that encases both microbial cells and mitochondria (Fig. 35). Mitochondria were abundant inside the cytoplasm. At higher magnification, the microbes were clustered intracellularly with as many as 7 bacteria within each tunicate "bacteriocyte" cell (Fig. 30). From several cross-sections analyzed, an average of approximately 5-7 bacteria was observed within each cell (Fig. 31-40). However, SEM showed a different three-dimensional perspective, with each bacterial cluster having around 25-50 bacteria. Cells containing these bacteria are associated with abundant mitochondria and endoplasmic reticulum (Fig. 31-40). In some cases, the mitochondria are closely associated with the bacteria (Fig. 38-40). Clusters of microbes and mitochondria are shown for comparison (Fig. 40), and these membrane-bound bacteria cell clusters are reminiscent of "bacteriocytes", which are cells that contain multiple bacteria in intracellular vacuoles. The bacteria can be easily distinguished from the mitochondria by the presence of prominent cristae in the mitochondria (Fig. 39, 40).

In some cases, the bacteria are clustered around an "opening" that suggests excretion activity (Fig. 35). It appears that fluid filled vesicles are pinching off and moving to the

extracellular environment. The nature of these is unknown, or whether these excretory products are associated with bioluminescence.

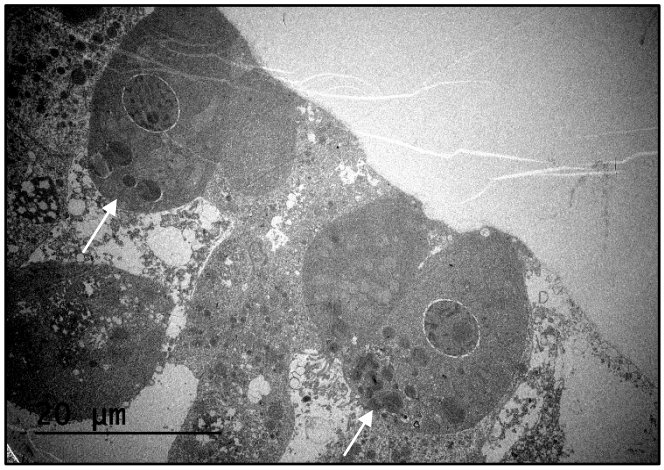

Figure 31. Lower magnification view of both light organs (white arrow). Bacteriocytes nuclei, bacteria, and mitochondria visible in both organs.

Figure 32. Higher magnification of the light organ shown in Fig. 31. It is exhibiting excretion functions shown in detail in Fig. 35.

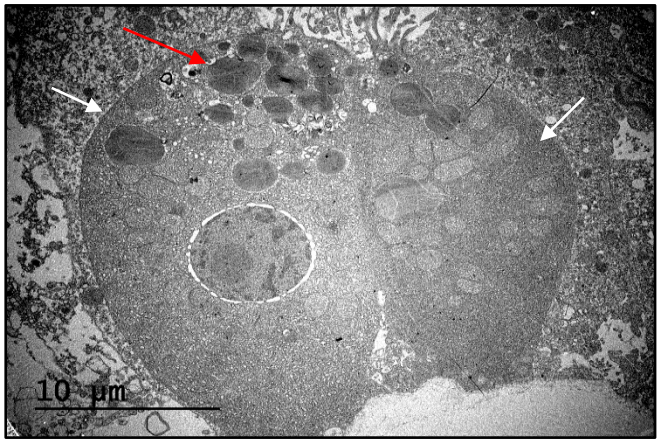

Figure 33. Higher magnification view of Fig. 32. Intact light organ with clear distinction between the two regions of the organ (white arrow). Bacteria are clustered near the edge of the organ (red arrow). See light micrograph photo (Fig.10) for comparison.

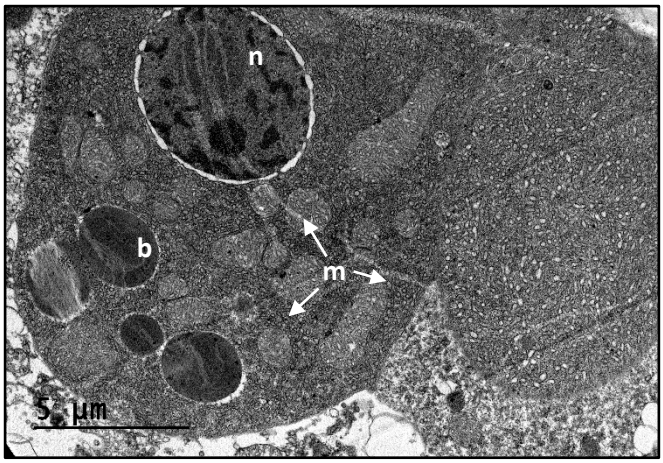

Figure 34. Light organ with bacteria (b) present, large nucleus (n) and mitochondria (m) shown.

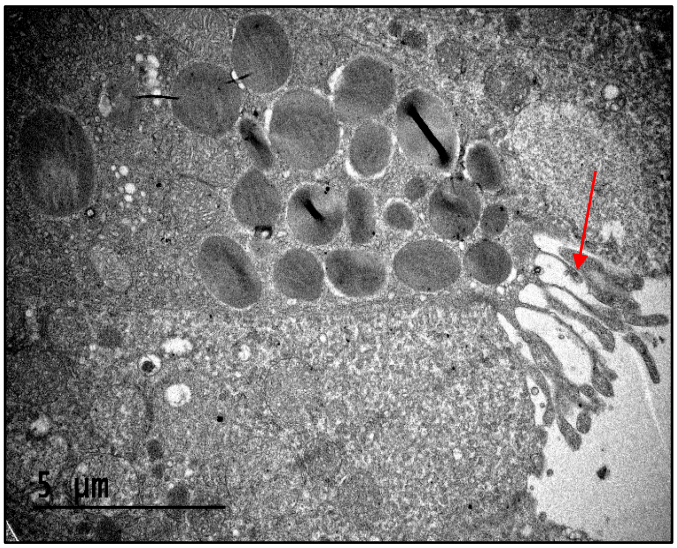

Figure 35. Bacteria within the light organ suggest intracellular to extracellular excretion activity (red arrow) of the light organ.

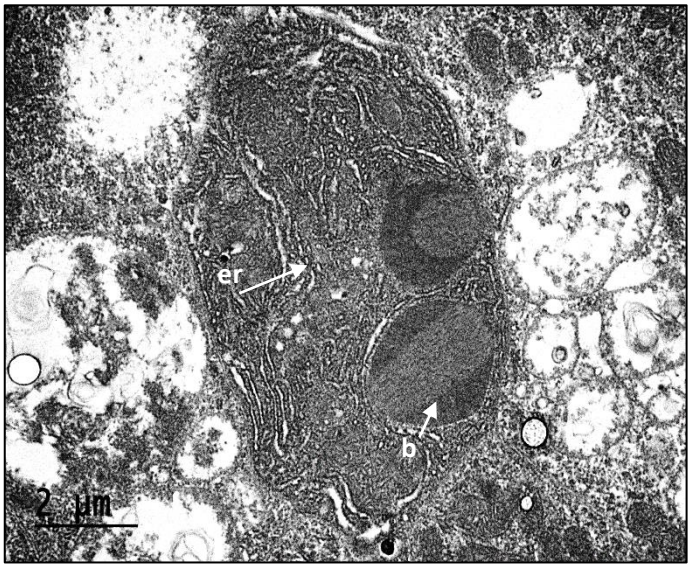

Figure 36. Intracellular microbes (b) with endoplasmic reticulum (er) distributed throughout the cell.

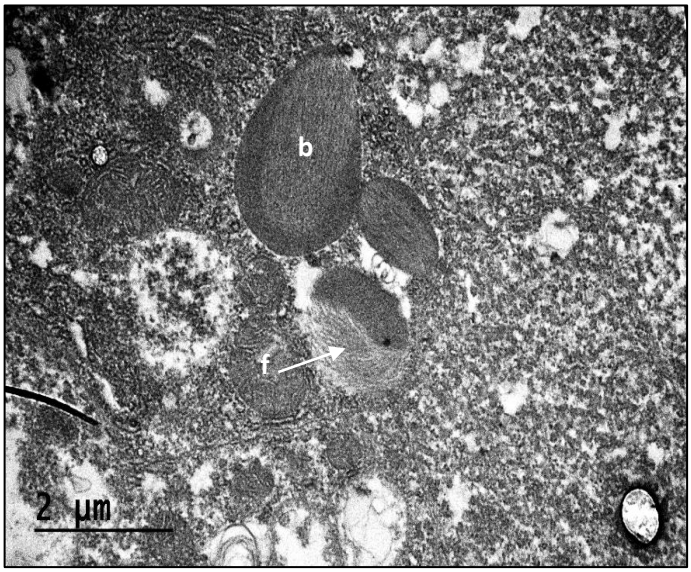

Figure 37. Featherlike structure (f) of microbes (b) exhibiting variability in cell wall thickness. The double membrane is visible.

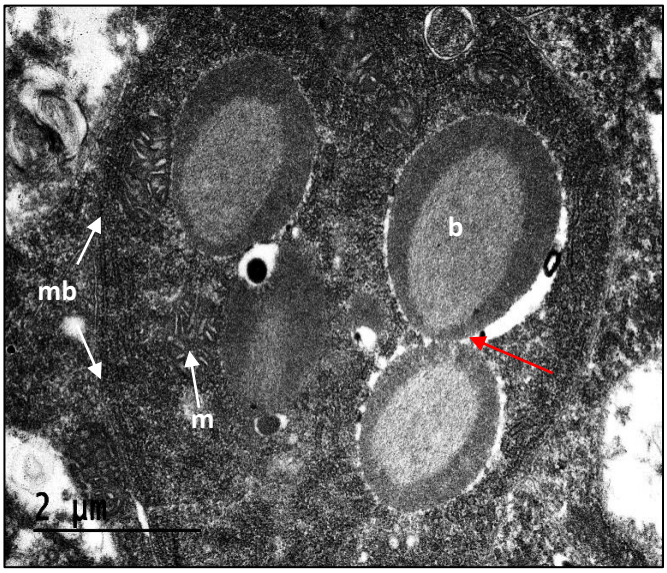

Figure 38. Cristae of the mitochondria (m) distinctly shown compared to the intracellular microbes (b) within the cell (membrane – mb). The cells on the right appear to have just divided (red arrow).

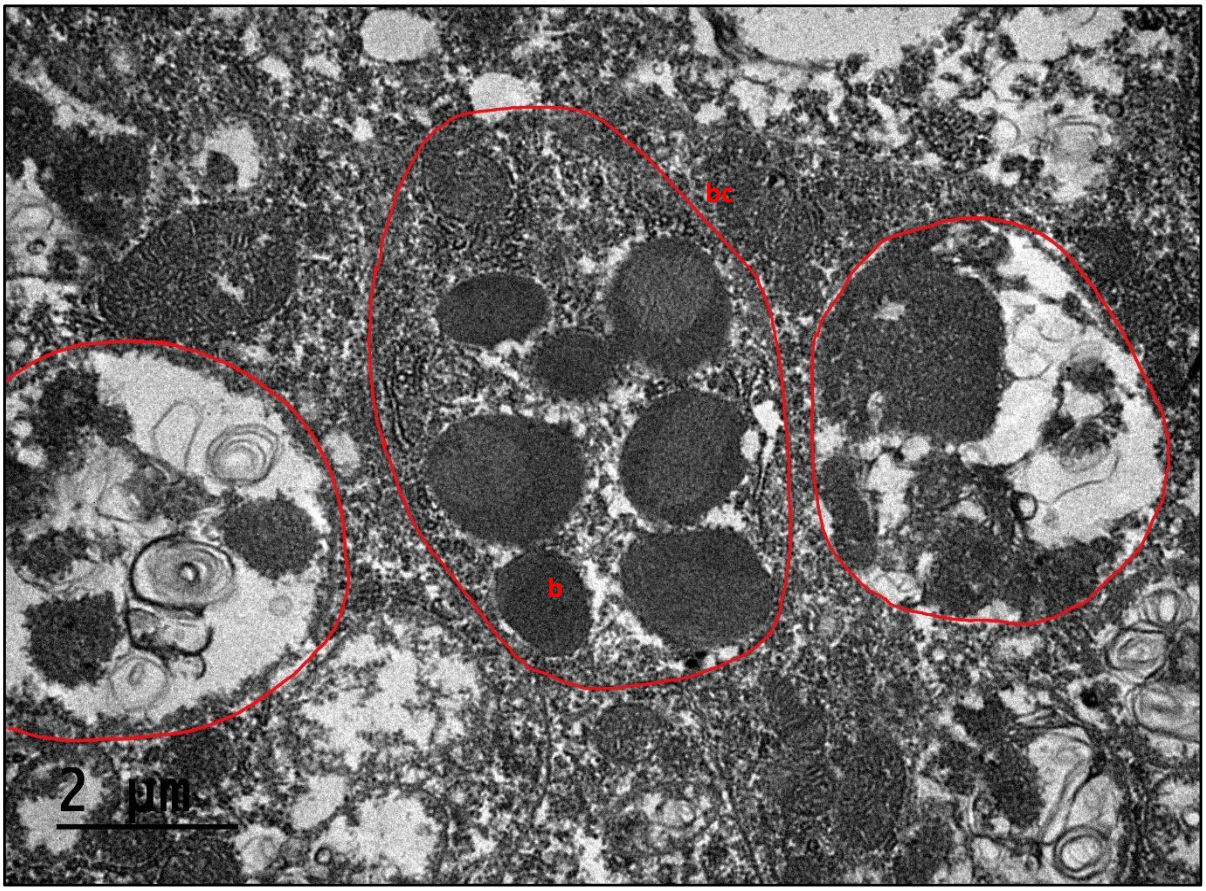

Figure 39. Intracellular microbes (b) in bacteriocytes (bc) displaying different cell thicknesses. In addition, cells on either side of the one containing bacteria appear to contain bacteria in various stages of degradation.

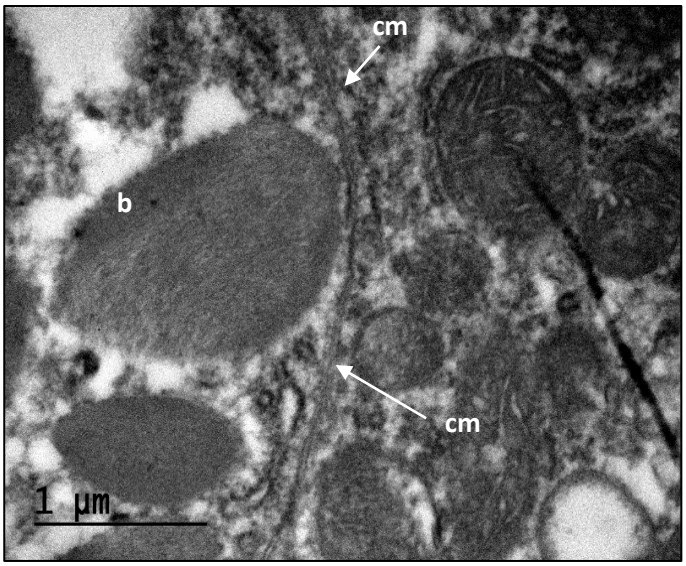

Figure 40. Cell membrane (cm) surrounding the bacteria (b) are visible, confirming the intracellular or bacteriocyte nature of the photobacterial clusters.

16S rRNA Analysis

A total of 13 samples were analyzed, 3 *P. atlanticum* and 10 seawater samples. Tissue samples were analyzed for pyrosomes with water samples for comparison at the same depths – each pyrosome sample had a corresponding water sample. Seawater samples were from two different sites at the same sample depth of 1500m. A total of 396K MiSeq reads and 497 Operational Taxonomic Units (OTUs) were produced.

In all three pyrosome samples, *Photobacterium sp. r33* showed the best match to the most abundant 16S rRNA sequences in our pyrosome microbiomes (Table 4). In order to confirm the identity of the symbiont, the sequence derived from the MiSeq run was aligned with the sequence of *Photobacterium sp. r33* from NCBI (Fig. 41). This was done through the NCBI BLAST program (https://blast.ncbi.nlm.nih.gov/Blast.cgi). This alignment showed it was a 99% match with only a single base pair that was different, however, until its identity is 100% confirmed with further genomic data, it will be referred to as *Photobacterium Pa-1* outside of 16S analytics.

In the CTD samples, it is shown that the relative abundance of *Photobacterium sp. r33* is less than 0.12%, while in DMSO1 it was 74.20%, RNALater6 had 70.88%, and RNALater7 had 39.60%. These numbers were calculated through CosmosID. When pyrosome samples are

compared to the water samples from the same trawl depths (Easson and Lopez, 2018), there are dramatic differences in diversity of bacterial types between the pyrosome and water samples (Fig. 42). The water samples were diverse while the pyrosome samples are more homogenous. The top two bacteria in the pyrosome samples are *Photobacterium sp. r33 and Vibrio_us* (unidentified species). *Photobacterium, Vibrio, Enterovibrio, and* Vibrionaceae are known luminescent genera and family (Hastings and Nealson, 1977), respectively, and they comprise about 50% of the most abundant bacteria found in the pyrosome samples (Fig. 42) (Hastings and Nealson, 1977). There are over a 1100 species found in the water samples. Some of these species are found solely in the water samples, with no trace in the pyrosomes and they include *Deltaproteobacteria sp., Gammaproteobacteria sp., Thermoplasmata sp., Halomans sp.,* and *Pseudofulvibacter geojdeonensis*.

```
Query: Photobacterium sp. r33 gene for 16S rRNA, partial sequence Query ID: AB470939

>
Sequence ID: Query_23873 Length: 236
Range 1: 1 to 236

Score:420 bits(465), Expect:2e-121,
Identities:236/237(99%),  Gaps:1/237(0%), Strand: Plus/Plus

Query  518  ACGGAGGGTGCGAGCGTTAATCGGAATTACTGGGCGTAAAGCGCATGCAGGCGGTCTGTT  577
            ||||||||||||||||||||||||||||||||||||||||||||||||||||||||||||
Sbjct  1    ACGGAGGGTGCGAGCGTTAATCGGAATTACTGGGCGTAAAGCGCATGCAGGCGGTCTGTT  60

Query  578  AAGCAAGATGTGAAAGCCCGGGGCTCAACCTCGGAACAGCATTTTGAACTGGCAGACTAG  637
            ||||||||||||||||||||||||||||||||||||||||||||||||||||||||||||
Sbjct  61   AAGCAAGATGTGAAAGCCCGGGGCTCAACCTCGGAACAGCATTTTGAACTGGCAGACTAG  120

Query  638  AGTCTTGTAGAGGGGGGTAGAATTTCAGGTGTAGCGGTGAAATGCGTAGAGATCTGAAGG  697
            ||||||||||||||||||||||||||||||||||||||||||||||||||||||||||||
Sbjct  121  AGTCTTGTAGAGGGGGGTAGAATTTCAGGTGTAGCGGTGAAATGCGTAGAGATCTGAAGG  180

Query  698  AATACCGGTGGCGAAGGCGGCCCCCTGGACAAAGACTGACGCTCAGAATGCGAAAGC  754
            |||||||||||||||||||||||||||||||||||||||||||| ||||||||||
Sbjct  181  AATACCGGTGGCGAAGGCGGCCCCCTGGACAAAGACTGACGCTCAG-ATGCGAAAGC  236
```

Figure 41. BLAST alignment of recorded *Photobacterium sp. r33* from NCBI and sequence of *Photobacterium* pulled from the 16S rRNA analysis.

Table 4. Relative abundance of the top 13 bacterial species found with *Photobacterium sp. r33* highlighted.

Name	DMSO 1	RNALater 6	RNALater 7	Water 1m	Water 12m	Water 64m	Water 72m	Water 500m	Water 1500m (a)	Water 1500m (b)	Water 1500m (c)	Water 1500m (d)	Water 1501m
Photobacterium sp. r33	0.742008	0.708790	0.396044	0.000185	0.000302	0.000000	0.000172	0.001193	0.001364	0.000112	0.001364	0.000292	0.000196
Vibrio u s	0.064947	0.000400	0.052508	0.000037	0.000121	0.000000	0.000000	0.000000	0.000138	0.000144	0.000138	0.000000	0.000147
Synechococcus u s	0.027416	0.001274	0.000471	0.025033	0.143685	0.052674	0.054037	0.008459	0.011172	0.018247	0.011172	0.006229	0.003742
Algicola u s	0.025933	0.000000	0.000000	0.000000	0.000000	0.000000	0.000000	0.000000	0.000000	0.000032	0.000000	0.000083	0.000954
Photobacterium u s	0.024748	0.021553	0.009654	0.000000	0.000000	0.000000	0.000000	0.000000	0.000000	0.000000	0.000000	0.000021	0.000000
Amphritea u s	0.022027	0.000000	0.000000	0.000000	0.000000	0.000000	0.000000	0.000000	0.000000	0.000000	0.000000	0.000063	0.000000
Enterovibrio u s	0.021486	0.020304	0.011773	0.000037	0.000000	0.000050	0.000000	0.000186	0.000158	0.000080	0.000158	0.000083	0.000000
Vibrionaceae u s	0.014336	0.005360	0.001648	0.002311	0.003047	0.002181	0.001806	0.000261	0.003500	0.001021	0.003500	0.000021	0.000367
Bd1-7 clade u s	0.007900	0.170001	0.035084	0.000259	0.000000	0.000852	0.000241	0.000000	0.000000	0.000048	0.000000	0.000021	0.000098
Moritella sp.	0.007307	0.007722	0.006828	0.000000	0.000000	0.000000	0.000000	0.000000	0.000079	0.000000	0.000079	0.000021	0.000000
Agarivorans u s	0.003453	0.000025	0.000706	0.000000	0.000000	0.000000	0.000034	0.000000	0.001206	0.000080	0.001206	0.000042	0.000269
Sagittula stellata	0.002476	0.000087	0.000942	0.000129	0.000272	0.000000	0.000327	0.001043	0.000277	0.001420	0.000277	0.001586	0.000098
Pirellulaceae u s	0.002302	0.000537	0.000471	0.001054	0.028719	0.002983	0.000808	0.004658	0.006011	0.017258	0.006011	0.008441	0.013967

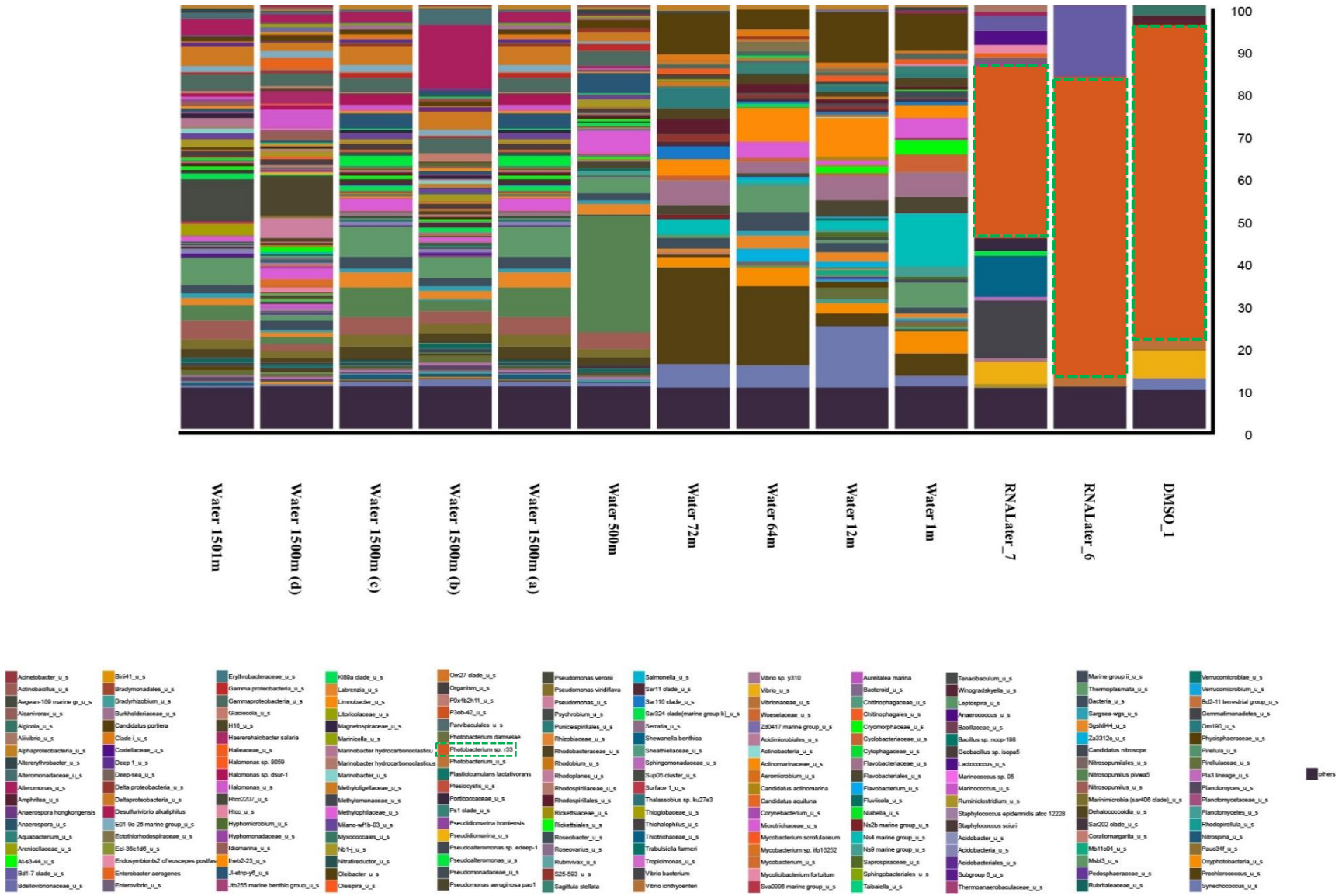

Figure 42. Stacked Bar Chart of water (CTD) vs. Pyrosome samples highlighting the most abundant symbiont (*Photobacterium sp. r33* and *Vibrio sp.*

The 16S rRNA phylogenetic tree generated by MAFFT shows a clear division between the genera *Vibrio* and *Aliivibrio* with the genus *Photobacterium.* All sequences used in this tree are from known bioluminescent species (Fig. 43). The sequence "MiSeq_Photobacterium" is grouped with only *Photobacterium* species, which indicates how closely related these species are. Based on CosmosID, this specific strand has been identified as *Photobacterium sp. r33* and it is shown in this same grouping as the other species of *Photobacterium*.

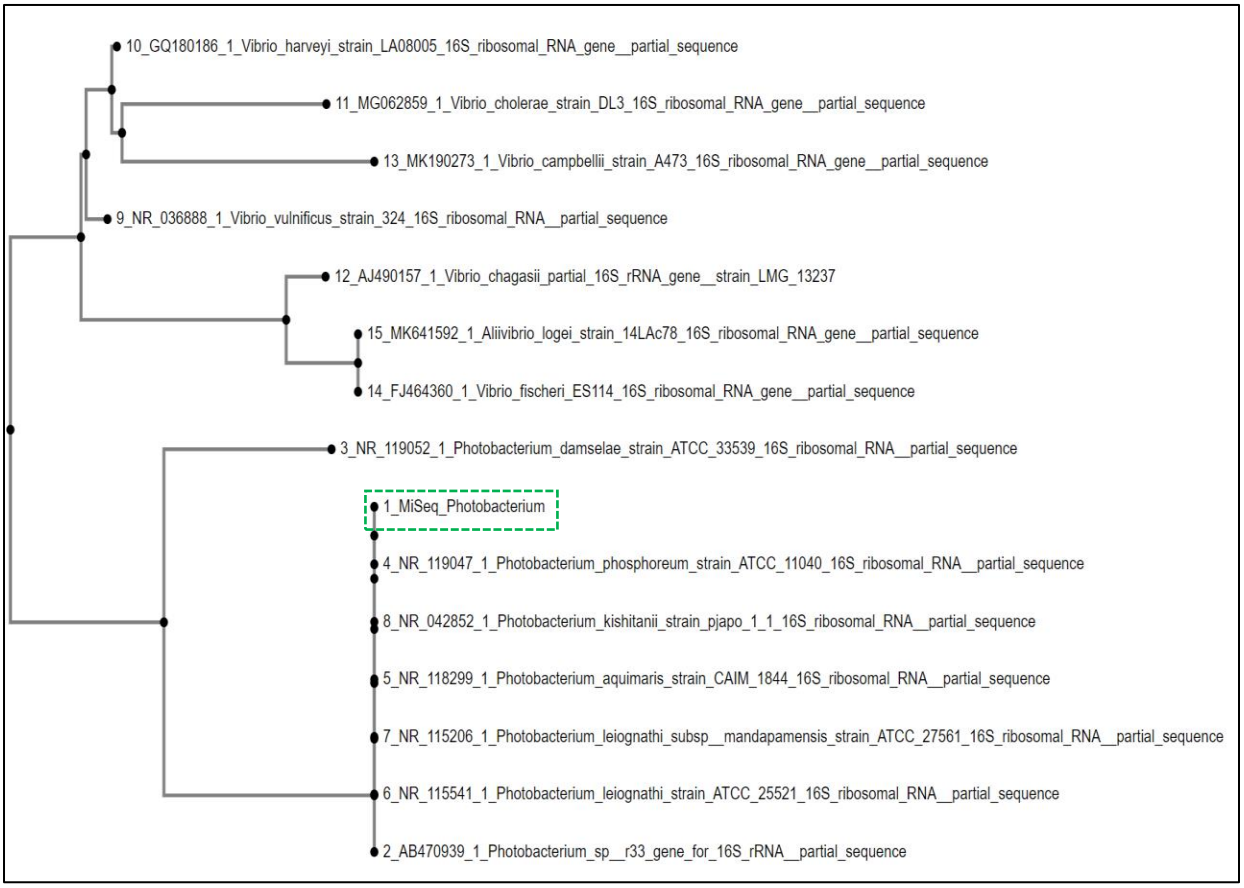

Figure 43. Phylogenetic tree based on 16S rRNA sequences of marine bioluminescent bacteria. Sequence pulled from MiSeq boxed in green.

Genome Sequencing

The 16S rRNA data showed that *Photobacterium sp. R33* had the highest relative abundance (Table 4). Whole genome sequencing was conducted in order to extract *lux* genes to determine if this bacterium caused the bioluminescence. However, there was more pyrosome than *Photobacterium* DNA within the samples, meaning that the mitochondrial genome of *Pyrosoma atlanticum* was sequenced instead. Due to more pyrosome DNA, *lux* genes were not extracted, and deeper sequencing would be needed in order to do so. Whole genome sequencing produced a contig of 14,302 base pairs (bp) long with 26X coverage. A preliminary phylogeny based on the mitochondrial cytochrome oxidase subunit 1 (COI) genes shows how distinct *P. atlanticum* is from other tunicate species (Fig. 44), especially between another pelagic tunicate.

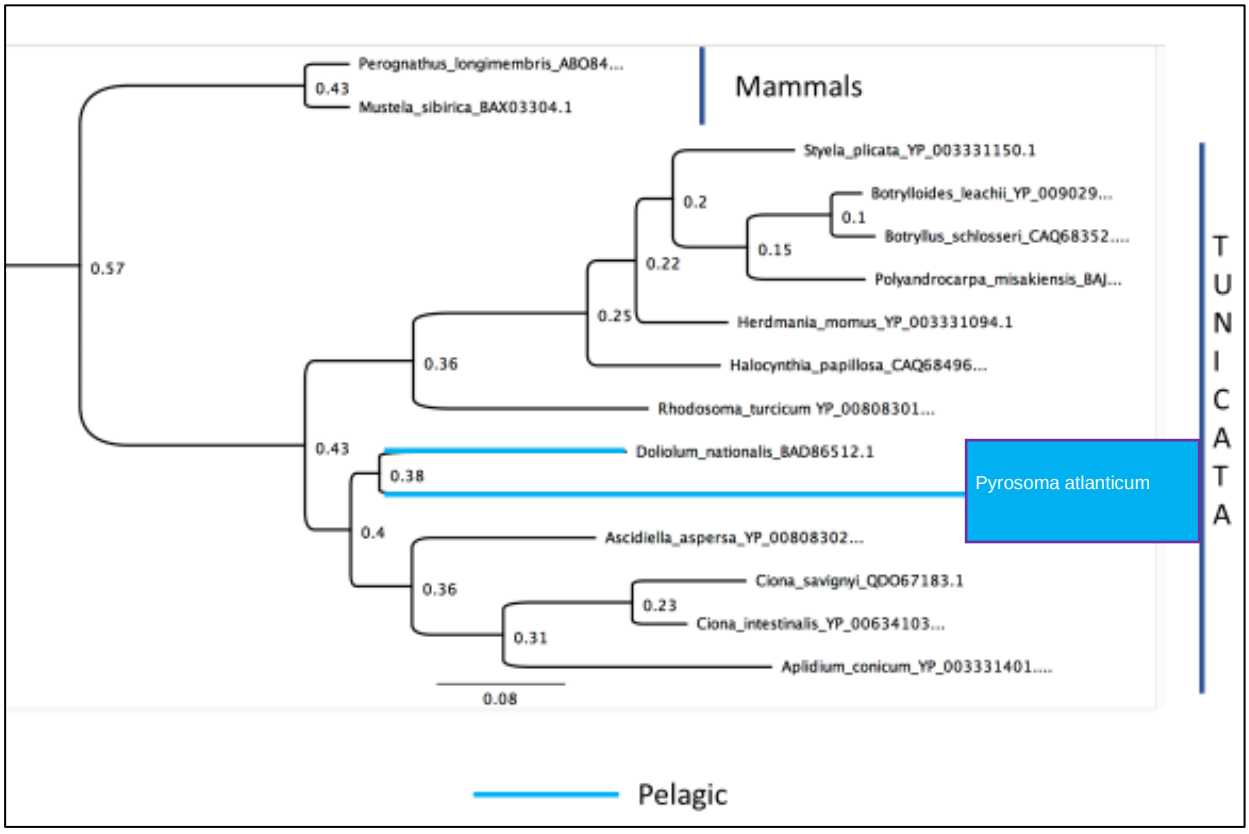

Figure 44. Preliminary phylogeny based on the Mitochondrial COI gene sequences.

Discussion

P. atlanticum Structure of the Light Organ

Based on *P. atlanticum* image and genetic analyses (light, TEM, SEM, FISH, and 16s rRNA sequencing), it evident that bioluminescent *Photobacterium Pa-1* are contained intracellularly in "bacteriocytes". The bacteriocytes can be found packed around the outer edges within the light organ. Therefore, images and genetic data suggest an intracellular location of *Photobacterium Pa-1* in bacteriocyte cells. These cell types have intracellular vacuoles which contain multiple bacteria, and have been found in several different marine holobionts including tunicates (Kwan et al., 2012;Lopez, 2019).

Source of Bioluminescence in *Pyrosoma atlanticum*

The genus *Photobacterium* is known to show substantial ecophysiological diversity, which includes free-living, symbiotic, and parasitic lifestyles (Labella et al., 2017). The bioluminescent species, in particular *P. aquimaris, P. damselae, P. kishitanii, P. leiognathi,* and *P. phosphoreum,* exhibit free-living and symbiotic lifestyles. They can be found in dense populations associated with tissues in the light organs of their selective hosts (Labella et al., 2017). These tissues could be reflectors, shutter lens, or other tissues that are used to control, target, and diffuse the bacterial light produced from the organisms' body (Urbanczyk et al., 2011). Some of the hosts of *P. kishitanii* and *P. leiognathi* are marine fish, squid, and octopus. However, *P. leiognathi* has established a highly specific symbiosis with fish families Leiognathidae, Acropomatidae, and Apogonidae, while *P. damselae* has been found to form a symbiosis only with damselfish (Labella et al., 2017). Similar host specificity is exhibited by *Photobacterium Pa-1* as indicated by the high relative abundance of *Photobacterium sp. r33* from 16S sequencing as well as the micrographs from light microscopy. SEM, TEM, and FISH confirm that *Photobacterium Pa-1* inhabits the light organ of *P. atlanticum*.

Photobacterium sp. hosts range from fish to squid and are found throughout the water column. The bacterially luminous fish are widely distributed in coastal demersal, epibenthic, and pelagic waters (Urbanczyk et al., 2011). The fishes that house *P. leiognathi* and *P. mandapamensis* are more commonly found in shallower and warmer waters, whereas *P. kishitanii* can be found in fish inhabiting deeper waters (Dunlap et al., 2007;Kaeding et al.,

2007;Nelson et al., 2016). The pelagic tunicate, *P. atlanticum*, can now be added now as a host of *Photobacterium Pa-1*.

The acquisition of the *Photobacterium* remains quite a mystery. There is much to be learned when it comes to how and when the hosts of *Photobacterium* initiate symbioses. *Nuchequula nuchalis* and *Siphanic versicolor*, both fish species, have light organs that develop before the symbiotic bacteria are acquired (Urbanczyk et al., 2011). This poses the question of whether there is horizontal or vertical transmission of microbial symbionts in these hosts. Horizontal transmission is the acquisition of symbionts from the environment, while vertical transmission is the acquisition of symbionts from the previous generation (Bright and Bulgheresi, 2010). In deep-sea ceratioid fishes it is believed that the bioluminescent symbionts are acquired from the environment during the larval migration of the fish from surface waters to the bathypelagic water, albeit in low levels of abundance (Freed et al., 2019). These symbionts were found in low levels of abundance in both mesopelagic and bathypelagic zones which suggest that the microbes are not obligately dependent on the hosts for growth. Anglerfish appear to not acquire the symbionts from the environment until they mature and move to lower depths (Freed et al., 2019). Another example of an organism that acquires its bioluminescent symbionts from the environment is the Hawaiian Bobtail squid (Nyholm and McFall-Ngai, 2004). In the case of *P. atlanticum*, the data show (Table 4) for *Photobacterium Pa-1* transmission it is most likely vertical because the water samples contained 0-0.14% while pyrosome samples contained 40-74% of the symbiont. Since *P. atlanticum* is specifically known to reproduce both sexually and asexually through internal fertilization and budding (Holland, 2016), vertical transmission of the *Photobacterium Pa-1* symbiont is plausible. The 16S rRNA analyses and micrographs support the concept that the acquisition of symbionts is through vertical transmission.

Fluorescence *in situ* Hybridization

Several control probe controls were used to demonstrate that *Photobacterium Pa-1* was located in the light organ of *P. atlanticum.* The protocol of using sections taken from the same individual, with different probes demonstrated this. Although in microscopy there is, by its nature variability in orientation, the light organ itself may exhibit some variability in morphology in micrographs. However, in the FISH analyses the signals produced essentially remain the same. In some cases, the probe was very bright, and the microscope shutter had to be partially closed in

order to record an image. This also explains why some images have a green or red tint compared to those with no probes. The probes likely emitted a strong signal because of the number and specificity of hybridized probes. The hybridization was also effective because of the formamide concentration used (35%) within the buffer. This concentration is important because formamide serves to lower the DNA melting temperature that allows for hybridization to occur without compromising the stringency of the probe (Meinkoth and Wahl, 1984).

The EUB338 probe bound to more bacteria than the *Photobacterium* probe due to having a more conservative sequence than the variable region V4 of the *Photobacterium*. The *Photobacterium* probe needed to be highly specific in order to bind to just *Photobacterium Pa-1*. The EUB338 probe fluoresced a greenish tint under the green filter cube (500-570nm) and produced more signals than the *Photobacterium* probe. With this general probe a wider variety of bacteria was shown throughout the zooids. The red filter cube (610~750 nm) served as the defining filter for the *Photobacterium* probe. The EUB338 probe showed that all bacterium fluoresced red and not orange while the slides with both probes or the solely *Photobacterium* probe fluoresced orange while using the red filter cube. What made the red filter the distinguishing factor was the fact that *Photobacterium* fluoresced orange while the other bacteria fluoresced red. The orange fluorophores confirmed that *Photobacterium Pa-1* was located in the light organ. All the results described above demonstrate the presence of bacteria in the light organ using all methods employed: light, fluorescence, electron microscopy, or genetic techniques.

P. atlanticum Bacteria Morphology

Bacterial symbionts have been described in many invertebrates (McFall-Ngai et al, 2013; Lopez 2019), however only one paper has produced a description of the ultrastructure of photogenic organelles assumed to be bacteria in pyrosomes (Mackie and Bone, 1978). There is precedence for bacteria to be contained intracellularly or within bacteriocytes, including tunicates (Kwan et al., 2012). The *P. atlanticum* photobacteria were found to be exclusively coccoid in morphology and 1-2 μm in diameter, in agreement with previous bacterial ultrastructural descriptions in other eukaryotic hosts (Nealson et al., 1981). The SEM, TEM, light microscopy, and histology images produced a more detailed description of the bacteria found in *P. atlanticum* than in any previous work done on pyrosomes. Extracellular and free living

bacterial symbionts are typically rod shape and are more elongated (Nealson et al., 1981) than the bacteria present in the pyrosomes. With the morphological similarities to Gram-negative bacteria, this provides strong support that these cells are of microbial origin aiding in the validation of the hypothesis that *P. atlanticum* uses bacterial symbiosis in their bioluminescence mechanism (Dunlap, 2009). Gram staining could not be done directly on the bacteria because neither they, nor the light organ, could be isolated.

Distribution of Bacteria in Organisms Related to Bioluminescence

In context of the mechanisms of bioluminescence, thus far both microbial and mineralogical evidence of the interaction between microbes and pyrosome cells has been generated. The SEM and TEM findings of degraded microbial cells supports the concept of the release of enzymes by the bacteria, with subsequent loss of bacterial cell function. Clusters of bacteria at the interior borders of the cells in the light organ, as well as of fluid filled vesicles migrating to the extracellular environment suggests the presence of an excretory function.

Previous work on *P. atlanticum* had not determined whether the bacteria are intra- or extracellular, and only one study has hypothesized an intracellular organization for pyrosome bacterial symbionts (Nealson et al., 1981). The current study provides strong evidence of an intracellular location of the bacteria through visualizing the light organs in light, fluorescence, and electron microscopy. Intracellular organization, in conjunction with host mediated bacteriocyte structure, indicates a highly interdependent and specialized biochemical relationship between the bacteria and host cells (Nealson et al., 1981). These micrographs provide the first evidence of such an intracellular configuration for these bacterial symbionts in *P. atlanticum*.

Intracellular symbionts represent the most highly adapted of bacterial symbionts (Shigenobu et al., 2000), which would be the case of the highly adapted bioluminescent bacterial symbionts found in *P. atlanticum*. These bacteria were found previously associated with mitochondria inside pyrosome cells (Nealson et al., 1981). It has been noted that there are several similarities between the respiratory chain of mitochondria and bioluminescent bacteria (Rees et al., 1998;Bourgois et al., 2001). Bacterial luciferase has previously been viewed as “an alternative” electron transport pathway, however, it is actually considered an “alternative” oxidase (Bourgois et al., 2001). This is why the entire photogenic system of bioluminescent bacteria scavenges not only reducing equivalents (luciferase), but also ATP and NADPH. The

close association also ties into the fact that the organism needs to consume a certain amount of energy to produce the visible spectrum of the bioluminescent light (Rees et al., 1998). In most cases it would be the blue photon (~470 nm), which requires about 255 J mol^{-1}. The fact that bioluminescence requires a lot of energy and mitochondria produces ATP, might explain why the mitochondria and microbes are so closely associated and densely packed into the cells (Bourgois et al., 2001).

Light microscopy revealed microbial localization within the luminous organ, and the bacterial symbionts were identified by FISH. TEM clearly indicated intracellular bacteria concentrated in the organ. There were as many as 72 discrete bacteriocytes found in a single light organ in light microscopy. However, in SEM and TEM there is a much lower range in number of bacteria present. This could be due to the plane in which it was sectioned so there were likely more *Photobacterium sp.* per cell than that observed using EM. In each micrograph, regardless of the type of microscopy used, the bacteria were concentrated on the interior border of the cells with clear space in the center. This begs the question as to what point do the bacteria concentrate at the edges.

It can be estimated that as many as 684~1140 bacteria can be found within the *P. atlanticum* light organ, based on how many bacteria can fit in the bacteriocytes and the volume of the light organ. This observation would be interesting for future research, to determine if the orientation of bacteria in the luminous organ plays a role in the production of, or stages in, luminescence production. The observation of secretion from the light organ to the extracellular environment in the TEM images suggests some compounds are being excreted from the light organ. The nature of these is not known but suggests they may be involved in the production of light.

Comment on Preservation Methods

Samples were stored in a variety of preservation methods – frozen, DMSO, or RNALater. The preservation methods that provided the best quality DNA were DMSO and RNALater. DMSO over time has shown that it is the most reliable and successful preservation method of tissue samples (Dawson et al., 1998). The importance of preservation method is the quality of DNA. The higher quality the DNA, the better and more reliable the 16S rRNA results will be.

The samples that were stored in DMSO and RNALater showed the most defined molecular weight and amplified the best.

Significance

Bioluminescence is found in many invertebrates. While most are not bacterial in nature, in the case of the pyrosomes the phenomenon appears due to bacterial symbionts. The degree to which this bioluminescent mechanism is similar in terms of the organelles and symbionts involved, compared to other bacterial based bioluminescence, is not known. The results obtained in this study identify the specific bacterial symbionts involved using genetic methods, which were also enhanced by an ultrastructural study to discern morphological characteristics of both the bacteria and the host organism. These ultrastructure and microscopy studies also helped produce a more detailed description of the pyrosome light organ and its potential mechanism for bioluminescence, contributing to our knowledge of pyrosomes. Identifying the bacteria intracellular location provides additional understanding into a unique luminescent mechanism, because most bacterial bioluminescence is extracellular. If highly specialized intracellular microbes are identified, critical insight into the holobiont's evolutionary path may be discerned. This study also determined that the bacterial symbionts are different in the light organ compared to those found in the rest of the organism. Understanding the taxonomy of this bioluminescent microbe could indicate how it is acquired by the tunicate, since many bioluminescent microbes exist in marine habitats and hosts (McFall-Ngai, 2014;Freed et al., 2019).

The fact that the *P. atlanticum* light organs has a relatively homogenous microbiome, with *Photobacterium Pa-1* making up a majority of the signal, supports the concept that symbionts are transferred vertically throughout generations. The pyrosome inherits the bacteria from previous generations and hosts them in an environment only in which the bioluminescent bacteria can survive (the light organ). Most bioluminescent bacterial symbionts have been shown to be acquired through the environment. For example, the horizontal transmission mode has been seen in the Hawaiian bobtail squid as well as deep sea anglerfish (Lee and Ruby, 1994;Nyholm and McFall-Ngai, 1998;Ruby and Lee, 1998;Baker et al., 2019). When comparing the pyrosome microbiome to the seawater samples, less than 0.001% of the water sample microbiome was composed of *Photobacterium sp.33*. Nonetheless, unequivocal proof of vertical transfer would be the identification of these bacteria in *P. atlanticum* larvae. Although interesting, this question

is beyond the scope of this thesis. Although bioluminescence has been described in pyrosomes for over 100 years, and pyrosomes are found in all the world's oceans, this is the first in-depth characterization of the light organ microbiome in the pyrosome. By utilizing both genetic and microscopy methods, more complete and complementary data was analyzed for the assessment of bacterial symbiosis in *P. atlanticum*. This is the first study to document that *Photobacterium Pa-1* is found symbiotically within the light organ of *P. atlanticum* and suggest they may be vertically transmitted.

Relevance to Ongoing Research Programs

This project dovetails with other deep-sea and molecular marine projects such as DEEPEND (Deep-Pelagic Nekton Dynamics of the Gulf of Mexico), the characterization of marine organisms such as GIGA (Global Invertebrate Genomics Alliance) (Lopez JV, 2013;Scientists, 2014) and the Earth Microbiome Project (Thompson et al., 2017). The DEEPEND Consortium's research initiative is to characterize the oceanic ecosystem of the northern Gulf of Mexico in order to surmise baseline conditions throughout the water column. Since the deep-pelagic is one of the largest and understudied habitats on Earth, DEEPEND has shed light on this mysterious environment. *P. atlanticum* is one of the inhabitants encountered on DEEPEND cruises throughout the water column with little known about the organism. This project contributes key insight into one of the major players in this understudied ecosystem.

GIGA's research goals are to sequence, assemble, and annotate whole genomes and/or transcriptomes of the world's invertebrates (Scientists, 2014). Currently only three tunicates have been sequenced, *Ciona intestinalis, Ciona savignyi,* and *Oikopleura dioica*. *Ciona sp.* are sessile tunicates and *O. dioica* is a pelagic tunicate. Due to this study, *P. atlanticum* is a viable candidate to sequence for its whole genome since the almost complete mitochondrial genome has been sequenced. Sequencing this tunicate further provides data that falls in line with the goals of GIGA. *P. atlanticum* serves as a tractable model for exploring symbioses, more specifically an intracellular bioluminescent symbiosis. Constructing the whole genome of *P. atlanticum* would provide additional evidence of the bioluminescent evolutionary pathway.

Future Work

A comparative study of the light organ and body of the pyrosome, in terms of the microbiome present, could show even more specificity of the symbionts in the light organ. It is estimated that less than 2% of bacteria can be cultured in a laboratory setting (Wade, 2002), so being able to culture a highly specific bacteria would add to the ground work for studying intracellular bacteria in a laboratory setting without the host organism. A comparative study of the light organ and whole body would also build on extraction techniques using Laser Capture Microdissection.

Future work could focus on the ultrastructure during stimulated bioluminescence and compare it to pyrosomes which have not been stimulated. This would elucidate potential ultrastructural variability related to these mechanisms. The bacteria have been seen in differing states of degradation and clustering in the SEM and TEM micrographs. In previous studies, the luciferase assayed from the disrupted pyrosomes displayed fast kinetics akin to that of *Photobacterium* species (Nealson et al., 1981). Since little is known of the production mechanisms of luciferase and it has been confirmed that *Photobacterium Pa-1* is the bacterial symbiont, these mechanisms should be studied in more detail. If the states of degradation are correlated to the production of the luciferase, it would give insight into where exactly the chemical reactions occur.

Conclusions

This study provides new insights into the bioluminescent mechanism of *P. atlanticum.* Our findings support bioluminescence is bacterial based and is caused by *Photobacterium Pa-1*. Family Vibrionaceae is known to contain three genera of bioluminescent bacteria, including *Photobacterium. Photobacterium Pa-1* are found intracellularly and within the light organs of *P. atlanticum.* They were found in great relative abundances in these pyrosomes at about 40-74%, dominating the microbiome. More specifically, the bioluminescent symbiont community primarily contained this species of *Photobacterium* while the next abundant symbiont was found in family Vibrionaceae. Future studies could focus on comparing the microbiome of the whole tunicate to that of the light organ in order to show just how selective an environment the light organ is.

References

Afgan, E., Baker, D., Batut, B., Van Den Beek, M., Bouvier, D., Čech, M., Chilton, J., Clements, D., Coraor, N., and Grüning, B.A. (2018). The Galaxy platform for accessible, reproducible and collaborative biomedical analyses: 2018 update. *Nucleic acids research* 46**,** W537-W544.

Alldredge, A., and Madin, L. (1982). Pelagic tunicates: unique herbivores in the marine plankton. *Bioscience* 32**,** 655-663.

Amann, R.I., Ludwig, W., and Schleifer, K.-H. (1995). Phylogenetic identification and in situ detection of individual microbial cells without cultivation. *Microbiol. Mol. Biol. Rev.* 59**,** 143-169.

Baker, L.J., Freed, L.L., Easson, C.G., Lopez, J.V., Fenolio, D., Sutton, T.T., Nyholm, S.V., and Hendry, T.A. (2019). Diverse deep-sea anglerfishes share a genetically reduced luminous symbiont that is acquired from the environment. *eLife* 8.

Baldwin, T., Devine, J., Heckel, R., Lin, J.W., and Shadel, G. (1989). The complete nucleotide sequence of the lux regulon of Vibrio fischeri and the luxABN region of Photobacterium leiognathi and the mechanism of control of bacterial bioluminescence. *Journal of bioluminescence and chemiluminescence* 4**,** 326-341.

Barer, R. (1974). Microscopes, microscopy, and microbiology. *Annual Reviews in Microbiology* 28**,** 371-390.

Bauermeister, A., Branco, P.C., Furtado, L.C., Jimenez, P.C., Costa-Lotufo, L.V., and Da Cruz Lotufo, T.M. (2018). Tunicates: A model organism to investigate the effects of associated-microbiota on the production of pharmaceuticals. *Drug Discovery Today: Disease Models* 28**,** 13-20.

Beveridge, T.J. (2006). Visualizing bacterial cell walls and biofilms. *MICROBE-AMERICAN SOCIETY FOR MICROBIOLOGY* 1**,** 279.

Blackwelder, P. (2019). "The Equipment/LM Marine Organisms Under Light and Electron Microscopy ", in: *Histology and Ultrastructure of Marine Organisms* (ed.) P. Blackwelder. Nova Southeastern University).

Bourgois, J.-J., Sluse, F., Baguet, F., and Mallefet, J. (2001). Kinetics of light emission and oxygen consumption by bioluminescent bacteria. *Journal of bioenergetics and biomembranes* 33**,** 353-363.

Bouvier, T., and Del Giorgio, P.A. (2003). Factors influencing the detection of bacterial cells using fluorescence in situ hybridization (FISH): a quantitative review of published reports. *FEMS Microbiology Ecology* 44**,** 3-15.

Bowlby, M.R., Widder, E.A., and Case, J.F. (1990). Patterns of Stimulated Bioluminescence in 2 Pyrosomes (Tunicata, Pyrosomatidae). *Biological Bulletin* 179**,** 340-350.

Bright, M., and Bulgheresi, S. (2010). A complex journey: transmission of microbial symbionts. *Nature Reviews Microbiology* 8**,** 218-230.

Brown, T.A. (2007). *Genomes 3.* New York and London: Garland Science.

Burghause, F. (1914). *Kreislauf und Herzschlag bei Pyrosoma giganteum nebst Bemerkungen zum Leuchtvermögen: Aus d. Zool. Inst. zu Leipzig.* W. Engelmann.

Cahill, P.L., Fidler, A.E., Hopkins, G.A., and Wood, S.A. (2016). Geographically conserved microbiomes of four temperate water tunicates. *Environmental microbiology reports* 8**,** 470-478.

Campbell, A.M., Fleisher, J., Sinigalliano, C., White, J.R., and Lopez, J.V. (2015). Dynamics of marine bacterial community diversity of the coastal waters of the reefs, inlets, and wastewater outfalls of southeast F lorida. *MicrobiologyOpen* 4**,** 390-408.

Caporaso, J.G., Kuczynski, J., Stombaugh, J., Bittinger, K., Bushman, F.D., Costello, E.K., Fierer, N., Pena, A.G., Goodrich, J.K., and Gordon, J.I. (2010). QIIME allows analysis of high-throughput community sequencing data. *Nature methods* 7**,** 335.

Caporaso, J.G., Lauber, C.L., Walters, W.A., Berg-Lyons, D., Lozupone, C.A., Turnbaugh, P.J., Fierer, N., and Knight, R. (2011). Global patterns of 16S rRNA diversity at a depth of millions of sequences per sample. *Proceedings of the national academy of sciences* 108**,** 4516-4522.

Chakravorty, S., Helb, D., Burday, M., Connell, N., and Alland, D. (2007). A detailed analysis of 16S ribosomal RNA gene segments for the diagnosis of pathogenic bacteria. *Journal of microbiological methods* 69**,** 330-339.

Cuvelier, M.L., Blake, E., Mulheron, R., Mccarthy, P.J., Blackwelder, P., Thurber, R.L.V., and Lopez, J.V. (2014). Two distinct microbial communities revealed in the sponge Cinachyrella. *Frontiers in microbiology* 5**,** 581.

Datye, A.K. (2003). Electron microscopy of catalysts: recent achievements and future prospects. *Journal of Catalysis* 216**,** 144-154.

Dawson, M.N., Raskoff, K.A., and Jacobs, D.K. (1998). Field preservation of marine invertebrate tissue for DNA analyses. *Molecular marine biology and biotechnology* 7**,** 145-152.

Décima, M., Stukel, M.R., López-López, L., and Landry, M.R. (2019). The unique ecological role of pyrosomes in the Eastern Tropical Pacific. *Limnology and Oceanography* 64**,** 728-743.

Dunlap, P. (2009). Bioluminescence, microbial.

Dunlap, P.V., Ast, J.C., Kimura, S., Fukui, A., Yoshino, T., and Endo, H. (2007). Phylogenetic analysis of host–symbiont specificity and codivergence in bioluminescent symbioses. *Cladistics* 23**,** 507-532.

Dunlap, P.V., and Urbanczyk, H. (2013). Luminous bacteria. *The Prokaryotes: Prokaryotic Physiology and Biochemistry***,** 495-528.

Easson, C.G., and Lopez, J.V. (2018). Depth-dependent environmental drivers of microbial plankton community structure in the northern Gulf of Mexico. *Frontiers in microbiology* 9**,** 3175.

Easson, C.G., and Lopez, J.V. (2019). Depth-Dependent environmental drivers of microbial plankton community structure in the Northern Gulf of Mexico. *Frontiers in microbiology* 9**,** 3175.

Emmert-Buck, M.R., Bonner, R.F., Smith, P.D., Chuaqui, R.F., Zhuang, Z., Goldstein, S.R., Weiss, R.A., and Liotta, L.A. (1996). Laser capture microdissection. *Science* 274**,** 998-1001.

Espina, V., Wulfkuhle, J.D., Calvert, V.S., Vanmeter, A., Zhou, W., Coukos, G., Geho, D.H., Petricoin, E.F., and Liotta, L.A. (2006). Laser-capture microdissection. *Nature protocols* 1**,** 586.

Farmer Iii, J., Michael Janda, J., Brenner, F.W., Cameron, D.N., and Birkhead, K.M. (2015). Vibrio. *Bergey's Manual of Systematics of Archaea and Bacteria***,** 1-79.

Farmer, J., and Hickman-Brenner, F. (2006). The genera vibrio and photobacterium. *The Prokaryotes: Volume 6: Proteobacteria: Gamma Subclass***,** 508-563.

Freed, L.L. (2018). *Characterization of the Bioluminescent Symbionts from Ceratioids Collected in the Gulf of Mexico.* Master Masters Nova Southeastern University

Freed, L.L., Easson, C., Baker, L.J., Fenolio, D., Sutton, T.T., Khan, Y., Blackwelder, P., Hendry, T.A., and Lopez, J.V. (2019). Characterization of the microbiome and bioluminescent symbionts across life stages of Ceratioid Anglerfishes of the Gulf of Mexico. *FEMS microbiology ecology* 95**,** fiz146.

Götz, S., García-Gómez, J.M., Terol, J., Williams, T.D., Nagaraj, S.H., Nueda, M.J., Robles, M., Talón, M., Dopazo, J., and Conesa, A. (2008). High-throughput functional annotation and data mining with the Blast2GO suite. *Nucleic acids research* 36**,** 3420-3435.

Haddock, S.H., and Case, J. (1999). Bioluminescence spectra of shallow and deep-sea gelatinous zooplankton: ctenophores, medusae and siphonophores. *Marine Biology* 133**,** 571-582.

Haddock, S.H., Moline, M.A., and Case, J.F. (2010). Bioluminescence in the sea. *Annual review of marine science* 2**,** 443-493.

Hastings, J., and Nealson, K.H. (1977). Bacterial bioluminescence. *Annual review of microbiology* 31**,** 549-595.

Haygood, M.G. (1993). Light Organ Symbioses In Fishes. *Critical Reviews in Microbiology* 19**,** 191-216.

Hendry, T.A., Freed, L.L., Fader, D., Fenolio, D., Sutton, T.T., and Lopez, J.V. (2018). Ongoing transposon-mediated genome reduction in the luminous bacterial symbionts of deep-sea ceratioid anglerfishes. *mBio* 9**,** e01033-01018.

Herring, P.J. (1985). Bioluminescence in the Crustacea. *Journal of crustacean biology* 5**,** 557-573.

Hirose, E., Kimura, S., Itoh, T., and Nishikawa, J. (1999). Tunic morphology and cellulosic components of pyrosomas, doliolids, and salps (Thaliacea, Urochordata). *The Biological Bulletin* 196**,** 113-120.

Holland, L.Z. (2016). Tunicates. *Current Biology* 26**,** R146-R152.

Hughes, G.M., Leech, J., Puechmaille, S.J., Lopez, J.V., and Teeling, E.C. (2018). Is there a link between aging and microbiome diversity in exceptional mammalian longevity? *PeerJ* 6**,** e4174.

Huxley, T.H. (1851). XXIV. Observations upon the anatomy and physiology of salpa and pyrosoma. *Philosophical transactions of the Royal Society of London***,** 567-593.

Janda, J.M., and Abbott, S.L. (2007). 16S rRNA gene sequencing for bacterial identification in the diagnostic laboratory: pluses, perils, and pitfalls. *Journal of clinical microbiology* 45**,** 2761-2764.

Johnsen, S., Widder, E.A., and Mobley, C.D. (2004). Propagation and perception of bioluminescence: factors affecting counterillumination as a cryptic strategy. *The Biological Bulletin* 207**,** 1-16.

Kaeding, A.J., Ast, J.C., Pearce, M.M., Urbanczyk, H., Kimura, S., Endo, H., Nakamura, M., and Dunlap, P.V. (2007). Phylogenetic diversity and cosymbiosis in the bioluminescent symbioses of "Photobacterium mandapamensis". *Appl. Environ. Microbiol.* 73**,** 3173-3182.

Katoh, K., and Standley, D.M. (2013). MAFFT multiple sequence alignment software version 7: improvements in performance and usability. *Molecular biology and evolution* 30**,** 772-780.

Kerk, N.M., Ceserani, T., Tausta, S.L., Sussex, I.M., and Nelson, T.M. (2003). Laser capture microdissection of cells from plant tissues. *Plant physiology* 132**,** 27-35.

Kita-Tsukamoto, K., Yao, K., Kamiya, A., Yoshizawa, S., Uchiyama, N., Kogure, K., and Wada, M. (2006). Rapid identification of marine bioluminescent bacteria by amplified 16S ribosomal RNA gene restriction analysis. *FEMS microbiology letters* 256**,** 298-303.

Krishnaveni, M., Asha, S., Vini, S.S., and Punitha, S.M.J. (2018). "Metagenomics of Marine Invertebrate-Microbial Consortium," in *Metagenomics*. Elsevier), 255-272.

Kuczynski, J., Stombaugh, J., Walters, W.A., González, A., Caporaso, J.G., and Knight, R. (2011). Using QIIME to analyze 16S rRNA gene sequences from microbial communities. *Current protocols in bioinformatics* 36**,** 10.17. 11-10.17. 20.

Kwan, J.C., Donia, M.S., Han, A.W., Hirose, E., Haygood, M.G., and Schmidt, E.W. (2012). Genome streamlining and chemical defense in a coral reef symbiosis. *Proceedings of the National Academy of Sciences* 109**,** 20655-20660.

Labella, A.M., Arahal, D.R., Castro, D., Lemos, M.L., and Borrego, J.J. (2017). Revisiting the genus Photobacterium: taxonomy, ecology and pathogenesis. *Int Microbiol* 20**,** 1-10.

Land, M., Hauser, L., Jun, S.-R., Nookaew, I., Leuze, M.R., Ahn, T.-H., Karpinets, T., Lund, O., Kora, G., and Wassenaar, T. (2015). Insights from 20 years of bacterial genome sequencing. *Functional & integrative genomics* 15**,** 141-161.

Lee, K.-H., and Ruby, E.G. (1994). Effect of the squid host on the abundance and distribution of symbiotic Vibrio fischeri in nature. *Appl. Environ. Microbiol.* 60**,** 1565-1571.

Leisman, G., Cohn, D.H., and Nealson, K.H. (1980). Bacterial Origin of Luminescence in Marine Animals. *Science* 208**,** 1271-1273.

Lemaire, P., and Piette, J. (2015). Tunicates: exploring the sea shores and roaming the open ocean. A tribute to Thomas Huxley. *Open biology* 5**,** 150053.

Lewin, H.A., Robinson, G.E., Kress, W.J., Baker, W.J., Coddington, J., Crandall, K.A., Durbin, R., Edwards, S.V., Forest, F., and Gilbert, M.T.P. (2018). Earth BioGenome Project: Sequencing life for the future of life. *Proceedings of the National Academy of Sciences* 115**,** 4325-4333.

Lopez, J.V. (2019). "After the taxonomic identification phase: addressing the functions of symbiotic communities within marine invertebrates," in *Symbiotic Microbiomes of Coral Reefs Sponges and Corals*. Springer), 105-144.

Lopez Jv, G.C.O.S. (2013). The Global Invertebrate Genomics Alliance (GIGA): developing community resources to study diverse invertebrate genomes. *Journal of Heredity* 105**,** 1-18.

Mackie, G.O., and Bone, Q. (1978). Luminescence and Associated Effector Activity in Pyrosoma (Tunicata Pyrosomida). *Proceedings of the Royal Society Series B-Biological Sciences* 202**,** 483-+.

Martini, S., and Haddock, S.H. (2017). Quantification of bioluminescence from the surface to the deep sea demonstrates its predominance as an ecological trait. *Scientific reports* 7**,** 45750.

Mcfall-Ngai, M. (2014). Divining the essence of symbiosis: insights from the squid-vibrio model. *PLoS biology* 12**,** e1001783.

Mcfall-Ngai, M., Hadfield, M.G., Bosch, T.C., Carey, H.V., Domazet-Lošo, T., Douglas, A.E., Dubilier, N., Eberl, G., Fukami, T., and Gilbert, S.F. (2013). Animals in a bacterial world, a new imperative for the life sciences. *Proceedings of the National Academy of Sciences* 110**,** 3229-3236.

Meinkoth, J., and Wahl, G. (1984). Hydridization of nucleic acids immobilized on solid supports. *Analytical biochemistry* 138**,** 267-284.

Munk, O. (1998). Light Guides of the Escal Light Organs in Some Deep-Sea Anglerfishes (Pisces; Ceratioidei). *Acta Zoologica* 79**,** 175-186.
Nealson, K., Cohn, D., Leisman, G., and Tebo, B. (1981). Co-evolution of luminous bacteria and their eukaryotic hosts. *Annals of the New York Academy of Sciences* 361**,** 76-91.
Negandhi, K., Blackwelder, P.L., Ereskovsky, A.V., and Lopez, J.V. (2010). Florida reef sponges harbor coral disease-associated microbes. *Symbiosis* 51**,** 117-129.
Nelson, J.S., Grande, T.C., and Wilson, M.V. (2016). *Fishes of the World.* John Wiley & Sons.
Nyholm, S.V., and Mcfall-Ngai, M. (2004). The winnowing: establishing the squid–Vibrio symbiosis. *Nature Reviews Microbiology* 2**,** 632-642.
Nyholm, S.V., and Mcfall-Ngai, M.J. (1998). Sampling the light-organ microenvironment of Euprymna scolopes: description of a population of host cells in association with the bacterial symbiont Vibrio fischeri. *The Biological Bulletin* 195**,** 89-97.
O'connell, L., Gao, S., Mccorquodale, D., Fleisher, J., and Lopez, J.V. (2018). Fine grained compositional analysis of Port Everglades Inlet microbiome using high throughput DNA sequencing. *PeerJ* 6**,** e4671.
Pace, N.R. (1997). A molecular view of microbial diversity and the biosphere. *Science* 276**,** 734-740.
Polimanti, O. (1911). *Über das leuchten von Pyrosoma elegans Les.* R. Oldenbourg.
Rader, B.A., and Nyholm, S.V. (2012). Host/microbe interactions revealed through "omics" in the symbiosis between the Hawaiian bobtail squid Euprymna scolopes and the bioluminescent bacterium Vibrio fischeri. *The Biological Bulletin* 223**,** 103-111.
Rees, G.N., Baldwin, D.S., Watson, G.O., Perryman, S., and Nielsen, D.L. (2004). Ordination and significance testing of microbial community composition derived from terminal restriction fragment length polymorphisms: application of multivariate statistics. *Antonie van Leeuwenhoek* 86**,** 339-347.
Rees, J.-F., De Wergifosse, B., Noiset, O., Dubuisson, M., Janssens, B., and Thompson, E.M. (1998). The origins of marine bioluminescence: turning oxygen defence mechanisms into deep-sea communication tools. *Journal of Experimental Biology* 201**,** 1211-1221.
Ruby, E.G., and Lee, K.-H. (1998). The Vibrio fischeri-Euprymna scolopes light organ association: current ecological paradigms. *Appl. Environ. Microbiol.* 64**,** 805-812.
Ruppert, E.E., and Barnes, R.D. (1994). *Invertebrate Zoology.* Saunders College Publishing New York.
Schauder, S., and Bassler, B.L. (2001). The languages of bacteria. *Genes & Development* 15**,** 1468-1480.
Schimak, M.P., Kleiner, M., Wetzel, S., Liebeke, M., Dubilier, N., and Fuchs, B.M. (2016). MiL-FISH: Multilabeled oligonucleotides for fluorescence in situ hybridization improve visualization of bacterial cells. *Appl. Environ. Microbiol.* 82**,** 62-70.
Schimak, M.P., Toenshoff, E.R., and Bright, M. (2012). Simultaneous 16S and 18S rRNA fluorescence in situ hybridization (FISH) on LR White sections demonstrated in Vestimentifera (Siboglinidae) tubeworms. *Acta histochemica* 114**,** 122-130.
Schnitzler, C.E., Pang, K., Powers, M.L., Reitzel, A.M., Ryan, J.F., Simmons, D., Tada, T., Park, M., Gupta, J., and Brooks, S.Y. (2012). Genomic organization, evolution, and expression of photoprotein and opsin genes in Mnemiopsis leidyi: a new view of ctenophore photocytes. *BMC biology* 10**,** 107.

Scientists, G.C.O. (2014). The Global Invertebrate Genomics Alliance (GIGA): developing community resources to study diverse invertebrate genomes. *Journal of heredity* 105**,** 1-18.

Sfanos, K., Harmody, D., Dang, P., Ledger, A., Pomponi, S., Mccarthy, P., and Lopez, J. (2005). A molecular systematic survey of cultured microbial associates of deep-water marine invertebrates. *Systematic and Applied Microbiology* 28**,** 242-264.

Shigenobu, S., Watanabe, H., Hattori, M., Sakaki, Y., and Ishikawa, H. (2000). Genome sequence of the endocellular bacterial symbiont of aphids Buchnera sp. APS. *Nature* 407**,** 81-86.

Sutherland, K.R., Sorensen, H.L., Blondheim, O.N., Brodeur, R.D., and Galloway, A.W. (2018). Range expansion of tropical pyrosomes in the northeast Pacific Ocean. *Ecology* 99**,** 2397-2399.

Thompson, F.L., Iida, T., and Swings, J. (2004). Biodiversity of vibrios. *Microbiol. Mol. Biol. Rev.* 68**,** 403-431.

Thompson, L.R., Sanders, J.G., Mcdonald, D., Amir, A., Ladau, J., Locey, K.J., Prill, R.J., Tripathi, A., Gibbons, S.M., and Ackermann, G. (2017). A communal catalogue reveals Earth's multiscale microbial diversity. *Nature* 551**,** 457.

Tringe, S.G., and Hugenholtz, P. (2008). A renaissance for the pioneering 16S rRNA gene. *Current opinion in microbiology* 11**,** 442-446.

Urbanczyk, H., Ast, J.C., and Dunlap, P.V. (2011). Phylogeny, genomics, and symbiosis of Photobacterium. *FEMS microbiology reviews* 35**,** 324-342.

Wade, W. (2002). Unculturable bacteria—the uncharacterized organisms that cause oral infections. *Journal of the Royal Society of Medicine* 95**,** 81-83.

Widder, E.A. (2010). Bioluminescence in the Ocean: Origins of Biological, Chemical, and Ecological Diversity. *Science* 328**,** 704-708.

Woese, C.R. (1987). Bacterial evolution. *Microbiological reviews* 51**,** 221.

Zaneveld, J.R., Burkepile, D.E., Shantz, A.A., Pritchard, C.E., Mcminds, R., Payet, J.P., Welsh, R., Correa, A.M., Lemoine, N.P., and Rosales, S. (2016). Overfishing and nutrient pollution interact with temperature to disrupt coral reefs down to microbial scales. *Nature communications* 7**,** 11833.

Appendix I

Laser Capture Microdissection for Light Organ Isolation

Laser capture microdissection (LCM) was developed in order to overcome limitations and drawbacks of current methods for isolating tissue samples (Emmert-Buck et al., 1996). Such methods were dissection of frozen blocks to enrich tissue samples, irradiation of manually inked-stained sections, and microdissection with manual tools (Emmert-Buck et al., 1996). With the development of LCM, it became a method to obtain subpopulations of tissue cells under direct microscopic observation (Espina et al., 2006). It can either harvest the target cells directly or cut away unwanted tissue from the target cells. This method provides histologically pure cell populations, especially important in pathology (Espina et al., 2006). The advantages of using LCM to isolate cells compared to previous methods is that it is simple, requires no moving parts and no manual steps that enable one-step transfer of cells/tissue. The transferred tissue retains its original morphology and it is performed quickly, whereas when manual microdissection was performed, it took many intensive and labor grueling hours to obtain the same results (Emmert-Buck et al., 1996).

This method is mainly used in the medical field, more specifically for pathology purposes. Today, it is branching out with its applicability and is even being implemented in the microbiology field. LCM can provide samples for a variety of downstream applications since it is compatible with a many tissue types, cellular staining and preservation methods (Espina et al., 2006). The samples can be used for molecular profiling of tissue, detecting and comparing cellular molecular signatures, and even cellular elements within microenvironments (Espina et al., 2006). More importantly, LCM can be used for real time- PCR (RT-PCR), genomic and proteomic profiling, and plant and cell biology (Espina et al., 2006). Previously hard and near impossible regions can now be reached and has become particularly useful in studying plant structures (Kerk et al., 2003).

With all of the advancements and applications of LCM, this study attempted to utilize this procedure in order to isolate the light organs of *P. atlanticum*. The isolation of the light organ would provide a more specific/concentrated bacterial population. The light organ is described to be about 20-30 μm in diameter deeming it a perfect candidate to undergo LCM for isolation. The goal was to be able to dissect out the pairs of light organs from each slide so there

was enough cells and DNA to amplify in PCR. The PCR product would then be used for 16S rRNA sequencing for a more concentrated population and compare that with the microbiome of the whole pyrosome.

Six samples were fixed in RNALater and one was fixed in 2% Glutaraldehyde in Sodium Cacodylate Buffered Sea-water fixative. In order to avoid contamination samples were hand processed instead of using a tissue processor. They underwent an ethanol series for dehydration, starting at 50% EtOH in order to rinse samples of the original fixative. They were then cleared using 100% xylene and molten Paraplast Plus®, then embedded in Paraplast Xtra®. Sections (4 μm thick) were made using the Leica RM 2125 microtome and mounted on Leica PEN (polyethylene naphthalate) slides. Sections were stained with Harris's hematoxylin and eosin following a modified protocol. The deparaffinizing stage included 3 xylene washes for 2 minutes each and 2 100% EtOH washes for 2 minutes each. The sections were then hydrated in 95% EtOH, then 80% EtOH, and DI H 2O for 2 minutes each. They sat in hematoxylin for 1 minute then the excess stain was washed in tap water. Then sections were placed in Eosin for 30 seconds and then destained for 45 seconds with 95% EtOH. They were then dehydrated in 2 washes in 100% EtOH for 3 minutes each. Sections air dried for 30 seconds then were checked using an Olympus BX43 light microscope. Samples were dissected out from slides using a Leica LMD 7000 laser capture microdissection microscope. Samples that were used for PCR were dissected out using 40x magnification with power 15, aperture 1, and speed 10 for the laser.

Once the samples were dissected using the LCM, they were checked for their DNA concentration using gel electrophoresis. The samples were identified to have no DNA and therefore unable to be amplified for sequencing. There are a few possible reasons as to why this procedure did not yield usable DNA. One being that a modified staining protocol was used and not the recommended protocol from Leica. Another is that Chelex solution was used for a one-step extraction instead of a specific LCM extraction kit. The sections used were about 4 μm thick instead of 8-10 μm, which could have not provided enough tissue to use. If this procedure were to be run again, samples would be thicker (10 μm) and the Leica protocol would be used for H&E staining. For extraction, the PicoPure DNA extraction kit would be used since it is tailored specifically for LCM products. Although this attempt was unsuccessful, it paved the way for incorporating a medical technique in a bacterial study. Using LCM on an organism other than a

human or even a plant could have greater implications in future research in other fields including microbiology.

Appendix II

R Code

Collection Maps – Courtesy of Dr. Rosanna Milligan

```
library(rgdal) ## Lets us read ESRI shapefiles into R
library(rgeos)
library(maptools)
library(tmap)
library(raster)
#library(SDMTools)
library(RNetCDF)
library(sp)
library(vegan)
library(plyr)
library(reshape)
library(marmap)
library(gridExtra)

#####################################################################

source("Functions/points_to_line.R")

#####################################################################

## To update, need (at a minimum) are your own lat / lon data in a .csv file with
## a column for "cruise", and a column for "day/night"

#all.stations <- read.csv("Combined ONSAP & NRDA datasheets for total abundance
analysis_NEW VOLUMES (JUL 2018).csv")
all.deepend <- read.csv("DEEPEND ALL DATA + MOCNESS + CHLA (MAR 2020).csv")
levels(as.factor(all.deepend$cruise_no))

all.deepend$cruise <- paste("DP0", all.deepend$cruise_no, sep="")

deployments <- ddply(all.deepend, .(cruise, deployment, day_night),
                     summarise,
                     "mean_lon" = mean(mean_lon),
                     "mean_lat" = mean(mean_lat))
```

```
#####################################################################

dp05 <- subset(deployments, deployments$cruise=="DP05")
dp06 <- subset(deployments, deployments$cruise=="DP06")

dp05 <- unique(dp05)
dp05 <- unique(dp06)

#####################################################################################
#Started Here for my data
gebco.bathy <- open.nc("GEBCO_2014_2D_-98.5833_17.3654_-78.5192_31.5321.nc")
print.nc(gebco.bathy)

tmp <- read.nc(gebco.bathy)
names(tmp)

## http://menugget.blogspot.com/2014/01/importing-bathymetry-and-coastline-data.html#more

z <- array(tmp$elevation, dim=dim(tmp$elevation))
z <- z[,seq(ncol(z))]

xran <- range(tmp$lon)
yran <- range(tmp$lat)
zran <- range(tmp$elevation)
lon <- tmp$lon
lat <- tmp$lat
rm(tmp)
close.nc(gebco.bathy)


colfunc <- colorRampPalette(c("darkblue","blue", "lightblue","lightblue","yellow", "orange",
"red"))

breakpoints <- seq(-1,1,0.1)
colfunc.manual <- colfunc(20)


## FOr colour maps, run this:
ocean.pal <- colorRampPalette(
  c("#000000", "#000209", "#000413", "#00061E", "#000728", "#000932", "#002650",
    "#00426E", "#005E8C", "#007AAA", "#0096C8", "#22A9C2", "#45BCBB",
    "#67CFB5", "#8AE2AE", "#ACF6A8", "#BCF8B9", "#CBF9CA", "#DBFBDC",
```

```
    "#EBFDED")
)

land.pal <- colorRampPalette(
  c("#336600", "#F3CA89", "#D9A627",
    "#A49019", "#9F7B0D", "#996600", "#B27676", "#C2B0B0", "#E5E5E5",
    "#FFFFFF")
)


## For black and white, run this:
#ocean.pal <- colorRampPalette(c("grey20", "grey80"))

#land.pal <- colorRampPalette(
#  c("#FFFFFF"))

zbreaks <- seq(-7500, 5500, by=10)
cols <-c(ocean.pal(sum(zbreaks<=0)-1), land.pal(sum(zbreaks>0)))

####### Temperatures

colfunc <- colorRampPalette(c("darkblue","blue", "lightblue","yellow", "orange", "red"))

breakpoints <- seq(7, 15, 0.1)
colfunc.manual <- colfunc(81)

#########

## In my datasets, I have some duplicated rows. If you don't, you can ignore this one step.
dp05n <- unique(subset(dp05, dp05$day_night=="Night"))
dp05d <- unique(subset(dp05, dp05$day_night=="Day"))

dp06n <- unique(subset(dp06, dp06$day_night=="Night"))
dp06d <- unique(subset(dp06, dp06$day_night=="Day"))


## DP05 & DP06 only

##Change to your own working directory

## DP05 & DP06 only

#(remove the ) # in front of the lines below to save your maps as jpeg files (don't forget the
```

```
## one in front of dev.off())

#jpeg(filename="Environmental Comparison Plots/DP05 locations.jpg", pointsize=48,
#     height=2400, width=3000, units="px")
windows(15,10)
image(lon, lat, z=z, col=cols, breaks=zbreaks, useRaster=TRUE, ylim=c(27, 31),
     xlim=c(-90, -84), xlab="Longitude", ylab="Latitude", asp=1/1)
box()

contour(x=lon, y=lat, z=z, levels=(0.0), col="black", lwd=1.5, add=T)
contour(x=lon, y=lat, z=z, col="grey30", levels=c(seq(-200, -5000, -500)), add=T,
       labels=c(seq(200, 5000, 200)), drawlabels=FALSE)
points(DP05$Lat~DP05$Lon, pch=17, lwd=2,  col="black", cex=2)
points(DP06$Lat~DP06$Lon, pch=17, lwd=2,  col="red", cex=2)
points(OER$Lat~OER$Lon, pch=17, lwd=2,  col="purple", cex=2)

legend("topright", legend=c("DP05", "DP06", "OER"), fill=c("red", "black", "purple"),
bg="white")#, bty="n")

#dev.off()


#jpeg(filename="Environmental Comparison Plots/DP06 locations.jpg", pointsize=48,
#     height=2400, width=3000, units="px")

image(lon, lat, z=z, col=cols, breaks=zbreaks, useRaster=TRUE, ylim=c(26, 31),
     xlim=c(-93, -85), xlab="Longitude", ylab="Latitude", asp=1/1)
box()

contour(x=lon, y=lat, z=z, levels=(0.0), col="black", lwd=1.5, add=T)
contour(x=lon, y=lat, z=z, col="grey30", levels=c(seq(-200, -5000, -500)), add=T,
       labels=c(seq(200, 5000, 200)), drawlabels=FALSE)
points(dp06d$mean_lat~dp06d$mean_lon, pch=21, lwd=2,  col="black", bg="white", cex=2)
points(dp06n$mean_lat~dp06n$mean_lon, pch=21, lwd=2,  col="black", bg="black", cex=2)

legend("topleft", legend="July 2018")#, bty="n")
legend("topright", legend=c("Day", "Night"), fill=c("white", "black"))#, bty="n")

#dev.off()
```

```
##DeepSearch only for Thesis- Modified Dr. Milligan Code
windows(15,10)
image(lon, lat, z=z, col=cols, breaks=zbreaks, useRaster=TRUE, ylim=c(26, 31),
     xlim=c(-93, -85), xlab="Longitude", ylab="Latitude", asp=1/1)
box()

contour(x=lon, y=lat, z=z, levels=(0.0), col="black", lwd=1.5, add=T)
contour(x=lon, y=lat, z=z, col="grey30", levels=c(seq(-200, -5000, -500)), add=T,
       labels=c(seq(200, 5000, 200)), drawlabels=FALSE)

points(OER$Lat~OER$Lon, pch=19, lwd=2,  col="black", cex=2)

legend("topleft", legend="June 2019", bg="white")
legend("topright", legend=c("OER"), fill=c( "black"), bg="white")#, bty="n")
```

Simper

```
dat <-table.from.biom
t.dat <- as.data.frame(t(dat))
dat <-t.dat
metadata<-pyro_meta_g
common.rownames <- intersect(rownames(dat),rownames(metadata))
dat <- dat[common.rownames,]
metadata <- metadata[common.rownames,]
all.equal(rownames(dat),rownames(metadata))
otu.abund<-which(colSums(dat)>2)
dat.dom<-dat[,otu.abund]
library(vegan)
library(base)
dat.pa<-decostand(dat.dom, method ="pa")
dat.otus.05per<-which(colSums(dat.pa) > (0.05*nrow(dat.pa)))
dat.05per<-dat.dom[,dat.otus.05per]
dat.ra<-decostand(dat.05per, method = "total")
dat.rat <- as.data.frame(t(dat.ra))
View(dat.rat) #double check it worked before making a txt file
write.table(dat.rat, "C:/Users/ajber/Documents/Lex_16S_data/dat.rat.txt", sep="\t",row.names =
T)

dat.simp<-simper(dat.ra, metadata$Sample.Type, permutations = 99)
sink("Simper_by_TYPE.csv")
summary(dat.simp)
sink()
```

Appendix III

Draft Manuscript

Microscopic and Genetic Characterization of Bacterial Bioluminescent Symbionts of the Pyrosome, *Pyrosoma atlanticum* in the Gulf of Mexico

Running title: Bioluminescent symbionts of the pyrosome

Alexis Berger, Patricia Blackwelder, Tracey Sutton, Nina Pruzinsky, Natalie Slayden, Jose V. Lopez

Halmos College of Natural Sciences and Oceanography, Nova Southeastern University, Dania Beach, FL 33004

Corresponding Author: Alexis Berger, a.j.berger@outlook.com

Abstract

The pelagic tunicate, *Pyrosoma atlanticum*, is known for its brilliant bioluminescence, but the mechanism causing this bioluminescence has not been fully characterized. This study identifies the bacterial bioluminescent symbionts of *P. atlanticum* collected in the northern Gulf of Mexico using various methods such as electron microscopy, light microscopy, and molecular genetics. The bacteria are localized within a specific pyrosome light organ. Bioluminescent symbiotic bacteria of Vibrionaceae composed >50% of taxa in tunicate samples (n=13), which was shown by utilizing current molecular genetics methodologies. While searching for bacterial lux genes in 2 tunicate samples, we also serendipitously generated a draft tunicate mitochondrial genome which was used for *P. atlanticum* pyrosome identification. Furthermore, a total of 396K MiSeq16S rRNA reads provided pyrosome microbiome profiles to determine bacterial symbiont taxonomy. After comparing with the Silva rRNA database, a 99% sequence identity matched a *Photobacterium sp. R33*-like bacterium (which we refer to as *Photobacterium Pa-1*) as the most abundant bacteria within *P. atlanticum* samples. Specifically-designed 16S rRNA V4 probes for fluorescence in situ hybridization (FISH) verified the *Photobacterium Pa-1* location around the periphery of each pyrosome luminous organ. Scanning and transmission electron microscopy (SEM, TEM respectively) confirmed a rod-like bacterial presence which also appears intracellular in the light organs. This intracellular bacterial localization may represent a bacteriocyte formation reminiscent of other invertebrates.

Keywords: symbiosis, bioluminescence, Pyrosome, microscopy, 16S, high throughput sequencing

Introduction

Bioluminescence is an important adaptive trait in ocean dwelling taxa and appears to be more prevalent than previously thought (Martini and Haddock, 2017). Over 700 animal genera are known to include luminous species, with more than 80% being marine organisms(Widder, 2010). Within this group, 90% of pelagic organisms between 200-1000m are known to have bioluminescent capabilities. In addition, fishes, squid, and shrimp are able to modify aspects of their light production, such as the intensity, kinetics, wavelength, and angular distribution. The emission of light by organisms has evolved independently over 40 times in marine and terrestrial organisms(Haddock et al., 2010). This emphasizes the evolutionary importance of the bioluminescence mechanism (Haddock and Case, 1999). There are several critical ways bioluminescence can aid an organism's survival. Bioluminescence can facilitate food location and capture, attract a mate, allow for species recognition, and functions as a defense mechanism (Widder, 2010).

With regard to bioluminescence, the tunicate pyrosomes derive their name from the Greek words pyro ("fire") and soma ("body") from the "fiery" bioluminescence that is produced at night (Sutherland et al., 2018). Pyrosomes were classified by Lamarck and Huxley under the subphylum Tunicata (previously known as Urochordata) due to the zooids that composed these organisms being encased by a tunic (Huxley, 1851;Lemaire and Piette, 2015). Pyrosomes are approximately 95% water and are extremely well adapted for rapid growth and efficient energy use. Transparency makes pyrosomes difficult to see at any depth, which is why they can be found throughout the pelagic realm. Aside from being transparent, and of limited nutritional value, pyrosomes have few sensory or predator-avoidance adaptations. Most biological processes, such as feeding, respiration, and swimming occur simultaneously through contraction of the same muscles (Alldredge and Madin, 1982).

Pyrosome tunicates remain one of the least studied planktonic grazers, despite their widespread distribution and ecological significance. Pyrosomes are characterized as highly successful planktonic grazers, and swarms of these colonies can consume substantial amounts of phytoplankton (Alldredge and Madin, 1982;Décima et al., 2019). The tunicates have been noted for their potential to restructure the food web when aggregating in large quantities (Sutherland et

al., 2018). The species of our study *Pyrosoma atlanticum* been observed since the 1840s worldwide and can be found in tropical and temperate waters ranging from 45°N to 45°S.

Bioluminescence in planktonic colonial tunicates is not as common as in other pelagic organisms (Haddock et al., 2010). The pyrosome is the most well-known example of bioluminescence in colonial tunicates, but it has recently been found that two other urochordate groups have luminous members. A deep-sea doliolid was recently described to have bioluminescence (Robison et al., 2005) as well as a shallow living benthic ascidian, *Clavelina miniate* (Aoki et al., 1989;Chiba et al., 1998;Hirose, 2009). The bioluminescence mechanisms are not well understood in these tunicates, but in Appendicularians they secrete luminous inclusions or use a coelenterazine + luciferase system (Galt and Sykes, 1983;Galt and Flood, 1998). Pyrosome bioluminescence appears unique compared to other pelagic organisms and is likely to be bacterial in nature (Mackie and Bone, 1978). The bacterial origin of luminescence is generally proposed on the basis of microscopic observation of bacteria in the light organ. The bacteria-like cells in the light organ of *Pyrosoma atlanticum* are intracellular and may have undergone considerable biochemical specialization (Mackie and Bone, 1978;Holland, 2016). However, since these symbionts have not been successfully cultivated, little is known about the physiology of the microbial symbionts associated with bioluminescence.

Microbial symbionts occur in almost every organism and many partnerships have not been sufficiently studied (McFall-Ngai et al., 2013). Discrete and innovative symbioses are widespread throughout the oceans, ranging from tropical and temperate coastal regions (e.g. coral reefs) to midwater and deep-sea habitats (e.g. brine pools) (Cordes et al., 2009;Roth, 2014). Luminous bacteria are all Gram-negative, non-spore-forming, have cell walls difficult to penetrate, are motile, and are generally chemoorganotrophic (Dunlap, 2009). Bioluminescent symbiosis is fundamentally different than other types of symbiotic associations (Dunlap, 2009). With most microbial mutualisms, the host relies nutritionally on the microbial symbiont, such as chemosynthetic bacterium or photosynthetic algae, and without these symbionts, the host growth suffers significantly (Dunlap, 2009). In bioluminescent symbioses, the host without bacterial symbionts has been found in laboratory settings to grow and develop at the same level as its counterparts with their bioluminescent bacterial symbionts (Dunlap, 2009). Another distinctive feature is that many bacterial bioluminescent symbionts appear to be extracellular, suggesting a

facultative association, whereas in obligate symbiosis the bacteria are found intracellularly (Dunlap, 2009). Even though most bacterial symbionts are extracellular, there are a few that appear intracellularly. The intracellular luminescent bacteria differ morphologically and biochemically from almost all other bacteria since they appear longer than oval or subspherical rods and without granules (Mackie and Bone, 1978). The present study on a relatively unknown pelagic tunicate, *P. atlanticum*, intends to reveal various aspects of its bioluminescence such as its ultimate source, anatomical and cellular location

Methods

Sample Collection and Fixation

Tunicate samples were collected through the Deep Pelagic Nekton Dynamics of the Gulf of Mexico (DEEPEND) consortium (Milligan et al., 2018). In 2017, a number of midwater trawls were conducted on DEEPEND Cruise DP05, during which various species of fish, crustaceans, cephalopods, and other pelagic species were collected from the Gulf of Mexico, among those was *P. atlanticum.* Five individuals were stored in dimethyl sulfoxide (DMSO) in our Microbiology and Genetics Laboratory at Nova Southeastern University after DEEPEND cruises. In addition to these 2017 samples, 29 more samples were collected from the Gulf of Mexico on the July 2018 DEEPEND Cruise DP06. Samples were collected from depths of 0-1500 meters at multiple collection sites for both cruises and stored in DMSO and RNALater. However, only 2 samples were viable candidates for genetic sequencing (Table 1'). In 2019, an additional 12 *P. atlanticum* samples in the Gulf of Mexico were collected during the NOAA DeepSearch Cruise aboard the R/V Point Sur (Supp. Fig. 1'). A total of 15 samples from 3 cruises to utilize for the several methodologies employed in this study (Table 1').

Light and Fluorescence Microscopy (Histology)

Samples were fixed in 2% Glutaraldehyde in Sodium Cacodylate Buffered Sea-water fixative. They were placed in 70% EtOH overnight and processed through a graded series of ethanols, cleared, and infiltrated with molten *Paraplast Plus*®, and embedded in *Paraplast Xtra*®. Using a Leica RM 2125 microtome, 4 μm thick sections were cut and mounted on microscope slides. Sections were then stained with Harris's hematoxylin and eosin. Slides were examined using an Olympus BX43 light microscope at 4–60x magnification. Fluorescence

microscopy was performed on an Olympus IX70 Fluorescence Microscope with green (500-570nm) and red (610 ~750nm) filter cubes. Bacteriocytes were counted in section using the histology sections. A structure was considered a bacteriocyte if it was dark and within the interior of the light organ. Further estimations of the quantity of bacteria able to fit within the light organ used TEM and SEM micrographs in addition to the light micrographs.

Electron Microscopy – Scanning and Transmission

SEM samples were stored in a 2% glutaraldehyde in sodium cacodylate buffered seawater fixative. Pyrosomes were dissected in the fixative and divided into three sections per sample. They were rinsed three times in sodium cacodylate buffered sea water, postfixed in 1% osmium tetroxide, rinsed in the sea water buffer, dehydrated through a graded series of ethanol (20, 50, 70, 95, and 100%), and dried in hexamethyldisilazane (HMDS). Dried samples were outgassed overnight, coated with palladium in a sputter coater, and examined in a Philips XL-30 Field Emission SEM at the University of Miami Center for Microscopy (UMCAM) located in the Chemistry Department at the University of Miami Coral Gables Campus.

TEM samples were prepared similarly to SEM except that samples at the last dehydration step (100% ETOH) were embedded in Spurr resin and polymerized for 3 days at 60°C. Blocks were trimmed, sectioned, floated onto grids, stained with either Uranyl Acetate and/or Lead Citrate and examined in a JEOL 1400X TEM located at the University of Miami Miller School of Medicine TEM Core Lab. Semi-thin sections of TEM prepared samples were examined in an IX-70 fluorescent microscope to examine gross structures.

DNA Extraction and Polymerase Chain Reaction (PCR)

Total microbiome DNAs were extracted with the standard protocol for the Qiagen PowerLyzer PowerSoil kit. this study focused on amplifying the 16S gene of the unknown bacteria in the luminescent organ of the pyrosome. Once DNA extractions were completed, the polymerase chain reactions (PCR) was run using Invitrogen Platinum Hot Start PCR Master Mix (2x) and the universal primers 515F and 806R. The 515F and 806R primers were used to amplify the 200bp sequence of the V3 and V4 region of the 16S gene (Caporaso et al., 2011;Easson and Lopez, 2019). The PCR products were cleaned via AMPure XP beads. This process was used to purify the 16S V3 and V4 amplicon away from free primers and primer dimer species.

(Chakravorty et al., 2007). The final DNA concentration was checked using a Qubit2.0 (Life Technologies).

Illumina High- Throughput Metagenomic Sequencing

The 16S rRNA gene fragment was the target for bacterial identification via high throughput sequencing (Easson and Lopez, 2018;O'Connell et al., 2018). Samples were prepared for sequencing following the 16S Illumina Amplicon Protocol per the Earth Microbiome Project (Kuczynski et al., 2011;Thompson et al., 2017). The final PCR products were checked for their DNA concentrations using a Qubit 2.0, which is a fluorometer created to precisely measure nucleic acids or proteins. Once concentrations were obtained, each sample was diluted to a normalization of 4pM. All DNA samples were library pooled and rechecked on the Qubit to make sure the concentration is between 4-6 ng/μL. A final quality check was done using an Agilent Bio analyzer Tapestation 2000, which reads the quality of the template DNA and for any possible contamination.. The final product was loaded into an Illumina MiSeq system for 16S metagenomics DNA at 500 cycles using V2 chemistry. The sequencing followed a modified Illumina workflow protocol.

Mitochondrial and Microbiome Sequencing and Analysis

For whole genome sequencing, the Illumina Nextera XT DNA Sample Prep Kit was used for library preparation previously described (Urakawa et al., 2019). A final quality check was done using an Agilent Bio Analyzer Tapestation 2000 as well. The Illumina MiSeq was used for sequencing, running samples at 300 cycles (for 150 bp library) due to the small library sizes of 254 and 292 bp. For genome assembly and annotation, Galaxy and Blast2Go were utilized (Götz et al., 2008;Afgan et al., 2018).

The Quantitative Insights into Microbial Ecology v.2 (QIIME2) pipeline was used to demultiplex, quality filter, assign taxonomy, reconstruct phylogeny, and produce diversity analysis and visualizations from the FASTQ DNA sequence files (Caporaso et al., 2010). The quality filtering and trimming of the data was conducted in DADA2, which was used to create a feature table that was utilized in R Studio. The QIIME2-generated sequences were assigned taxonomy through a learned SILVA classifier (silva-132-99- 515-806-nb-classifier.qza). This feature table was used for SIMPER statistical analysis in R Studios. A SIMPER analysis was

used to determine which taxa are driving the differences in the water and pyrosome samples (Rees et al., 2004). Additional comparisons were made in CosmosID, a bioinformatic pipeline used for microbial analysis that employs a phylogenetic and k-mer based approach to metagenomics. FASTQ files were uploaded to CosmosID, which provided relative abundance described in a heatmap comparison. Further data analysis used 16S rRNA multiple sequence alignments with MAFFT, the Multiple Alignment using Fast Fourier Transform program (Katoh and Standley, 2013) in order to generate a phylogeny to compare the extracted 16S sequence from the MiSeq run with known luminescent bacterial species. Pyrosome sequences have been deposited to the NCBI Sequence Read Archive (#PRJNA636187).

Fluorescence in situ hybridization (FISH)

Pyrosome (*P. atlanticum*) samples were stored in paraformaldehyde and dehydrated through an ethanol series, cleared in xylenes, and infiltrated with paraffin. Serial sections were cut at 4 μm and 8 μm and mounted. They were then deparaffinized with xylene and ethanol series (100-70%). After mounting the sections, specialized probes were added to localize the bacteria within the light organs of the pyrosome. Optimal probe sequences were designed by using MAFFT alignments (Katoh and Standley, 2013). MAFFT utilized the novel tunicate 16S rRNA sequences of the Illumina MiSeq run we generated, combined with previously determined 16S sequences from various bacterial species (DQ889917, DQ889916, DQ889915, DQ889914, DQ889913) from NCBI database to find the most specific V4 region of *Photobacterium sp. r33* for the probe to identify bioluminescent symbiont location within the pyrosome zooid (Table 2). The alignment is shown as a supplementary figure (Supp. Fig. 1).

MAFFT aligned the 16S rRNA sequences from the selected samples. The *Photobacterium* sequence, TTCAGGTGTAGCGGTGAAATGC, was chosen because it specific to *Photobacterium* in the most variable V4 region alignment. This signified that there was no similarity in this sequence with the various bacterial sequences chosen for comparison. The high specificity was required in order to specifically detect the *Photobacterium* in FISH prepared slides. The probes were then tested on NCBI PROBE Database (www.ncbi. nlm.nih.gov/probe) and Microbial Ribosomal Databases Probe Match (http://rdp.cme.msu.edu/probematch/search.jsp) (Negandhi et al., 2010).

Labeled probes for FISH were manufactured by IDT Inc (Iowa, US) The dye used for the *Photobacterium*-specific probe was Cy3, which is a standard orange-fluorescent label for nucleic acids and was attached at the 5' end (Table 3). The control probe EUB338 is a universal bacteria probe and was dyed with 6-FAM (fluorescein)(Negandhi et al., 2010). FAM (fluorescein) is the most commonly used fluorescent dye attachment for oligonucleotides and this particular dye was attached at the 3' end and will appear green. The probes attach to one end or the other to allow for overlap. This is possible because the two probes' nucleotide sequences are at different location on the ribosome (either the 5' or 3' end). When imaging the samples, only orange and green fluorescence should appear, and red fluorescence should be excluded due to double binding. This means both probes should bind to the targeted *Photobacterium sp.* which will present the orange fluorescence with the rest of the bacteria appearing green.

FISH protocols followed closely to previously described methods (Sharp et al., 2007;Negandhi et al., 2010). For example, FISH hybridization buffer (35% formamide) was made to contain 5M NaCl, 40 µl 1M Tris-HCl, 700 µl formamide, 900 µl H_2O, and 2 µl 10% SDS, and applied as 45 µl mixed with 5 ng/µl of the desired probe, for a total of 50 µl per slide. Pyrosome tissues were then incubated inside a humidity chamber with a paper towel that was saturated with the hybridization buffer for 2 hours at 46°C. After hybridization, slides were put in a buffer wash for 20 minutes at 48°C (buffer consists of 700 µl 5M NaCl, 1 ml 1M Tris-HCl, 500 µl 0.5 EDTA, 50 ml H_2O, and 50 µl 10% SDS). Slides were quickly rinsed with dH_2O and air dried.

FISH was performed on three samples with two sections each. The control runs utilized probe EUB338. In addition to the control, a slide with no probes as well as slides with both EUB338 and *Photobacterium* probes were hybridized. This allowed for an autofluorescence assessment and aided in eliminating background noise. Slides were examined using an Olympus IX70 Fluorescence Microscope with green (500-570nm) and red (610 ~750nm) filter cubes.

Results

Structure and Morphology of the Light Organ: Light and Fluorescence Microscopy

Light and fluorescent microscopy were able to identify the *P. atlanticum* luminous light organs, as well as any potential microbes observed. Due to the visible location of light organs in the tissue, it was straightforward to determine where the organs were in thin section, and anatomical structural features were evident even in unstained sections. The light organ and bacteria were well resolved under light microscopy, with the buccal siphon and the light organs, located on each side, clearly identified (Fig. 1a'). The left and right light organs were usually fully intact with the 30-50 μm luminous organ well resolved (Fig. 1a'). The light organs were oval shaped structures, with each exhibiting a nodule at the end. Within the light organ, there was a clear space in the center, with the bacteria clustered around the interior. At higher magnification, it is evident that what appear to be bacteria are clustered in the light organ with as many as 72 bacteriocytes evident in a single light organ (Fig. 1b'). This value was calculated by counting the number of dark structures within the light organ.

Sequencing of *P. atlanticum* Microbiomes and Partial Mitochondrial Genome

A total of 13 samples were sequenced, encompassing 3 *P. atlanticum* and 10 seawater samples. The seawater samples were sequenced at a different time by Easson and Lopez (Easson and Lopez, 2019). The samples are meant to give a general profile for comparison. In all three pyrosome samples, *Photobacterium sp. r33* showed the best match to the most abundant 16S rRNA sequences in our pyrosome microbiomes (Table 3). In order to confirm the identity of the symbiont, the sequence derived from the MiSeq run was aligned with the sequence of *Photobacterium sp. r33* from NCBI (Fig. 2'). This was done through the NCBI BLAST program (https://blast.ncbi.nlm.nih.gov/Blast.cgi). This alignment showed it was a 99% match with only a single base pair that was different. To compare tunicate microbiomes with seawater, each pyrosome sample was matched to a previously sequenced seawater microbiome at depth corresponding to the tunicate collections. Seawater samples were from two different sites at the same sample depth of 1500m. A total of 396K MiSeq reads and 497 Amplicon Sequence Variant (ASV) were produced.

In the 10 CTD samples, the relative abundance of *Photobacterium sp. r33* appears less than 0.12 %, while in DMSO1 it was 74.20%, RNALater6 had 70.88%, and RNALater7 had 39.60%. These numbers were calculated through CosmosID. When pyrosome samples are compared to the water samples from the same trawl depths (Easson and Lopez, 2018), there are dramatic differences in diversity of bacterial types between the pyrosome and water samples (Fig. 2'). The water samples showed a diverse bacterial community while all three pyrosome samples had more homogenous microbiomes. The top two bacterial taxa in the pyrosome samples are *Photobacterium sp. r33 and Vibrio_us* (unidentified species). *Photobacterium, Vibrio, Enterovibrio, and* Vibrionaceae are known luminescent genera and family (Hastings and Nealson, 1977), respectively, and they comprise about 50% of the most abundant bacteria found in the pyrosome samples (Fig. 2') (Hastings and Nealson, 1977). There are over a 1100 bacterial species found in the water samples.

In an effort to find detect and characterize *lux* genes of a bacterial photosymbiont causing bioluminescence, we ran a whole genome Illumina sequencing run. Unfortunately, bacterial *lux* genes were not detected in the assemblies. However, a mitochondrial DNA contig of 14,302 base pairs (bp) long was generated serendipitously with 26X coverage. The mtDNA sequences provided an opportunity to gain a genetic basis for the taxonomic identity of *P. atlanticum.* We found the closest match to *P. atlanticum* was another o thus found carried out a preliminary phylogeny based on the mitochondrial cytochrome oxidase subunit 1 (COI) genes shows how distinct *P. atlanticum* is from other tunicate species (Supplemental Fig. x), especially between another pelagic tunicate.

Fluorescence *in situ* Hybridization (FISH)

Under fluorescence microscopy, the pyrosome exhibited a considerable amount of autofluorescence. However, the bacteria were clearly discernable (Fig. 1'). If histology sections are compared with those prepared for FISH analyses, similar orientation, and morphology of the two light organs is evident (Fig. 3'). Shown in both methodologies are the putative "bacteriocytes" containing bacteria concentrated at the outer edges of the organ with a clear space in the center.

Control FISH included pyrosome sections that was incubated with no fluorescent probes. The control sections reflected native background autofluorescence and did not display the degree of fluorescence seen in sections hybridized with probes (Fig. 3a'). This comparison shows that the probes appear to be annealing specifically to their respective DNA targets and producing a signal after stringent washing. The pair of light organs illuminated without a probe, but not as brilliantly as when the EUB338 and *Photobacterium* probes were used (Fig. 3b'). The signal produced with both probes was very intense and, as anticipated, bacteria other than those in the light organ, can be seen emitting a signal. Due to the light intensity, the shutter on the microscope was partially closed for the sections hybridized with probes while the sections with no probes were imaged with the shutter remain fully open.

The EUB338 probe is designated as the universal bacteria probe and is designed to bind to almost all bacteria within the sample. As expected, the fluorescent signal is apparent not only in the light organ, but also in surrounding tissue as well (Fig 3c'). Most bacteria emit a slightly green signal. The morphology of bacteria is different in the tissue throughout the section, ranging from coccoid in the light organ, to bacterium with flagella-like structures in the tunic. When the *Photobacterium* probe was employed, only the light organ emitted a signal (Fig. 3d'). Other areas of the tunic do not emit a signal, confirming that the photobacteria were concentrated in, and were not present outside, the light organ.

When the EUB338 and *Photobacterium* probes were combined, variability in the intensity of signal emission was evident. *Photobacterium Pa-1* was brightest when both probes were combined. For example, under the green filter, the bacteria are seen as in previous observations, concentrated around the outer edges of the light organ with a clear space in the center (Fig. 3e'). When the red filter is used, the same outer edges are packed with *Photobacterium Pa-1* fluorescing orange (Fig. 3f'). This orange fluorescence confirms the presence of *Photobacterium Pa-1* in the light organ.

Fine Structure and Bacterial Cluster Location in *P. atlanticum* (SEM)

SEM was utilized to discern high resolution three dimensional fine structural details of *P. atlanticum* and the bacteria associated with the light organ. Confirmation of observations made in the light microscopy and FISH analysis described in the previous section was a goal of this

analyses. In some cases, the light organ was located intact within parts of the tunic, with crystalline structures near the bacterial clusters (Fig. 4').

Ultrastructure of the Microbial Population in *P. atlanticum* (TEM)

The microbial cells appear intracellular and associated with mitochondria (Fig. 5a'). Their intracellular location is confirmed by observation of a cell membrane that encases both microbial cells and mitochondria (Fig. 5a'). Cells containing these bacteria are associated with abundant mitochondria and endoplasmic reticulum (Fig. 5a, 5b'). In some cases, the mitochondria are closely associated with the bacteria (Fig. 5a'). Clusters of microbes and mitochondria are shown for comparison (Fig. 5a'), and these membrane-bound bacteria cell clusters are reminiscent of "bacteriocytes", which are eukaryotic structures or cells that contain multiple bacteria in intracellular vacuoles. The bacteria can be easily distinguished from the mitochondria by the presence of prominent cristae in the mitochondria (Fig. 5a'). In some cases, the bacteria are clustered around an "opening" that suggests excretion activity (Fig. 5c'). It appears that fluid filled vesicles are pinching off and moving to the extracellular environment. The nature of these is unknown, or whether these excretory products are associated with bioluminescence.

Discussion

P. atlanticum Structure of the Light Organ

The light organ of *P. atlanticum* appeared to conform to previous depictions (Holland 2016). This study now shows the first detailed image and genetic analyses (light, TEM, SEM, FISH, and 16s rRNA sequencing) of *P. atlanticum*, with *Photobacterium sp. r33*-like bioluminescent symbionts contained intracellularly in "bacteriocytes". The bacteriocytes can be found packed around the outer edges of the light organ. Therefore, our data suggest an intracellular location of *Photobacterium Pa-1* in bacteriocyte cells. These cell types have intracellular vacuoles which contain multiple bacteria, and have been found in several different marine holobionts including tunicates (Kwan et al., 2012;Lopez, 2019).

Source of Bioluminescence in *Pyrosoma atlanticum*

We have now demonstrated a likely bacterial source for bioluminescence in *P. atlanticum* which appears as the closest match to *Photobacterium sp. r33*. However, we cannot unequivocally claim the identity without further genomic data (Fox et al., 1992;Janda and Abbott, 2007). The genus *Photobacterium* is known to show substantial ecophysiological diversity, which includes free-living, symbiotic, and parasitic lifestyles (Labella et al., 2017). The bioluminescent species, in particular *P. aquimaris, P. damselae, P. kishitanii, P. leiognathi,* and *P. phosphoreum,* exhibit free-living and symbiotic lifestyles. They can be found in dense populations associated with tissues in the light organs of their selective hosts (Labella et al., 2017). These tissues could be reflectors, shutter lens, or other tissues that are used to control, target, and diffuse the bacterial light produced from the organisms' body (Urbanczyk et al., 2011). Some of the hosts of *P. kishitanii* and *P. leiognathi* are marine fish, squid, and octopus. However, *P. leiognathi* has established a highly specific symbiosis with fish families Leiognathidae, Acropomatidae, and Apogonidae, while *P. damselae* has been found to form a symbiosis only with damselfish (Labella et al., 2017). Similar host specificity is exhibited by *Photobacterium Pa-1* as indicated by the high relative abundance of *Photobacterium sp. r33* from 16S sequencing as well as the micrographs from light microscopy. SEM, TEM, and FISH confirm that *Photobacterium Pa-1* inhabits the light organ of *P. atlanticum*.

Photobacterium sp. hosts range from fish to squid and are found throughout the water column. The bacterially luminous fish are widely distributed in coastal demersal, epibenthic, and pelagic waters (Urbanczyk et al., 2011). The fishes that house *P. leiognathi* and *P. mandapamensis* are more commonly found in shallower and warmer waters, whereas *P. kishitanii* can be found in fish inhabiting deeper waters (Dunlap et al., 2007;Kaeding et al., 2007;Nelson et al., 2016). The pelagic tunicate, *P. atlanticum*, can now be added now as a host of *Photobacterium Pa-1*.

Symbiont location

Several control probe controls were used to demonstrate that *Photobacterium Pa-1* was located in the light organ of *P. atlanticum.* The protocol of using sections taken from the same individual, with different probes demonstrated this. Although in microscopy there is, by its

nature variability in orientation, the light organ itself may exhibit some variability in morphology in micrographs. However, in the FISH analyses the signals produced essentially remain the same. In some cases, the probe was very bright, and the microscope shutter had to be partially closed in order to record an image. This also explains why some images have a green or red tint compared to those with no probes. The probes likely emitted a strong signal because of the number and specificity of hybridized probes. The hybridization was also effective because of the formamide concentration used (35%) within the buffer. This concentration is important because formamide serves to lower the DNA melting temperature that allows for hybridization to occur without compromising the stringency of the probe (Meinkoth and Wahl, 1984).

The EUB338 probe bound to more bacteria than the *Photobacterium* probe due to having a more conservative rRNA sequence than the variable region V4 of the *Photobacterium*. The EUB338 probe fluoresced a greenish tint under the green filter cube (500-570nm) and produced more signals than the *Photobacterium* probe. With this general probe a wider variety of bacteria was shown throughout the zooids. The red filter cube (610~750 nm) served as the defining filter for the *Photobacterium* probe. The EUB338 probe showed that all bacterium fluoresced red and not orange while the slides with both probes or the solely *Photobacterium* probe fluoresced orange while using the red filter cube. What made the red filter the distinguishing factor was the fact that *Photobacterium* fluoresced orange while the other bacteria fluoresced red. The orange fluorophores confirmed that *Photobacterium Pa-1* was located in the light organ. All the results described above demonstrate the presence of bacteria in the light organ using all methods employed: light, fluorescence, electron microscopy, or genetic techniques.

P. atlanticum Bacteria Morphology

Bacterial symbionts have been described in many marine invertebrates (McFall-Ngai et al, 2013; Lopez 2019), however only one paper has produced a description of the ultrastructure of photogenic organelles assumed to be bacteria in pyrosomes (Mackie and Bone, 1978). There is precedence for bacteria to be contained intracellularly or within bacteriocytes, including tunicates (Kwan et al., 2012). The *P. atlanticum* photobacteria were found to be exclusively coccoid in morphology and 1-2 μm in diameter, in agreement with previous bacterial ultrastructural descriptions in other eukaryotic hosts (Nealson et al., 1981). The SEM, TEM, light microscopy, and histology images produced a more detailed description of the bacteria found in

P. atlanticum than in any previous work done on pyrosomes. Extracellular and free living bacterial symbionts are typically rod shape and are more elongated (Nealson et al., 1981) than the bacteria present in the pyrosomes. With the morphological similarities to Gram-negative bacteria, this provides strong support that these cells are of microbial origin aiding in the validation of the hypothesis that *P. atlanticum* uses bacterial symbiosis in their bioluminescence mechanism (Dunlap, 2009). Gram staining could not be done directly on the bacteria because neither they, nor the light organ, could be isolated.

Distribution and Acquisition of Bacteria in Organisms Related to Bioluminescence

In context of the mechanisms of bioluminescence, thus far both microbial and mineralogical evidence of the interaction between microbes and pyrosome cells has been generated. The SEM and TEM findings of degraded microbial cells supports the concept of the release of enzymes by the bacteria, with subsequent loss of bacterial cell function. Clusters of bacteria at the interior borders of the cells in the light organ, as well as of fluid filled vesicles migrating to the extracellular environment suggests the presence of an excretory function.

Previous work on *P. atlanticum* had not determined whether the bacteria are intra- or extracellular, and only one study has hypothesized an intracellular organization for pyrosome bacterial symbionts (Nealson et al., 1981). The current study provides strong evidence of an intracellular location of the bacteria through visualizing the light organs in light, fluorescence, and electron microscopy. Intracellular organization, in conjunction with host mediated bacteriocyte structure, indicates a highly interdependent and specialized biochemical relationship between the bacteria and host cells (Nealson et al., 1981). Our current microscopy data provide the first evidence an intracellular configuration for these bacterial symbionts in *P. atlanticum*. Intracellular symbionts represent the most highly adapted of bacterial symbionts (Shigenobu et al., 2000), which would be the case of the highly adapted bioluminescent bacterial symbionts found in *P. atlanticum*.

The intracellular feature also brings up questions of how the *Photobacterium Pa-1* symbiont may be acquired. There is much to be learned when it comes to how and when the hosts of *Photobacterium* initiate symbioses. *Nuchequula nuchalis* and *Siphanic versicolor*, both fish species, have light organs that develop before the symbiotic bacteria are acquired (Urbanczyk et al., 2011). This poses the question of whether there is horizontal or vertical

transmission of microbial symbionts in these hosts. Horizontal transmission is the acquisition of symbionts from the environment, while vertical transmission is the inheritance of symbionts from previous generations (Bright and Bulgheresi, 2010). In deep-sea ceratioid fishes it is believed that the bioluminescent symbionts are acquired from the environment during the larval migration of the fish from surface waters to the bathypelagic water, albeit in low levels of abundance (Freed et al., 2019). These symbionts were found in low levels of abundance in both mesopelagic and bathypelagic zones which suggest that the microbes are not obligately dependent on the hosts for growth. Anglerfish appear to not acquire their photosymbionts that illuminate esca from the environment until they mature and move to lower depths (Freed et al., 2019). In one of the best examples of horizontal transmission, bioluminescent *Vibrio fischeri* symbionts appear to move freely from the environment to a residence within the Hawaiian Bobtail squid via special ducts (Nyholm and McFall-Ngai, 2004). The light organ crypts have a small window for *V. fischeri* to inoculate - between 30 and 60 minutes after hatching do these crypts open (Nyholm and McFall-Ngai, 2004).

In the case of *P. atlanticum*, the data show (Table 4) that for *Photobacterium Pa-1,* transmission is most likely vertical. Finding a relative paucity of *Photobacterium Pa-1* sequences in our large pelagic GoM dataset (of Easson and Lopez 2019), support that the bioluminescent symbiont is probably transmitted vertically. The seawater samples showed virtually no presence of *Photobacterium sp. r33-like sequences* (0.0-0.12%) compared to pyrosome samples which contained a dominant concentration of 40-74% of the symbiont. Since *P. atlanticum* is specifically known to reproduce both sexually and asexually through internal fertilization and budding (Holland, 2016), vertical transmission of the *Photobacterium sp. r33* symbiont is plausible. The 16S rRNA analyses and micrographs support the concept that the acquisition of symbionts is through vertical transmission. However, we realize that full confirmation requires an analysis of pyrosome larvae which is beyond the scope of this study.

Association with mitochondria

Photobacteria were found previously associated with mitochondria inside pyrosome cells (Nealson et al., 1981). It has been noted that there are several similarities between the respiratory chain of mitochondria and bioluminescent bacteria (Rees et al., 1998;Bourgois et al., 2001). Bacterial luciferase has previously been viewed as “an alternative” electron transport pathway,

however, it is actually considered an “alternative” oxidase (Bourgois et al., 2001). This is why the entire photogenic system of bioluminescent bacteria scavenges not only reducing equivalents (luciferase), but also ATP and NADPH. The close association also ties into the fact that the organism needs to consume a certain amount of energy to produce the visible spectrum of the bioluminescent light (Rees et al., 1998). In most cases it would be the blue photon (~470 nm), which requires about 255 J mol^{-1}. The fact that bioluminescence requires a lot of energy and mitochondria produces ATP, might explain why the mitochondria and microbes are so closely associated and densely packed into the cells (Bourgois et al., 2001).

Light microscopy revealed microbial localization within the luminous organ, and the bacterial symbionts were identified by FISH. TEM clearly indicated intracellular bacteria concentrated in the organ. There were approximately 60 bacteriocytes found in a single light organ in light microscopy. Precise estimates of bacteriocyte numbers could be due to the plane in which tissues were sectioned, so there may likely more *Photobacterium sp.* per cell than that observed using EM. In each micrograph, regardless of the type of microscopy used, the bacteria were concentrated on the interior border of the cells, while the bacteriocytes made up the periphery of light organ itself, surrounding a non-cellular space in the center. This begs the question as to what point do the bacteria concentrate at the edges.

It can be estimated that as many as 480~1200 bacteria can be found within the *P. atlanticum* light organ, based on visualization of 5-7 bacteria within a single bacteriocyte (Fig. 5) and the volume of the light organ. To determine if the orientation of bacteria in the luminous organ plays a role in the production of, or stages in, luminescence production would pose interesting questions future research. The observation of secretion from the light organ to the extracellular environment in the TEM images suggests some compounds are being excreted from the light organ. The nature of these is not known but suggests they may be involved in the production of light.

Future Work

A comparative study of the light organ and body of the pyrosome, in terms of the microbiome present, could show even more specificity of the symbionts in the light organ. It is estimated that less than 2% of bacteria can be cultured in a laboratory setting (Wade, 2002), so being able to culture a highly specific bacteria would add to the ground work for studying

intracellular bacteria in a laboratory setting without the host organism. A comparative study of the light organ and whole body would also build on extraction techniques using Laser Capture Microdissection (Berger, 2020).

Future work could focus on the ultrastructure during stimulated bioluminescence and compare it to pyrosomes which have not been stimulated. This would elucidate potential ultrastructural variability related to these mechanisms. The bacteria have been seen in differing states of degradation and clustering in the SEM and TEM micrographs. In previous studies, the luciferase assayed from the disrupted pyrosomes displayed fast kinetics akin to that of *Photobacterium* species (Nealson et al., 1981). Since little is known of the production mechanisms of luciferase and it has been confirmed that *Photobacterium sp.* r33 is the bacterial symbiont, these mechanisms should be studied in more detail. If the states of degradation are correlated to the production of the luciferase, it would give insight into where exactly the chemical reactions occur.

This study provides new insights into the bioluminescent mechanism of *P. atlanticum.* Our findings support bacterial based bioluminescence which is caused by a closely matching to *Photobacterium sp. r33*. Family Vibrionaceae is known to contain three genera of bioluminescent bacteria, including *Photobacterium. Photobacterium sp. r33* are found intracellularly and within the light organs of *P. atlanticum.* They were found in great relative abundances in these pyrosomes at about 40-74%, dominating the microbiome. More specifically, the bioluminescent symbiont community primarily contained this species of *Photobacterium* while the next abundant symbiont was found in family Vibrionaceae.

Figures and Tables

Figure 1. Orientation of both light organs on either side of the buccal siphon (a). Higher magnification of individual light organ (LO) with bacteria (or more likely bacteriocytes) (b).

Figure 2. Relative abundance of bacterial taxa (at the species level) across different samples. Columns 1 – 3 represent microbiomes derived from tunicate specimens preserved under different conditions. The next ten samples show bacterial distributions in seawater samples from the same location.

Figure 3. The light organs (green arrows) with no probe and the shutter wide open (a) vs. 4 μl of both EUB338 and *Photobacterium* probe with the shutter partially closed (b). Scale bar = 100 μm. EUB338 probe (c) vs. *Photobacterium* probe (d). The EUB338 probe binds to many bacteria (green arrow) within the tunic (white arrow) and the light organ (yellow arrow). In contrast, the *Photobacterium* probe only illuminated the light organ. Scale bar = 100 μm and 50 μm, respectively. EUB338 and *Photobacterium* probes in green (e) vs. red (f). The orange fluorescence in *Photobacterium Pa-1* is found exclusively concentrated around the edges of the light organ (yellow arrow). Scale bar = 20 μm.

Figure 4. Intact light organ (~30 μm diameter) semi encased in the tunic. Red scale bar is set at 50 μm.

Figure 5. Cristae of the mitochondria (m) distinctly shown compared to the intracellular microbes (b) within the cell (membrane – mb). The cells on the right appear to have just divided (red arrow) (a). Intracellular microbes (b) with endoplasmic reticulum (er) distributed throughout the cell (b). Bacteria within the light organ suggest intracellular to extracellular excretion activity (red arrow) of the light organ (c).

Table 1. Collection Data from the 15 samples used from all three research cruises with DEEPEND and NOAA - DP05, DP06, OER.

Table 2. FISH probe sequences and dye used to identify the Photobacterium in samples.

Table 3. Relative abundance of the top 13 bacterial species found with *Photobacterium sp. r33* highlighted.

Supplemental Figure 1. Map of collection cruises from DP05, DP06, and NOAA OER

Supplemental Figure 2. BLAST alignment of recorded *Photobacterium sp. r33* from NCBI and sequence of Photobacterium pulled from the 16S rRNA analysis.

Supplemental Figure 3. Preliminary phylogeny based on the Mitochondrial COI gene sequences.

Acknowledgments. Shortened. This study was conceived jointly by AB, JVL and PB. Etc. Internal funding by JVL laboratory.

Table 1. Collection Data from the 15 samples used from all three research cruises with DEEPEND and NOAA - DP05, DP06, OER.

Sample ID	Sample Type	Count	Cruise Designation	Sample Date	Start Lat	Start Lon	Trawl Depth (m)	Protocol Used
RNALater6	RNALater	1	DP06-25JUL18-MOC10-B250N-108-N0	25-Jul-18	27°59'21.588"N	88°30'36.612"W	0-1503	16S Sequencing & Genome Sequencing
RNALater7	RNALater	1	DP06-26JUL18-MOC10-B250D2-109-N0	26-Jul-18	27°59'27.6"N	88°30'20.412"W	0-1504	16S Sequencing & Genome Sequencing
DMSO1	DMSO	1	DPO5-02MAY17-MOC10-B082N-085-N0	2-May-17	28°0'58.5612"N	88°2'53.98"W	0-1500	16S Sequencing & Genome Sequencing
PYRG1_6.19	Gluteraldehyde	1	15JUN19-OER2019T07	15-Jun-19	27°21'47" N	85°31'93" W	0-1200	TEM & SEM
PYRG2_6.19	Gluteraldehyde	1	15JUN19-OER2019T07	15-Jun-19	27°21'47" N	85°31'93" W	0-1200	TEM & SEM
PYRG3_6.19	Gluteraldehyde	1	15JUN19-OER2019T07	15-Jun-19	27°21'47" N	85°31'93" W	0-1200	TEM & SEM
PYRG4_6.19	Gluteraldehyde	1	15JUN19-OER2019T07	15-Jun-19	27°21'47" N	85°31'93" W	0-1200	TEM & SEM
PYRP1_6.19	Paraformaldehyde	1	15JUN19-OER2019T07	15-Jun-19	27°21'47" N	85°31'93" W	0-1200	Fluorescence in situ hybridization
PYRP2_6.19	Paraformaldehyde	1	15JUN19-OER2019T07	15-Jun-19	27°21'47" N	85°31'93" W	0-1200	Fluorescence in situ hybridization
PYRP3_6.19	Paraformaldehyde	1	16JUN19-OER2019T09	16-Jun-19	27°23'67" N	85°30'56" W	0-1200	Fluorescence in situ hybridization
PYRP4_6.19	Paraformaldehyde	1	16JUN19-OER2019T09	16-Jun-19	27°23'67" N	85°30'56" W	0-1200	Fluorescence in situ hybridization
PYRRNA1_6.19	RNALater	1	16JUN19-OER2019T09	16-Jun-19	27°23'67" N	85°30'56" W	0-1200	DNA Extraction
PYRRNA2_6.19	RNALater	1	17JUN19-OER2019T10	17-Jun-19	28°29'34" N	87°27'14" W	1000-1500	DNA Extraction
PYRRNA3_6.19	RNALater	1	17JUN19-OER2019T10	17-Jun-19	28°29'34" N	87°27'14" W	1000-1500	DNA Extraction
PYRRNA4_6.19	RNALater	1	18JUN19-OER2019T10	18-Jun-19	28°31'58" N	84°42'27" W	0-200	DNA Extraction

Table 2. FISH probe sequences and dye used to identify the *Photobacterium* in samples.

Probe	Sequence with dye TAG	Base Pairs	5' or 3' Attachment	Absorbance Max	Emission Max
Photobacterium sp.	/5Cy3/TTCAGGTGTAGCGGTG AAATGC	22	5' End	550 nm	564 nm
EUB3338	GCTGCCTCCCGTAGGAGT/36-FAM/	18	3' End	495 nm	520 nm

Table 3. Relative abundance of the top 13 bacterial species found with *Photobacterium sp. r33* highlighted.

Name	DMSO 1	RNALater 6	RNALater 7	Water 1m	Water 12m	Water 64m	Water 72m	Water 500m	Water 1500m (a)	Water 1500m (b)	Water 1500m (c)	Water 1500m (d)	Water 1501m
Photobacterium sp. r33	0.742008	0.708790	0.396044	0.000185	0.000302	0.000000	0.000172	0.001193	0.001364	0.000112	0.001364	0.000292	0.000196
Vibrio u s	0.064947	0.000400	0.052508	0.000037	0.000121	0.000000	0.000000	0.000000	0.000138	0.000144	0.000138	0.000000	0.000147
Synechococcus u s	0.027416	0.001274	0.000471	0.025033	0.143685	0.052674	0.054037	0.008459	0.011172	0.018347	0.011172	0.006229	0.003742
Algicola u s	0.025933	0.000000	0.000000	0.000000	0.000000	0.000000	0.000000	0.000000	0.000000	0.000032	0.000000	0.000083	0.000954
Photobacterium u s	0.024748	0.021553	0.009654	0.000000	0.000000	0.000000	0.000000	0.000000	0.000000	0.000000	0.000000	0.000021	0.000000
Amphritea u s	0.022027	0.000000	0.000000	0.000000	0.000000	0.000000	0.000000	0.000000	0.000000	0.000000	0.000000	0.000063	0.000000
Enterovibrio u s	0.021486	0.020304	0.011773	0.000037	0.000000	0.000050	0.000000	0.000186	0.000158	0.000080	0.000158	0.000083	0.000000
Vibrionaceae u s	0.014336	0.005360	0.001648	0.002311	0.003047	0.002181	0.001806	0.000261	0.003500	0.001021	0.003500	0.000021	0.000367
Bd1-7 clade u s	0.007900	0.170001	0.035084	0.000259	0.000000	0.000852	0.000241	0.000000	0.000000	0.000048	0.000000	0.000021	0.000098
Moritella sp.	0.007307	0.007722	0.006828	0.000000	0.000000	0.000000	0.000000	0.000000	0.000079	0.000000	0.000079	0.000021	0.000000
Agarivorans u s	0.003453	0.000025	0.000706	0.000000	0.000000	0.000000	0.000034	0.000000	0.001206	0.000080	0.001206	0.000042	0.000269
Sagittula stellata	0.002476	0.000087	0.000942	0.000129	0.000272	0.000000	0.000327	0.001043	0.000277	0.001420	0.000277	0.001586	0.000098
Pirellulaceae u s	0.002302	0.000537	0.000471	0.001054	0.028719	0.002983	0.000808	0.004658	0.006011	0.017258	0.006011	0.008441	0.013967

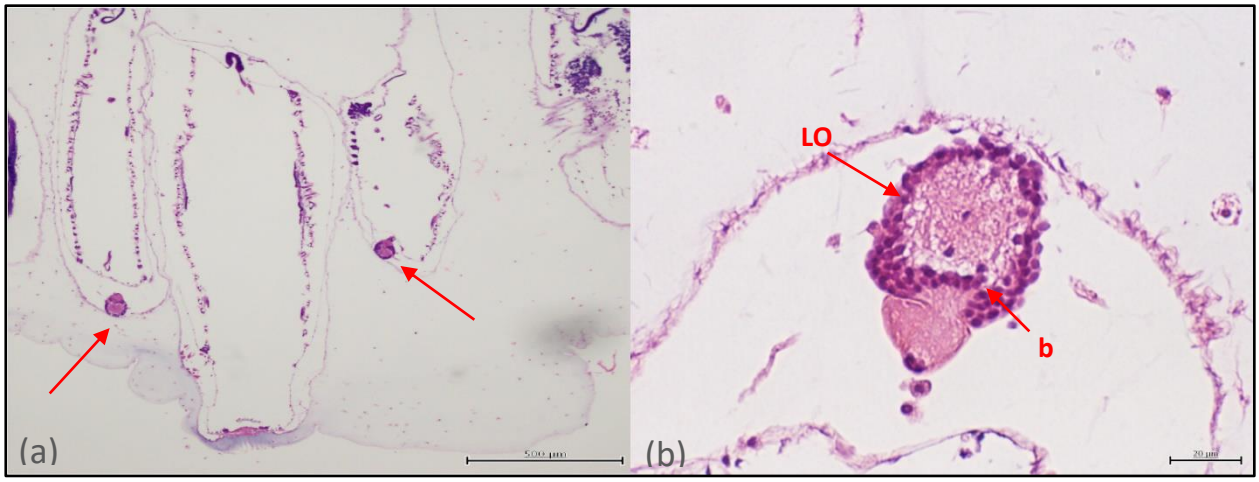

Figure 1'. Orientation of both light organs on either side of the buccal siphon (a). Higher magnification of individual light organ (LO) with bacteria (or more likely bacteriocytes) (b).

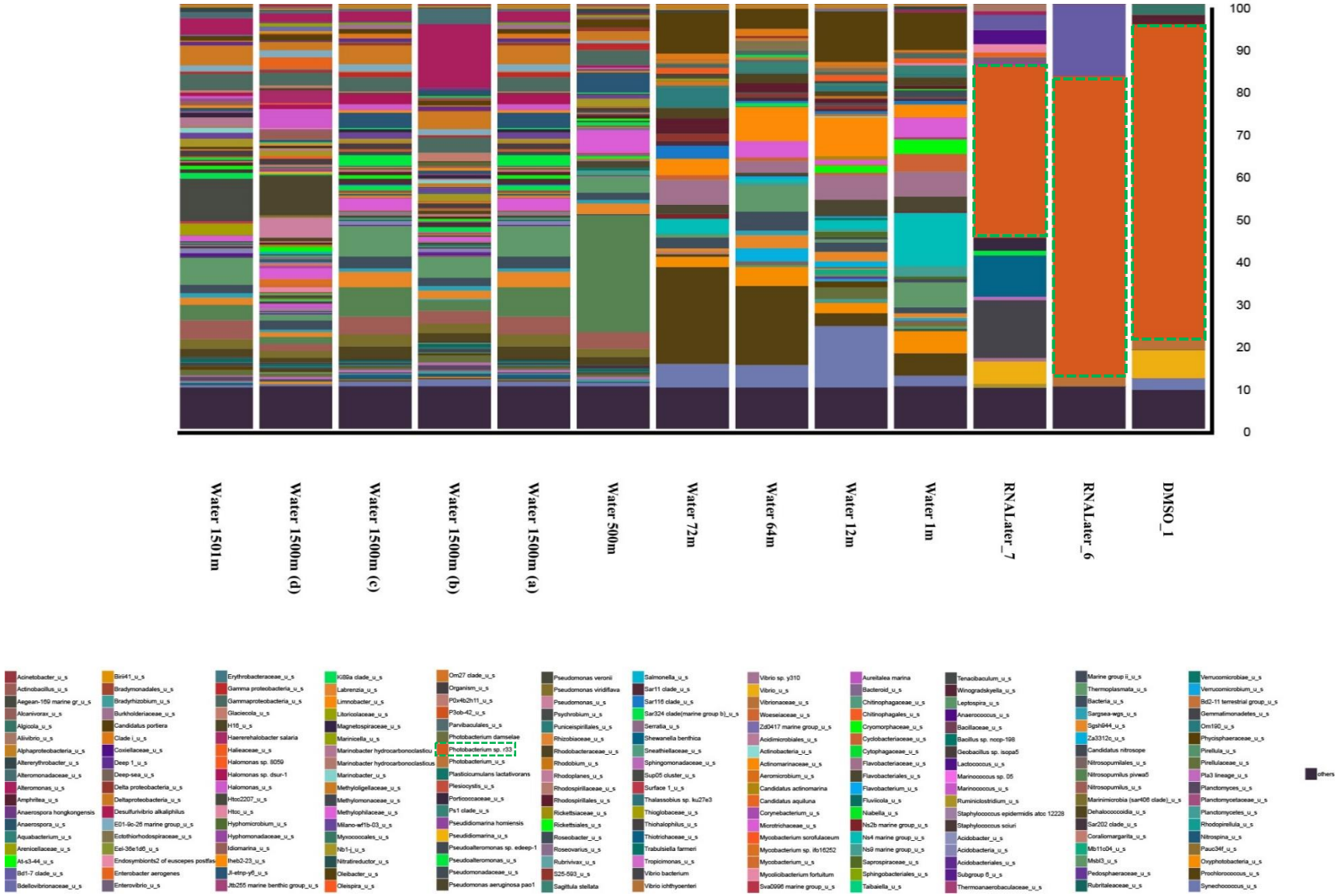

Figure 2'. Stacked Bar Chart of water (CTD) vs. Pyrosome samples highlighting the most abundant symbiont (*Photobacterium sp. r33* and *Vibrio sp.*

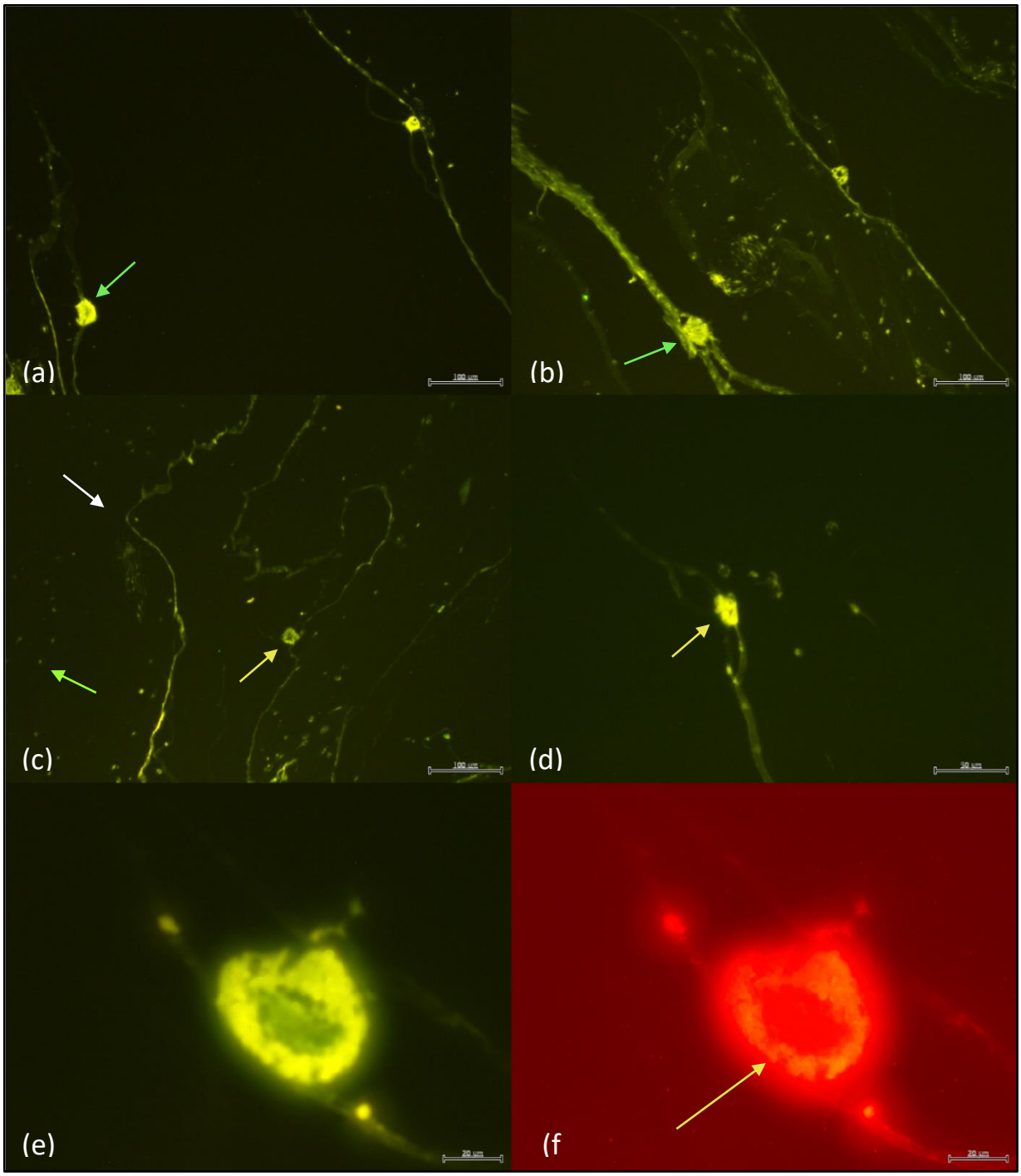

Figure 3'. The light organs (green arrows) with no probe and the shutter wide open (a) vs. 4 µl of both EUB338 and *Photobacterium* probe with the shutter partially closed (b). Scale bar = 100 µm. EUB338 probe (c) vs. *Photobacterium* probe (d). The EUB338 probe binds to many bacteria (green arrow) within the tunic (white arrow) and the light organ (yellow arrow). In contrast, the *Photobacterium* probe only illuminated the light organ. Scale bar = 100 µm and 50 µm, respectively. EUB338 and *Photobacterium* probes in green (e) vs. red (f). The orange fluorescence in *Photobacterium Pa-1* is found exclusively concentrated around the edges of the light organ (yellow arrow). Scale bar = 20 µm.

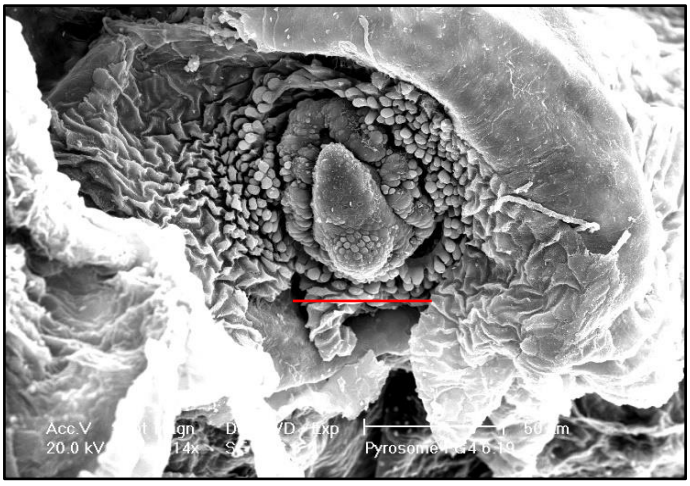

Figure 4'. Intact light organ (~30 µm diameter) semi encased in the tunic. Red scale bar is set at 50 µm.

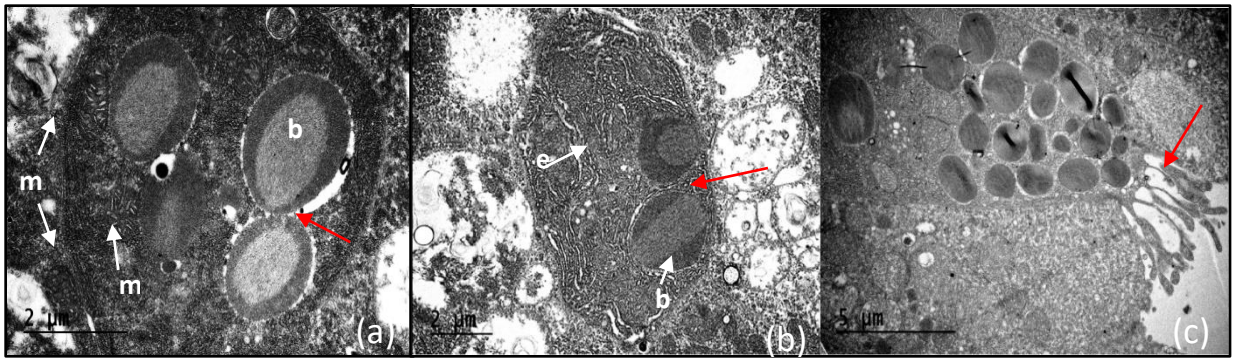

Figure 5'. Cristae of the mitochondria (m) distinctly shown compared to the intracellular microbes (b) within the cell (membrane – mb). The cells on the right appear to have just divided (red arrow) (a). Intracellular microbes (b) with endoplasmic reticulum (er) distributed throughout the cell (b). Bacteria within the light organ suggest intracellular to extracellular excretion activity (red arrow) of the light organ (c).

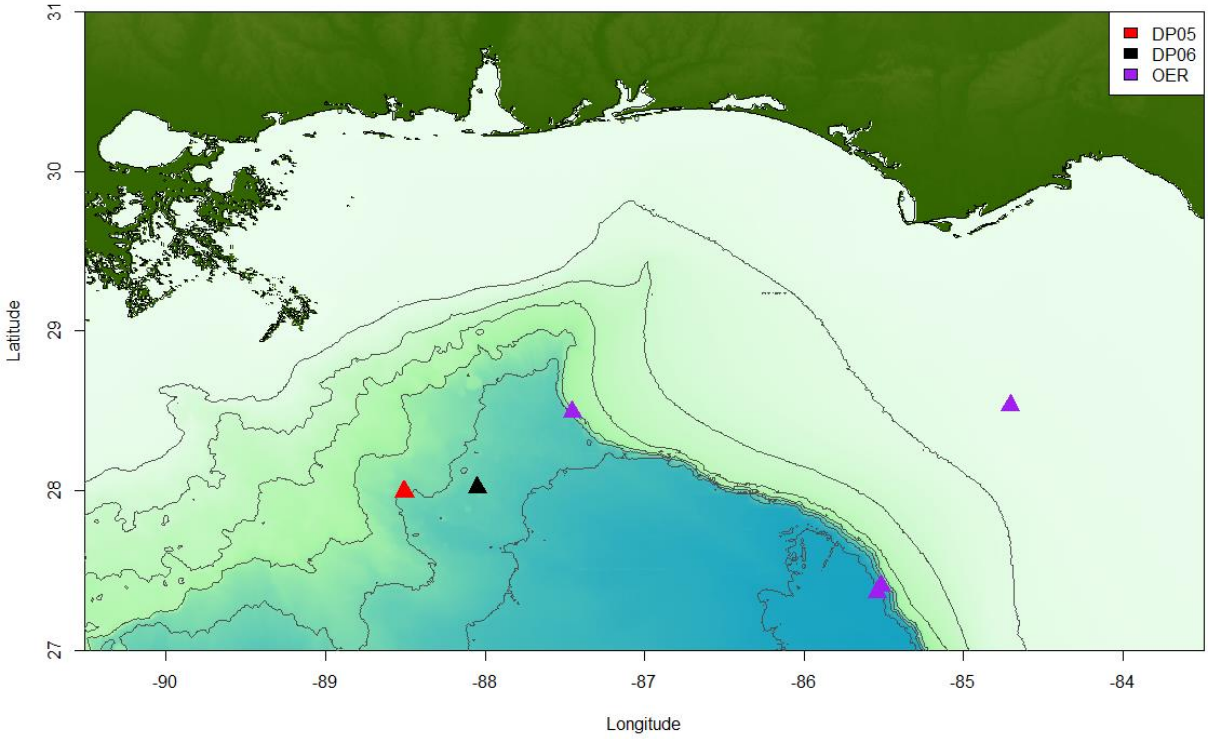

Supplemental Figure 1'. Map of collection cruises from DP05, DP06, and NOAA OER.

```
Query: Photobacterium sp. r33 gene for 16S rRNA, partial sequence Query ID: AB470939

>
Sequence ID: Query_23873 Length: 236
Range 1: 1 to 236

Score:420 bits(465), Expect:2e-121,
Identities:236/237(99%),  Gaps:1/237(0%), Strand: Plus/Plus

Query  518  ACGGAGGGTGCGAGCGTTAATCGGAATTACTGGGCGTAAAGCGCATGCAGGCGGTCTGTT  577
            ||||||||||||||||||||||||||||||||||||||||||||||||||||||||||||
Sbjct  1    ACGGAGGGTGCGAGCGTTAATCGGAATTACTGGGCGTAAAGCGCATGCAGGCGGTCTGTT  60

Query  578  AAGCAAGATGTGAAAGCCCGGGGCTCAACCTCGGAACAGCATTTTGAACTGGCAGACTAG  637
            ||||||||||||||||||||||||||||||||||||||||||||||||||||||||||||
Sbjct  61   AAGCAAGATGTGAAAGCCCGGGGCTCAACCTCGGAACAGCATTTTGAACTGGCAGACTAG  120

Query  638  AGTCTTGTAGAGGGGGGTAGAATTTCAGGTGTAGCGGTGAAATGCGTAGAGATCTGAAGG  697
            ||||||||||||||||||||||||||||||||||||||||||||||||||||||||||||
Sbjct  121  AGTCTTGTAGAGGGGGGTAGAATTTCAGGTGTAGCGGTGAAATGCGTAGAGATCTGAAGG  180

Query  698  AATACCGGTGGCGAAGGCGGCCCCCTGGACAAAGACTGACGCTCAGAATGCGAAAGC  754
            |||||||||||||||||||||||||||||||||||||||||||||||| ||||||||||
Sbjct  181  AATACCGGTGGCGAAGGCGGCCCCCTGGACAAAGACTGACGCTCAG-ATGCGAAAGC  236
```

Supplemental Figure 2. BLAST alignment of recorded *Photobacterium sp. r33* from NCBI and sequence of *Photobacterium* pulled from the 16S rRNA analysis.

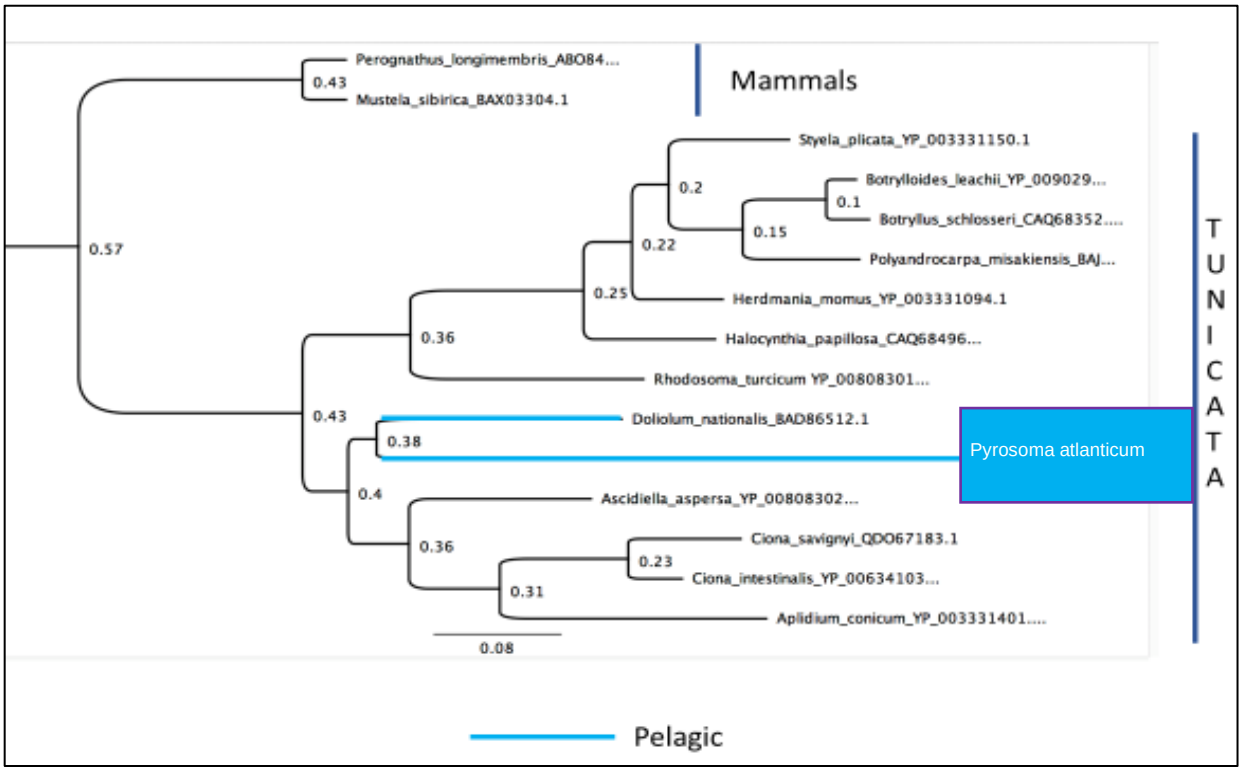

Supplemental Figure 3. Preliminary phylogeny based on the Mitochondrial COI gene sequences.

References

Afgan, E., Baker, D., Batut, B., Van Den Beek, M., Bouvier, D., Čech, M., Chilton, J., Clements, D., Coraor, N., and Grüning, B.A. (2018). The Galaxy platform for accessible, reproducible and collaborative biomedical analyses: 2018 update. *Nucleic acids research* 46**,** W537-W544.

Alldredge, A., and Madin, L. (1982). Pelagic tunicates: unique herbivores in the marine plankton. *Bioscience* 32**,** 655-663.

Amann, R.I., Ludwig, W., and Schleifer, K.-H. (1995). Phylogenetic identification and in situ detection of individual microbial cells without cultivation. *Microbiol. Mol. Biol. Rev.* 59**,** 143-169.

Aoki, M., Hashimoto, K., and Watanabe, H. (1989). The intrinsic origin of bioluminescence in the ascidian, Clavelina miniata. *The Biological Bulletin* 176**,** 57-62.

Baker, L.J., Freed, L.L., Easson, C.G., Lopez, J.V., Fenolio, D., Sutton, T.T., Nyholm, S.V., and Hendry, T.A. (2019). Diverse deep-sea anglerfishes share a genetically reduced luminous symbiont that is acquired from the environment. *eLife* 8.

Baldwin, T., Devine, J., Heckel, R., Lin, J.W., and Shadel, G. (1989). The complete nucleotide sequence of the lux regulon of Vibrio fischeri and the luxABN region of Photobacterium leiognathi and the mechanism of control of bacterial bioluminescence. *Journal of bioluminescence and chemiluminescence* 4**,** 326-341.

Barer, R. (1974). Microscopes, microscopy, and microbiology. *Annual Reviews in Microbiology* 28**,** 371-390.

Bauermeister, A., Branco, P.C., Furtado, L.C., Jimenez, P.C., Costa-Lotufo, L.V., and Da Cruz Lotufo, T.M. (2018). Tunicates: A model organism to investigate the effects of associated-microbiota on the production of pharmaceuticals. *Drug Discovery Today: Disease Models* 28**,** 13-20.

Berger, A. (2020). *The Role of Bacterial Symbionts and Bioluminescence in the Pyrosome, Pyrosoma atlanticum.* Master of Science, Nova Southeastern University

Beveridge, T.J. (2006). Visualizing bacterial cell walls and biofilms. *MICROBE-AMERICAN SOCIETY FOR MICROBIOLOGY* 1**,** 279.

Blackwelder, P. (2019). "The Equipment/LM Marine Organisms Under Light and Electron Microscopy ", in: *Histology and Ultrastructure of Marine Organisms* (ed.) P. Blackwelder. Nova Southeastern University).

Bourgois, J.-J., Sluse, F., Baguet, F., and Mallefet, J. (2001). Kinetics of light emission and oxygen consumption by bioluminescent bacteria. *Journal of bioenergetics and biomembranes* 33**,** 353-363.

Bouvier, T., and Del Giorgio, P.A. (2003). Factors influencing the detection of bacterial cells using fluorescence in situ hybridization (FISH): a quantitative review of published reports. *FEMS Microbiology Ecology* 44**,** 3-15.

Bowlby, M.R., Widder, E.A., and Case, J.F. (1990). Patterns of Stimulated Bioluminescence in 2 Pyrosomes (Tunicata, Pyrosomatidae). *Biological Bulletin* 179**,** 340-350.

Bright, M., and Bulgheresi, S. (2010). A complex journey: transmission of microbial symbionts. *Nature Reviews Microbiology* 8**,** 218-230.

Brown, T.A. (2007). *Genomes 3.* New York and London: Garland Science.

Burghause, F. (1914). *Kreislauf und Herzschlag bei Pyrosoma giganteum nebst Bemerkungen zum Leuchtvermögen: Aus d. Zool. Inst. zu Leipzig.* W. Engelmann.

Cahill, P.L., Fidler, A.E., Hopkins, G.A., and Wood, S.A. (2016). Geographically conserved microbiomes of four temperate water tunicates. *Environmental microbiology reports* 8**,** 470-478.

Campbell, A.M., Fleisher, J., Sinigalliano, C., White, J.R., and Lopez, J.V. (2015). Dynamics of marine bacterial community diversity of the coastal waters of the reefs, inlets, and wastewater outfalls of southeast F lorida. *MicrobiologyOpen* 4**,** 390-408.

Caporaso, J.G., Kuczynski, J., Stombaugh, J., Bittinger, K., Bushman, F.D., Costello, E.K., Fierer, N., Pena, A.G., Goodrich, J.K., and Gordon, J.I. (2010). QIIME allows analysis of high-throughput community sequencing data. *Nature methods* 7**,** 335.

Caporaso, J.G., Lauber, C.L., Walters, W.A., Berg-Lyons, D., Lozupone, C.A., Turnbaugh, P.J., Fierer, N., and Knight, R. (2011). Global patterns of 16S rRNA diversity at a depth of millions of sequences per sample. *Proceedings of the national academy of sciences* 108**,** 4516-4522.

Chakravorty, S., Helb, D., Burday, M., Connell, N., and Alland, D. (2007). A detailed analysis of 16S ribosomal RNA gene segments for the diagnosis of pathogenic bacteria. *Journal of microbiological methods* 69**,** 330-339.

Chiba, K., Hoshi, M., Isobe, M., and Hirose, E. (1998). Bioluminescence in the tunic of the colonial ascidian, Clavelina miniata: identification of luminous cells in vitro. *Journal of Experimental Zoology* 281**,** 546-553.

Cordes, E.E., Bergquist, D.C., and Fisher, C.R. (2009). Macro-ecology of Gulf of Mexico cold seeps. *Annual Review of Marine Science* 1**,** 143-168.

Cuvelier, M.L., Blake, E., Mulheron, R., Mccarthy, P.J., Blackwelder, P., Thurber, R.L.V., and Lopez, J.V. (2014). Two distinct microbial communities revealed in the sponge Cinachyrella. *Frontiers in microbiology* 5**,** 581.

Datye, A.K. (2003). Electron microscopy of catalysts: recent achievements and future prospects. *Journal of Catalysis* 216**,** 144-154.

Dawson, M.N., Raskoff, K.A., and Jacobs, D.K. (1998). Field preservation of marine invertebrate tissue for DNA analyses. *Molecular marine biology and biotechnology* 7**,** 145-152.

Décima, M., Stukel, M.R., López-López, L., and Landry, M.R. (2019). The unique ecological role of pyrosomes in the Eastern Tropical Pacific. *Limnology and Oceanography* 64**,** 728-743.

Dunlap, P. (2009). Bioluminescence, microbial.

Dunlap, P.V., Ast, J.C., Kimura, S., Fukui, A., Yoshino, T., and Endo, H. (2007). Phylogenetic analysis of host–symbiont specificity and codivergence in bioluminescent symbioses. *Cladistics* 23**,** 507-532.

Dunlap, P.V., and Urbanczyk, H. (2013). Luminous bacteria. *The Prokaryotes: Prokaryotic Physiology and Biochemistry***,** 495-528.

Easson, C.G., and Lopez, J.V. (2018). Depth-dependent environmental drivers of microbial plankton community structure in the northern Gulf of Mexico. *Frontiers in microbiology* 9**,** 3175.

Easson, C.G., and Lopez, J.V. (2019). Depth-Dependent environmental drivers of microbial plankton community structure in the Northern Gulf of Mexico. *Frontiers in microbiology* 9**,** 3175.

Emmert-Buck, M.R., Bonner, R.F., Smith, P.D., Chuaqui, R.F., Zhuang, Z., Goldstein, S.R., Weiss, R.A., and Liotta, L.A. (1996). Laser capture microdissection. *Science* 274**,** 998-1001.

Espina, V., Wulfkuhle, J.D., Calvert, V.S., Vanmeter, A., Zhou, W., Coukos, G., Geho, D.H., Petricoin, E.F., and Liotta, L.A. (2006). Laser-capture microdissection. *Nature protocols* 1**,** 586.

Farmer Iii, J., Michael Janda, J., Brenner, F.W., Cameron, D.N., and Birkhead, K.M. (2015). Vibrio. *Bergey's Manual of Systematics of Archaea and Bacteria***,** 1-79.

Farmer, J., and Hickman-Brenner, F. (2006). The genera vibrio and photobacterium. *The Prokaryotes: Volume 6: Proteobacteria: Gamma Subclass***,** 508-563.

Fox, G.E., Wisotzkey, J.D., and Jurtshuk Jr, P. (1992). How close is close: 16S rRNA sequence identity may not be sufficient to guarantee species identity. *International Journal of Systematic and Evolutionary Microbiology* 42**,** 166-170.

Freed, L.L. (2018). *Characterization of the Bioluminescent Symbionts from Ceratioids Collected in the Gulf of Mexico.* Master Masters Nova Southeastern University

Freed, L.L., Easson, C., Baker, L.J., Fenolio, D., Sutton, T.T., Khan, Y., Blackwelder, P., Hendry, T.A., and Lopez, J.V. (2019). Characterization of the microbiome and bioluminescent symbionts across life stages of Ceratioid Anglerfishes of the Gulf of Mexico. *FEMS microbiology ecology* 95**,** fiz146.

Galt, C., and Flood, P. (1998). Bioluminescence in the Appendicularia. *The Biology of Pelagic Tunicates***,** 215-229.

Galt, C., and Sykes, P. (1983). Sites of bioluminescence in the appendicularians Oikopleura dioica and O. labradoriensis (Urochordata: Larvacea). *Marine Biology* 77**,** 155-159.

Götz, S., García-Gómez, J.M., Terol, J., Williams, T.D., Nagaraj, S.H., Nueda, M.J., Robles, M., Talón, M., Dopazo, J., and Conesa, A. (2008). High-throughput functional annotation and data mining with the Blast2GO suite. *Nucleic acids research* 36**,** 3420-3435.

Haddock, S.H., and Case, J. (1999). Bioluminescence spectra of shallow and deep-sea gelatinous zooplankton: ctenophores, medusae and siphonophores. *Marine Biology* 133**,** 571-582.

Haddock, S.H., Moline, M.A., and Case, J.F. (2010). Bioluminescence in the sea. *Annual review of marine science* 2**,** 443-493.

Hastings, J., and Nealson, K.H. (1977). Bacterial bioluminescence. *Annual review of microbiology* 31**,** 549-595.

Haygood, M.G. (1993). Light Organ Symbioses In Fishes. *Critical Reviews in Microbiology* 19**,** 191-216.

Hendry, T.A., Freed, L.L., Fader, D., Fenolio, D., Sutton, T.T., and Lopez, J.V. (2018). Ongoing transposon-mediated genome reduction in the luminous bacterial symbionts of deep-sea ceratioid anglerfishes. *mBio* 9**,** e01033-01018.

Herring, P.J. (1985). Bioluminescence in the Crustacea. *Journal of crustacean biology* 5**,** 557-573.

Hirose, E. (2009). Ascidian tunic cells: morphology and functional diversity of free cells outside the epidermis. *Invertebrate Biology* 128**,** 83-96.

Hirose, E., Kimura, S., Itoh, T., and Nishikawa, J. (1999). Tunic morphology and cellulosic components of pyrosomas, doliolids, and salps (Thaliacea, Urochordata). *The Biological Bulletin* 196**,** 113-120.

Holland, L.Z. (2016). Tunicates. *Current Biology* 26**,** R146-R152.

Hughes, G.M., Leech, J., Puechmaille, S.J., Lopez, J.V., and Teeling, E.C. (2018). Is there a link between aging and microbiome diversity in exceptional mammalian longevity? *PeerJ* 6**,** e4174.
Huxley, T.H. (1851). XXIV. Observations upon the anatomy and physiology of salpa and pyrosoma. *Philosophical transactions of the Royal Society of London***,** 567-593.
Janda, J.M., and Abbott, S.L. (2007). 16S rRNA gene sequencing for bacterial identification in the diagnostic laboratory: pluses, perils, and pitfalls. *Journal of clinical microbiology* 45**,** 2761-2764.
Johnsen, S., Widder, E.A., and Mobley, C.D. (2004). Propagation and perception of bioluminescence: factors affecting counterillumination as a cryptic strategy. *The Biological Bulletin* 207**,** 1-16.
Kaeding, A.J., Ast, J.C., Pearce, M.M., Urbanczyk, H., Kimura, S., Endo, H., Nakamura, M., and Dunlap, P.V. (2007). Phylogenetic diversity and cosymbiosis in the bioluminescent symbioses of "Photobacterium mandapamensis". *Appl. Environ. Microbiol.* 73**,** 3173-3182.
Katoh, K., and Standley, D.M. (2013). MAFFT multiple sequence alignment software version 7: improvements in performance and usability. *Molecular biology and evolution* 30**,** 772-780.
Kerk, N.M., Ceserani, T., Tausta, S.L., Sussex, I.M., and Nelson, T.M. (2003). Laser capture microdissection of cells from plant tissues. *Plant physiology* 132**,** 27-35.
Kita-Tsukamoto, K., Yao, K., Kamiya, A., Yoshizawa, S., Uchiyama, N., Kogure, K., and Wada, M. (2006). Rapid identification of marine bioluminescent bacteria by amplified 16S ribosomal RNA gene restriction analysis. *FEMS microbiology letters* 256**,** 298-303.
Krishnaveni, M., Asha, S., Vini, S.S., and Punitha, S.M.J. (2018). "Metagenomics of Marine Invertebrate-Microbial Consortium," in *Metagenomics*. Elsevier), 255-272.
Kuczynski, J., Stombaugh, J., Walters, W.A., González, A., Caporaso, J.G., and Knight, R. (2011). Using QIIME to analyze 16S rRNA gene sequences from microbial communities. *Current protocols in bioinformatics* 36**,** 10.17. 11-10.17. 20.
Kwan, J.C., Donia, M.S., Han, A.W., Hirose, E., Haygood, M.G., and Schmidt, E.W. (2012). Genome streamlining and chemical defense in a coral reef symbiosis. *Proceedings of the National Academy of Sciences* 109**,** 20655-20660.
Labella, A.M., Arahal, D.R., Castro, D., Lemos, M.L., and Borrego, J.J. (2017). Revisiting the genus Photobacterium: taxonomy, ecology and pathogenesis. *Int Microbiol* 20**,** 1-10.
Land, M., Hauser, L., Jun, S.-R., Nookaew, I., Leuze, M.R., Ahn, T.-H., Karpinets, T., Lund, O., Kora, G., and Wassenaar, T. (2015). Insights from 20 years of bacterial genome sequencing. *Functional & integrative genomics* 15**,** 141-161.
Lee, K.-H., and Ruby, E.G. (1994). Effect of the squid host on the abundance and distribution of symbiotic Vibrio fischeri in nature. *Appl. Environ. Microbiol.* 60**,** 1565-1571.
Leisman, G., Cohn, D.H., and Nealson, K.H. (1980). Bacterial Origin of Luminescence in Marine Animals. *Science* 208**,** 1271-1273.
Lemaire, P., and Piette, J. (2015). Tunicates: exploring the sea shores and roaming the open ocean. A tribute to Thomas Huxley. *Open biology* 5**,** 150053.
Lewin, H.A., Robinson, G.E., Kress, W.J., Baker, W.J., Coddington, J., Crandall, K.A., Durbin, R., Edwards, S.V., Forest, F., and Gilbert, M.T.P. (2018). Earth BioGenome Project: Sequencing life for the future of life. *Proceedings of the National Academy of Sciences* 115**,** 4325-4333.

Lopez, J.V. (2019). "After the taxonomic identification phase: addressing the functions of symbiotic communities within marine invertebrates," in *Symbiotic Microbiomes of Coral Reefs Sponges and Corals*. Springer), 105-144.
Lopez Jv, G.C.O.S. (2013). The Global Invertebrate Genomics Alliance (GIGA): developing community resources to study diverse invertebrate genomes. *Journal of Heredity* 105**,** 1-18.
Mackie, G.O., and Bone, Q. (1978). Luminescence and Associated Effector Activity in Pyrosoma (Tunicata Pyrosomida). *Proceedings of the Royal Society Series B-Biological Sciences* 202**,** 483-+.
Martini, S., and Haddock, S.H. (2017). Quantification of bioluminescence from the surface to the deep sea demonstrates its predominance as an ecological trait. *Scientific reports* 7**,** 45750.
Mcfall-Ngai, M. (2014). Divining the essence of symbiosis: insights from the squid-vibrio model. *PLoS biology* 12**,** e1001783.
Mcfall-Ngai, M., Hadfield, M.G., Bosch, T.C., Carey, H.V., Domazet-Lošo, T., Douglas, A.E., Dubilier, N., Eberl, G., Fukami, T., and Gilbert, S.F. (2013). Animals in a bacterial world, a new imperative for the life sciences. *Proceedings of the National Academy of Sciences* 110**,** 3229-3236.
Meinkoth, J., and Wahl, G. (1984). Hydridization of nucleic acids immobilized on solid supports. *Analytical biochemistry* 138**,** 267-284.
Milligan, R.J., Bernard, A.M., Boswell, K.M., Bracken-Grissom, H.D., D'elia, M.A., Derada, S., Easson, C.G., English, D., Eytan, R.I., and Finnegan, K.A. (2018). The Application of Novel Research Technologies by the Deep Pelagic Nekton Dynamics of the Gulf of Mexico (DEEPEND) Consortium. *Marine Technology Society Journal* 52**,** 81-86.
Munk, O. (1998). Light Guides of the Escal Light Organs in Some Deep-Sea Anglerfishes (Pisces; Ceratioidei). *Acta Zoologica* 79**,** 175-186.
Nealson, K., Cohn, D., Leisman, G., and Tebo, B. (1981). Co-evolution of luminous bacteria and their eukaryotic hosts. *Annals of the New York Academy of Sciences* 361**,** 76-91.
Negandhi, K., Blackwelder, P.L., Ereskovsky, A.V., and Lopez, J.V. (2010). Florida reef sponges harbor coral disease-associated microbes. *Symbiosis* 51**,** 117-129.
Nelson, J.S., Grande, T.C., and Wilson, M.V. (2016). *Fishes of the World.* John Wiley & Sons.
Nyholm, S.V., and Mcfall-Ngai, M. (2004). The winnowing: establishing the squid–Vibrio symbiosis. *Nature Reviews Microbiology* 2**,** 632-642.
Nyholm, S.V., and Mcfall-Ngai, M.J. (1998). Sampling the light-organ microenvironment of Euprymna scolopes: description of a population of host cells in association with the bacterial symbiont Vibrio fischeri. *The Biological Bulletin* 195**,** 89-97.
O'connell, L., Gao, S., Mccorquodale, D., Fleisher, J., and Lopez, J.V. (2018). Fine grained compositional analysis of Port Everglades Inlet microbiome using high throughput DNA sequencing. *PeerJ* 6**,** e4671.
Pace, N.R. (1997). A molecular view of microbial diversity and the biosphere. *Science* 276**,** 734-740.
Polimanti, O. (1911). *Über das leuchten von Pyrosoma elegans Les.* R. Oldenbourg.
Rader, B.A., and Nyholm, S.V. (2012). Host/microbe interactions revealed through "omics" in the symbiosis between the Hawaiian bobtail squid Euprymna scolopes and the bioluminescent bacterium Vibrio fischeri. *The Biological Bulletin* 223**,** 103-111.
Rees, G.N., Baldwin, D.S., Watson, G.O., Perryman, S., and Nielsen, D.L. (2004). Ordination and significance testing of microbial community composition derived from terminal

restriction fragment length polymorphisms: application of multivariate statistics. *Antonie van Leeuwenhoek* 86**,** 339-347.

Rees, J.-F., De Wergifosse, B., Noiset, O., Dubuisson, M., Janssens, B., and Thompson, E.M. (1998). The origins of marine bioluminescence: turning oxygen defence mechanisms into deep-sea communication tools. *Journal of Experimental Biology* 201**,** 1211-1221.

Robison, B.H., Raskoff, K.A., and Sherlock, R.E. (2005). Ecological substrate in midwater: Doliolula equus, a new mesopelagic tunicate. *Journal of the Marine Biological Association of the United Kingdom* 85**,** 655-663.

Roth, M.S. (2014). The engine of the reef: photobiology of the coral–algal symbiosis. *Frontiers in Microbiology* 5**,** 422.

Ruby, E.G., and Lee, K.-H. (1998). The Vibrio fischeri-Euprymna scolopes light organ association: current ecological paradigms. *Appl. Environ. Microbiol.* 64**,** 805-812.

Ruppert, E.E., and Barnes, R.D. (1994). *Invertebrate Zoology.* Saunders College Publishing New York.

Schauder, S., and Bassler, B.L. (2001). The languages of bacteria. *Genes & Development* 15**,** 1468-1480.

Schimak, M.P., Kleiner, M., Wetzel, S., Liebeke, M., Dubilier, N., and Fuchs, B.M. (2016). MiL-FISH: Multilabeled oligonucleotides for fluorescence in situ hybridization improve visualization of bacterial cells. *Appl. Environ. Microbiol.* 82**,** 62-70.

Schimak, M.P., Toenshoff, E.R., and Bright, M. (2012). Simultaneous 16S and 18S rRNA fluorescence in situ hybridization (FISH) on LR White sections demonstrated in Vestimentifera (Siboglinidae) tubeworms. *Acta histochemica* 114**,** 122-130.

Schnitzler, C.E., Pang, K., Powers, M.L., Reitzel, A.M., Ryan, J.F., Simmons, D., Tada, T., Park, M., Gupta, J., and Brooks, S.Y. (2012). Genomic organization, evolution, and expression of photoprotein and opsin genes in Mnemiopsis leidyi: a new view of ctenophore photocytes. *BMC biology* 10**,** 107.

Scientists, G.C.O. (2014). The Global Invertebrate Genomics Alliance (GIGA): developing community resources to study diverse invertebrate genomes. *Journal of heredity* 105**,** 1-18.

Sfanos, K., Harmody, D., Dang, P., Ledger, A., Pomponi, S., Mccarthy, P., and Lopez, J. (2005). A molecular systematic survey of cultured microbial associates of deep-water marine invertebrates. *Systematic and Applied Microbiology* 28**,** 242-264.

Sharp, K.H., Eam, B., Faulkner, D.J., and Haygood, M.G. (2007). Vertical transmission of diverse microbes in the tropical sponge Corticium sp. *Appl. Environ. Microbiol.* 73**,** 622-629.

Shigenobu, S., Watanabe, H., Hattori, M., Sakaki, Y., and Ishikawa, H. (2000). Genome sequence of the endocellular bacterial symbiont of aphids Buchnera sp. APS. *Nature* 407**,** 81-86.

Sutherland, K.R., Sorensen, H.L., Blondheim, O.N., Brodeur, R.D., and Galloway, A.W. (2018). Range expansion of tropical pyrosomes in the northeast Pacific Ocean. *Ecology* 99**,** 2397-2399.

Thompson, F.L., Iida, T., and Swings, J. (2004). Biodiversity of vibrios. *Microbiol. Mol. Biol. Rev.* 68**,** 403-431.

Thompson, L.R., Sanders, J.G., Mcdonald, D., Amir, A., Ladau, J., Locey, K.J., Prill, R.J., Tripathi, A., Gibbons, S.M., and Ackermann, G. (2017). A communal catalogue reveals Earth's multiscale microbial diversity. *Nature* 551**,** 457.

Tringe, S.G., and Hugenholtz, P. (2008). A renaissance for the pioneering 16S rRNA gene. *Current opinion in microbiology* 11**,** 442-446.
Urakawa, H., Skutas, J., and Lopez, J.V. (2019). Draft Genome Sequence of Nitrosomonas sp. Strain APG5, a Betaproteobacterial Ammonia-Oxidizing Bacterium Isolated from Beach Sand. *Microbiology resource announcements* 8**,** e01573-01518.
Urbanczyk, H., Ast, J.C., and Dunlap, P.V. (2011). Phylogeny, genomics, and symbiosis of Photobacterium. *FEMS microbiology reviews* 35**,** 324-342.
Wade, W. (2002). Unculturable bacteria—the uncharacterized organisms that cause oral infections. *Journal of the Royal Society of Medicine* 95**,** 81-83.
Widder, E.A. (2010). Bioluminescence in the Ocean: Origins of Biological, Chemical, and Ecological Diversity. *Science* 328**,** 704-708.
Woese, C.R. (1987). Bacterial evolution. *Microbiological reviews* 51**,** 221.
Zaneveld, J.R., Burkepile, D.E., Shantz, A.A., Pritchard, C.E., Mcminds, R., Payet, J.P., Welsh, R., Correa, A.M., Lemoine, N.P., and Rosales, S. (2016). Overfishing and nutrient pollution interact with temperature to disrupt coral reefs down to microbial scales. *Nature communications* 7**,** 11833.